HeH^+ IN MODEL STELLAR ATMOSPHERES

Thesis by

Robert Henry Norton

In Partial Fulfillment of the Requirements

For the Degree of

Doctor of Philosophy

California Institute of Technology

Pasadena, California

1964

(Submitted May 1, 1964)

ACKNOWLEDGEMENTS

I am indebted to Professor Guido Münch, who first suggested the subject of this thesis and who has patiently guided me in its completion.

A special debt of gratitude is owed Dr. N. J. Sopkovich for his many helpful discussions and suggestions on the quantum mechanical calculations and especially for critically reading the manuscript.

I am grateful also to Dr. William Whitney and Professor Robert Christy for their helpful discussions of quantum mechanical calculations.

I wish to thank Dr. Dimitri Mihalas for the use of his partition function tables in advance of publication and for discussions on the computation of model stellar atmospheres.

Thanks are due the Jet Propulsion Laboratory for the grant of computing time on their equipment.

This thesis could never have been completed had it not been for the invaluable assistance of my wife Joanne. I am eternally in debt to her for her unfailing loyalty and patience in the typing, checking and preparation of the manuscript, and above all, for her faith.

ABSTRACT

Approximate quantum-mechanical calculations for the two lowest $^1\Sigma^+$ states of the helium hydride molecule ion HeH^+ have been made. The molecular potential energy curves resulting from these calculations have been found to agree reasonably well with the results of other investigators. Using classical statistics for the distribution of internuclear separations, approximate absorption coefficients for radiative transitions between these two states have been obtained.

A program to compute model stellar atmospheres in strict radiative equilibrium is described and was used to compute eight models with log g = 4.0 and effective temperatures between 9500° K. and 30000° K. Total flux constant to within 1% was attained for these models excluding HeH^+ as a source of opacity. When the final models were re-computed including the opacity of HeH^+, radiative equilibrium was found to be destroyed by as much as 15%. Radiative equilibrium was re-established for the model with $T_e = 16000^{\circ}$ K., and a comparison between this model with and without HeH^+ is given.

It is found that HeH^+ introduces a striking discontinuity in the continuous spectrum of the model at 1130 A; the ratio of the emergent monochromatic flux on the red side of the discontinuity to the flux on the violet side is 8.2 for the 16000° K. model. It is concluded that the wings of the Lyman lines, except L α, are probably weaker than previously supposed.

In addition, numerical quadrature formulae of high accuracy and efficiency are given for integrals of the Schwarzschild-Milne type.

TABLE OF CONTENTS

I. LIST OF TABLES

II. LIST OF FIGURES

III INTRODUCTION

It is indeed fortunate that the earth possesses a protective atmosphere, under which life could develop. This life-giving mantle, however, has been a source of frustration to the astronomer, for it has deprived him of badly needed observations in some of the most important spectral regions, for example the ultraviolet below 3000 A. The coming of the Space Age now holds out the promise that definitive observations in these long-inaccessible spectral regions can soon be made.

Recent observations have been made by Stecher and Milligan (38) from an unguided Aerobee rocket, which reached a peak altitude of 107 miles. The data consist of observations on 15 stars, of which 8 are of doubtful quality, secured with a modest grating spectrophotometer and telemetered to earth. The observations exhibit a fundamental disagreement with theoretical model atmospheres, in the sense that the model atmospheres predict monochromatic fluxes some 30 times as large as observed by Stecher and Milligan. This disagreement was found to decrease in a somewhat systematic manner, disappearing at spectral type F 0, to within the accuracy of either the observations or the models.

This disagreement is disturbing. One can consider three possibilities for the origin of this effect: 1) continuous absorption by an unknown source in the stellar atmosphere; 2) absorption by material in a circumstellar envelope; and 3) absorption in interstellar space.

Pecker (39) has considered origin No. 2 above as explaining the observed ultraviolet deficiency in early type stars. He considers a circumstellar envelope of dielectric dust particles and finds that to produce the observed extinction, the particles must have a radius of 0.4μ.

Hoyle and Wickramasinghe (40) suggest that the extinction may be caused by interstellar composite graphite - ice grains of radii less than or equal to 0.1μ.

In their paper presenting the rocket observations, Stecher and Milligan favor an atmospheric origin for the observed ultraviolet deficiency on the grounds that if half of a hot star's total flux were absorbed by a circumstellar envelope, the envelope should be visible; they reject an interstellar source on the grounds that the effect appears to be systematic with spectral type, and that α Carinae, the most distant star observed, does not show the effect at all. They propose instead an opacity source within the stellar atmosphere, due to quasi-molecular absorption by various combinations of hydrogen and helium atoms and ions. In particular, they suggest the helium hydride molecule ion HeH^+.

The purpose of this thesis is to obtain approximate quantum mechanical cross-sections for the HeH^+ molecule and to investigate the effectiveness of HeH^+ as an opacity source in a theoretical model atmosphere. We will make no attempt to explain the ultraviolet deficiencies observed by Stecher and Milligan.

The general theory of formation of molecules by radiative association and the absorption coefficient due to radiative dissociation is discussed in Chapter IV, where are also given the specific results obtained for HeH^+ in this investigation. A comparison between the rate coefficient for radiative association of HeH^+ and the rate coefficients of other atomic and molecular processes is also made.

A description of a non-gray model atmosphere computer program follows in Chapter V. Several main sequence model atmospheres, with effective temperatures between $9500^{\circ}K$ and $30000^{\circ}K$, were computed using this computer program, and the results obtained, both with and without the HeH^+ molecule as an opacity source, are contained in Chapter VI. Mathematical derivations and discussions that were lengthy have been put in the Appendices wherever possible.

IV SEMI-CLASSICAL MOLECULAR ABSORPTION COEFFICIENTS

1. General Theory

At low gas densities, as for example in the outer layers of a stellar atmosphere, a significant fraction of molecules present may be formed by radiative association, typified by

$$A + B \rightarrow (AB) \rightarrow (AB)' + h\nu \qquad \text{(IV-1)}$$

since the densities are frequently too low for the three-body reaction

$$A + B + C \rightarrow (AB) + C$$

to compete. Our particular interest is in the inverse of process (IV-1), or an absorption process. We follow the semi-classical procedure of Bates (6, 7), who supposes that two atoms approach each other along a trajectory AB(R). This trajectory is asymptotic to the initial state A + B at infinite separation and corresponds to the potential energy curve $U_1(R)$ indicated schematically in Figure 1. Since we are talking in completely general terms, let us suppose that we can write a complete Hamiltonian for state (AB(R)) along the trajectory and solve Schrodinger's time-independent equation at each internuclear separation R. We assume that there exists a second state (CD(R)) to which radiative transitions from the initial state (AB(R)) occur. This state (CD(R)) is asymptotic to the final state C + D at infinite separation and corresponds to the potential energy curve $U_2(R)$ in Figure 1.

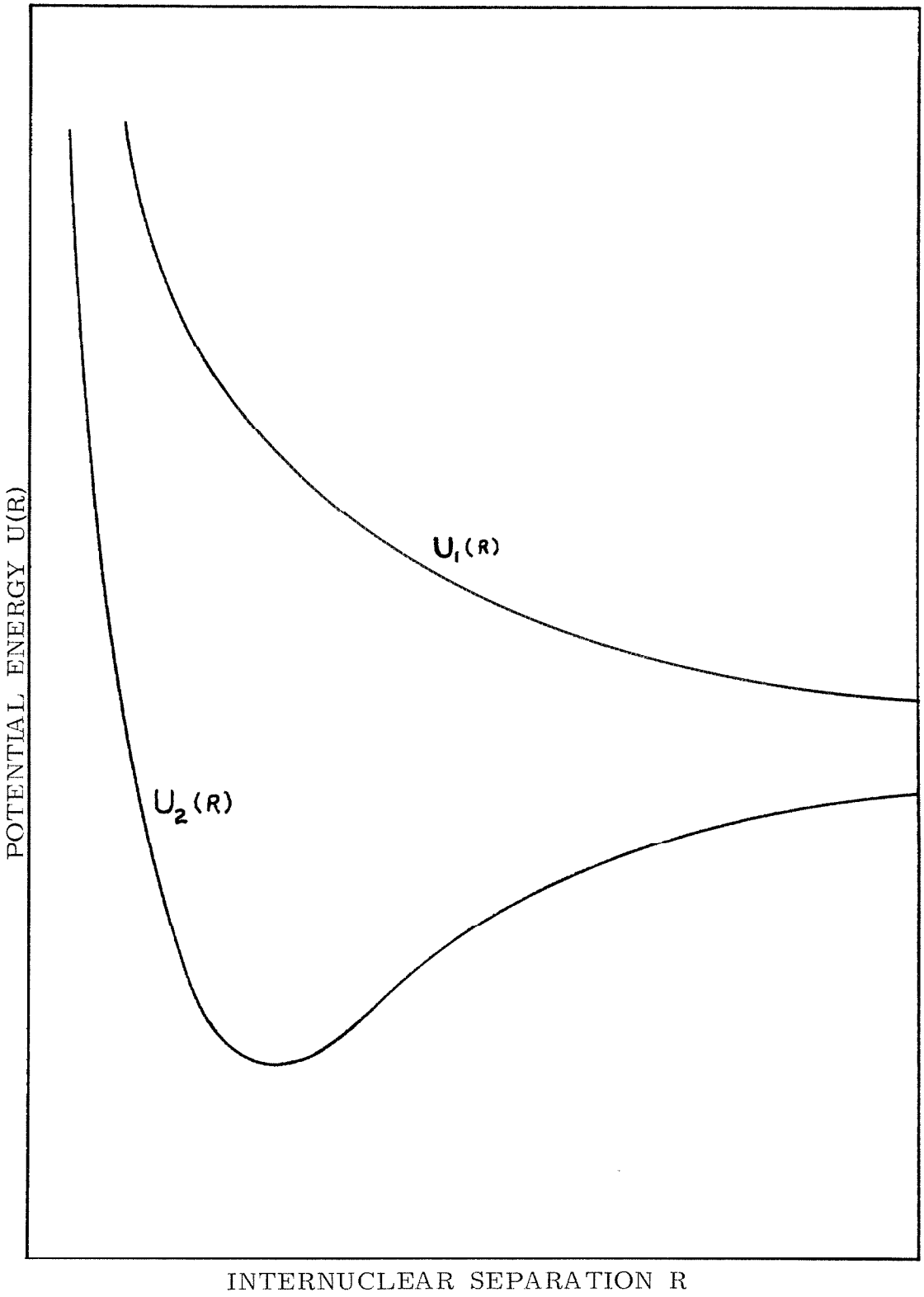

Figure 1. Schematic Molecular Potential Energy Curves

We write the reaction as

$$A + B \rightarrow (AB)$$
$$(AB) \rightarrow (CD) + h\nu$$
$$(CD) \rightarrow C + D \qquad \text{(IV-2)}$$

After the electronic transition, the state (CD) may or may not be stable, depending upon the amount of kinetic energy possessed by the atomic systems after the transition. If the kinetic energy is greater than the depth of the potential well shown in Figure 1, the atoms can separate. If it is not, the system remains bound until another event occurs, such as the absorption of radiation.

The absorption coefficient per unit volume $k(\nu,T)$ associated with the inverse reaction of (IV-2) is related to the photon emissivity $j(\nu,T)$ of (IV-2) by Kirchhoff's law

$$k(\nu,T) = \frac{c^2}{8\pi\nu^2}\left(e^{\frac{h\nu}{kT}} - 1\right) j(\nu,T) \qquad \text{(IV-3)}$$

where ν is the frequency of the radiation and T is the temperature. We define a rate coefficient $\gamma(\nu,T)$ for process (IV-2) giving the number of particles (AB) formed per unit volume per unit time in the frequency range ν to $\nu + d\nu$. The photon emissivity $j(\nu,T)$ is then

$$j(\nu,T) = \gamma(\nu,T)\, N_A\, N_B \qquad \text{(IV-4)}$$

where N_A and N_B are the concentrations per unit volume of atoms A and B.

We relate the reaction rate coefficient $\gamma(\nu,T)$ for the frequency range ν to $\nu+d\nu$ to a reaction rate coefficient $\gamma(R,T)$ for photon emission from atoms whose internuclear separation lie between R and R + dR by the definition

$$\gamma(\nu,T) = \gamma(R,T) \Big/ \left| d\nu/dR \right| . \qquad \text{(IV-5)}$$

By an equally simple definition, the frequency of the radiative transition is given by the difference in energy between the potential energies of the two states

$$h\nu(R) = U_1(R) - U_2(R) . \qquad \text{(IV-6)}$$

Bates assumes that the trajectory AB(R) along which the atoms A and B approach each other is given by the laws of motion for a classical orbit

$$\frac{dR}{dt} = \left[v^2 - \frac{p^2 v^2}{R^2} - \frac{2\,U_1(R)}{m} \right]^{1/2} \qquad \text{(IV-7)}$$

where m is the reduced mass, v is the relative velocity of approach, and p is the impact parameter. The rate coefficient $\gamma(R,T)$ is obtained by assuming a Maxwelliam velocity distribution and then averaging over all values of v and p consistent with a given internuclear separation R, yielding

$$\gamma(R,T) = 8\pi^2 g\, A(R) \left(\frac{m}{2\pi kT}\right)^{3/2} \iint e^{-\frac{mv^2}{2kT}} \times v^3 p \left[v^2 - \frac{p^2 v^2}{R^2} - \frac{2\,U_1(R)}{m} \right]^{-1/2} dv\, dp \qquad \text{(IV-8)}$$

where g is the statistical probability that the atoms will approach each other along the particular trajectory AB(R) out of all the possible trajectories, and A(R) is the Einstein transition probability for a radiative transition from state AB(R) to a lower state CD(R) at the separation R. g will be explicity defined later when we consider a specific transition between two electronic states of HeH^+. The integration of equation (IV-8) over p is carried out first between the limits p = 0 and $p = p_m$, the maximum value which p may achieve for given values of ν and R. At a point of closest approach, dR/dt vanishes and from equation (IV-7), Kramers and ter Haar (33) concluded that p_m is given by

$$p_m^2 = R^2 - \frac{2U_1(R)}{m\nu^2} \quad . \tag{IV-9}$$

Bates (6) pointed out that this is not always true and gave several limiting cases. One limiting case is of special interest, for it involves the approach of two atoms along a trajectory whose potential energy curve is repulsive. An example of a reaction such as this is the emission of photons from colliding hydrogen atoms and protons

$$H + H^+ \longrightarrow H + H^+ + h\nu \quad .$$

Bates shows that in this case where $U_1(R) > 0$ everywhere $(U_1(\infty) = 0)$, the maximum p_m is correctly given by equation (IV-9). As we shall show in Section 2 of this Chapter, this case applies also to the reactions involving hydrogen atoms and ionized helium atoms

$$He^+ + H \longrightarrow He + H^+ + h\nu \quad .$$

Another limiting case is where the atoms approach each other along a trajectory whose potential energy curve is attractive, exemplified by the doubly ionized helium hydride molecule

$$He^{2+} + H \rightarrow He^{+} + H^{+} + h\nu .$$

In this case equation (IV-9) is incorrect, and Bates gives several approximate expressions which can be used.

The integration of equation (IV-8) over p thus results in

$$\gamma(R,T) = 8\pi^2 g\, A(R)\, R^2 \left(\frac{m}{2\pi kT}\right)^{3/2}$$

$$\times \int_{v_1}^{v_2} e^{-\frac{mv^2}{2kT}} v \left[v^2 - \frac{2U_1(R)}{m}\right]^{1/2} dv . \qquad \text{(IV-10)}$$

From the equation of motion, equation (IV-7), we can see that the minimum value of v which enables a given separation R to be reached is

$$v_1 = \left[\frac{2}{m} U_1(R)\right]^{1/2}$$

since the derivative dR/dt must be real. If, after the transition, the atoms possess no kinetic energy, v must equal v_2 , where

$$v_2 = \left[\frac{2}{m}\left\{U_1(R) - U_2(R)\right\}\right]^{1/2}$$

but since they may possess excess kinetic energy, the upper limit of integration should be infinity. We integrate equation (IV-10) between $v = \left[2U_1(R)/m\right]^{1/2}$ and $v = \infty$ and obtain

$$\gamma(R,T) = 4\pi g A(R) R^2 e^{-\frac{U_1(R)}{kT}} \left[\frac{2}{\sqrt{\pi}} \int_0^{\infty} e^{-x^2} x^2 dx\right]$$

$$= 4\pi g A(R) R^2 e^{-\frac{U_1(R)}{kT}} \qquad \text{(IV-11)}$$

We emphasize that as used in this context, the potential energy $U_1(R)$ is considered to be zero at $R = \infty$. It should also be borne in mind that equation (IV-11) is valid only if $U_1(R) \geq 0$ everywhere.

The Einstein transition probability A(R) was shown by Mulliken (8) to be

$$A(R) = \frac{64\pi^4 e^2}{3hc^3} G_2 \nu^3 \left|\vec{Q}(R)\right|^2 \qquad \text{(IV-12)}$$

where G_2 is the orbital degeneracy factor of the lower state, defined by Mulliken (8) to be the number of suitable final orbitals to which a transition from a given initial orbital may occur. For diatomic molecules, transitions between states may be divided into parallel-type transitions, which are characterized by $\Delta\Lambda = 0$, and perpendicular-type transitions, where $\Delta\Lambda = \pm 1$. Λ is of course the projection of the electronic orbital angular moment on the line joining the nuclei. When we discuss the helium-hydride molecule ion in the next section, we will be considering only parallel-type transitions. Mulliken shows that for parallel-type transitions, the

orbital degeneracy factors of both the initial and final states are both unity. Mulliken also points out that while G_1 and G_2, associated with the upper (initial) and lower (final) states respectively, are not statistical weights, their ratio G_2/G_1 is always equal to the ratio of the statistical weights g_2/g_1 associated with the states.

In equation (IV-12), the quantity $\vec{Q}(R)$ is a dipole transition integral and is defined by

$$\vec{Q}(R) = \int \psi_2^* \left(\sum_s \vec{r}_s \right) \psi_1 \, d\tau \,, \qquad \text{(IV-13)}$$

where the subscript s and the summation refer to the electrons, $\vec{r}_s$ is the position vector of the electrons referred to a coordinate system to be described later, ψ_1 and ψ_2 are the electronic wave functions along the trajectory for the initial and final states respectively, and the integration is carried out over the coordinates of all electrons.

In practice, exact electronic wave functions are not available; approximate wave functions must then be used, and thus a knowledge of the exactness or inexactness of the trial wave functions becomes desirable. As Chandrasekhar (16) has pointed out, the expression for the dipole transition integral in equation (IV-13), designated the dipole-length formula, may be expressed in terms of the dipole-velocity formula

$$\vec{Q}(R) = \frac{1}{E(R)} \int \psi_2^* \left(\sum_s \vec{\nabla}_s \psi_1 \right) d\tau \qquad \text{(IV-14)}$$

or the dipole-acceleration formula

$$\vec{Q}(R) = \frac{1}{[E(R)]^2} \int \psi_2^* \left(\sum_a \vec{\nabla}_a V \right) \psi_1 \, d\tau \qquad \text{(IV-15)}$$

where E(R) is the energy difference between states at a specific internuclear separation R, and V is the potential energy arising from Coulomb interactions of the electrons with the nuclei and other electrons. The three formulas for $\vec{Q}(R)$ yield identical results when exact electronic wave functions are used. The extent to which they disagree when approximate wave functions are used may be considered to be an index to the inexactness of the wavefunctions.

We now obtain the absorption coefficient of a unit volume of atoms undergoing the inverse of process (IV-2) by combining equations (IV-3), (IV-4), (IV-5), (IV-11) and (IV-12). The result is

$$k(\nu,T) = \frac{32\pi^4 e^2}{3hc} g G_2 \left| \frac{\nu}{d\nu/dR} \right| R^2 \left| \vec{Q}(R) \right|^2$$

$$\times \; e^{-\frac{U_1(R)}{kT}} \left[e^{\frac{h\nu}{kT}} - 1 \right] N_A N_B \, . \qquad \text{(IV-16)}$$

In this expression, the quantity $\left| \frac{\nu}{d\nu/dR} \right|$ is computed from equation (IV-9), and $|\vec{Q}(R)|$ is computed from any of equations (IV-13), (IV-14) or (IV-15).

2. Applications to the Helium Hydride Molecule Ion HeH^+

Over a significant range of temperatures and electron pressures in a stellar atmosphere, helium is mostly neutral and hydrogen is mostly ionized, due to the fact that the ionization potential of He is some 11 ev greater than H. For this reason the singly ionized helium hydride molecule HeH^+, formed in its ground state by helium atoms and protons, may contribute significantly to the opacity in a stellar atmosphere if the absorption occurs in a transparent spectral region. The process involves a transfer of charge, viz

$$\left.\begin{aligned} He + H^+ &\rightarrow (HeH^+) \\ (HeH^+) + h\nu &\longrightarrow (He^+H) \\ (He^+H) &\rightarrow He^+ + H \end{aligned}\right\} \qquad \text{(IV-17)}$$

Electronic states and potential energy curves have been reported for the ground state by Evett (13) and Anex (14), who found the ground state to be slightly attractive, with a binding energy less then 2 ev and an equilibrium internuclear separation of 1.4 Bohr radii. Preliminary investigations by these two authors indicated that the first excited state was repulsive.

An estimate of the lower frequency limit for this absorption process may be obtained by considering the energies of the two states at infinite internuclear separation. The ground state dissociates into a neutral helium atom and a proton; its electronic orbital energy is the ground state energy of the helium atom, or

-2.90372 Hartrees, after Hart and Herzberg (15). The excited state dissociates into a singly ionized helium atom and a hydrogen atom, having electronic energies of -2.0 Hartrees for the He II atom and -0.5 Hartrees for the H I atom. This minimum energy difference of approximately 0.4 Hartrees corresponds roughly to 1140 Angstroms. The continuous absorption coefficient of a stellar atmosphere is small in this wavelength region, as absorption by photo-ionizations of hydrogen from the ground state cannot occur.

In atomic units the time-independent Schrödinger equation for the electronic states of the system (HeH^+) is

$$-\frac{1}{2}\left(\nabla_1^2 + \nabla_2^2\right)\psi + (V - W)\psi = 0 \qquad \text{(IV-18)}$$

where W is the electronic energy of the state for the electronic potential energy V

$$V = \frac{1}{r_{12}} - 2\left(\frac{1}{r_{a1}} + \frac{1}{r_{a2}}\right) - 2\left(\frac{1}{r_{b1}} + \frac{1}{r_{b2}}\right). \qquad \text{(IV-19)}$$

Here the subscripts a and b denote the helium and hydrogen nuclei respectively, the subscripts 1 and 2 denote the electrons, and R is the internuclear separation, as shown in Figure 2.

To find approximate electronic wave functions for this molecule, we use a variational approach, expanding the trial wave functions as linear combinations of atomic orbitals (LCAO) after Mulliken (8). For the sake of simplicity, we allow only two non-linear parameters, ζ_a and ζ_b one associated with each nucleus.

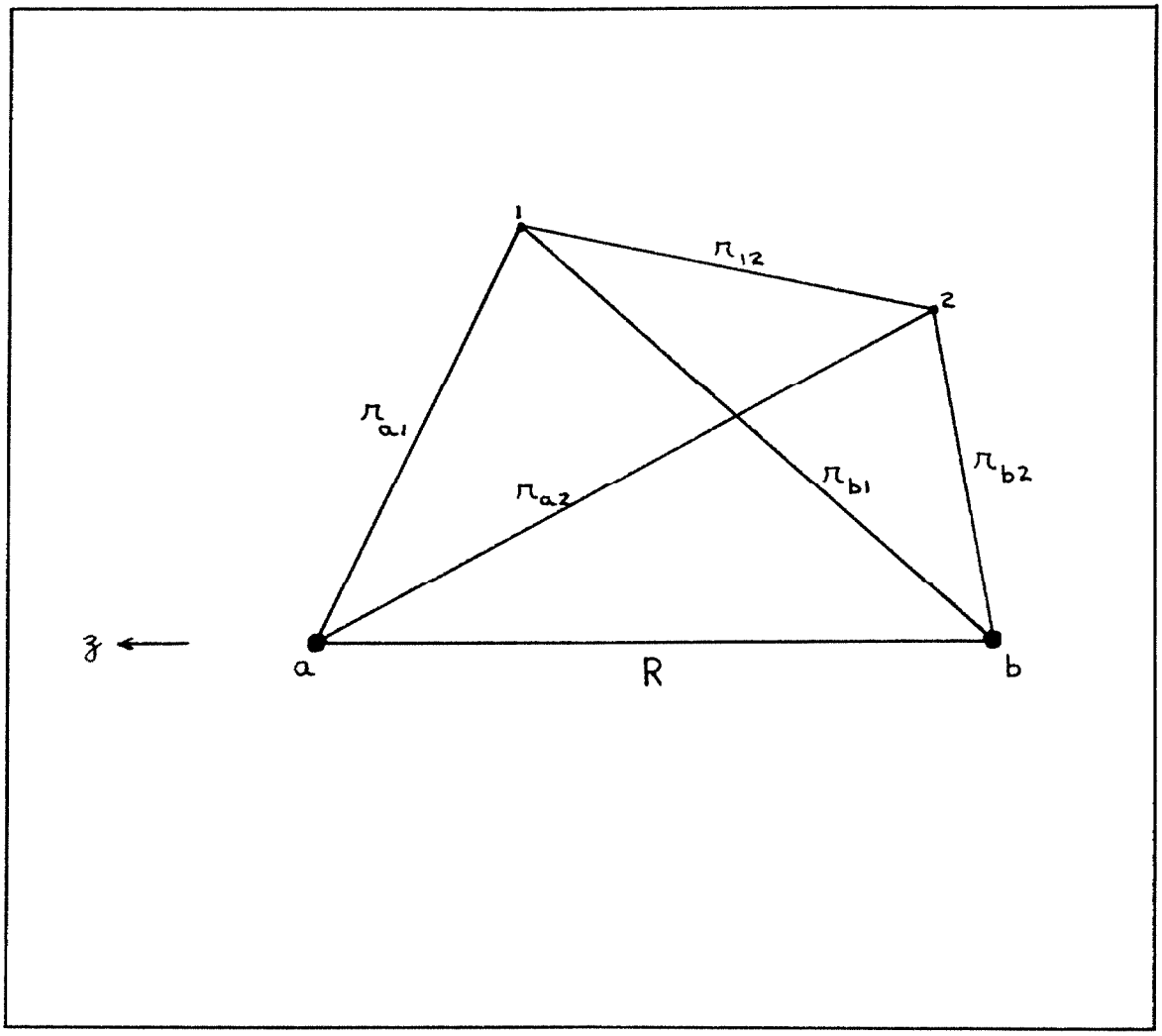

Figure 2. Hamiltonian Coordinate System

The atomic orbitals chosen are the normalized Slater orbitals; for the sake of simplicity we restrict ourselves to only s-type orbitals, defined by Roothaan (35) as

$$n\Delta = \frac{(2\zeta)^{n+\frac{1}{2}}}{[4\pi\,(2n)!\,]^{1/2}}\; r^{n-1}\; e^{-\zeta r} \qquad \text{(IV-20)}$$

where ζ is a non-linear variation parameter, n is the principle quantum number of the atomic orbital, and r is the electron-nucleus distance.

Anex (14) reports that the electronic ground state of HeH^+ is a $^1\Sigma^+$ state, in customary molecular notation. The meaning of this notation is that the component along the internuclear axis of the electronic orbital angular momentum is zero, hence the state is non-degenerate. The superscript 1 denotes the multiplicity of the state due to electron spin; in this case the component of the spin angular momentum on the internuclear axis is zero. The superscript + indicates that the electronic eigenfunction is symmetric about the internuclear axis (Herzberg (36)).

Radiative electric dipole transitions can occur only between states of the same orbital symmetry in the electrons. To prove this, let us consider the transition dipole moment as expressed in equation (IV-13), and let us denote real electronic wave functions for the ground state and some excited state by $\phi_i(x_1, x_2)$ and $\phi_f(x_1, x_2)$ respectively, where x_1 and x_2 are the coordinates of the two electrons. As the ground state of HeH^+ is symmetric, we assume

that the ground state wave function is symmetric with respect to an interchange of the electrons,

$$\phi_i(x_1 x_2) = \phi_i(x_2 x_1) \quad . \tag{IV-21}$$

The transition dipole moment is

$$\vec{Q} = \int \phi_f(x_1 x_2) \left[\vec{x}_1 + \vec{x}_2 \right] \phi_i(x_1 x_2) \, dx_1 \, dx_2 \quad . \tag{IV-22}$$

We also have

$$\vec{Q} = \int \phi_f(x_2 x_1) \left[\vec{x}_2 + \vec{x}_1 \right] \phi_i(x_2 x_1) \, dx_2 \, dx_1 \quad . \tag{IV-23}$$

If the excited state wavefunction is antisymmetric,

$$\phi_f(x_1 x_2) = - \phi_f(x_2 x_1) \tag{IV-24}$$

and we have

$$\vec{Q} = -\vec{Q}$$

which can be satisfied only if

$$\vec{Q} = 0$$

Thus the wave functions representing the ground and excited states of an electronic transition must both be symmetric or both anti-symmetric.

The following set of symmetric electronic orbital wave functions are constructedfrom Slater-type atomic orbitals with principle quantum numbers less than or equal to two.

$$
\left.
\begin{aligned}
\chi_1 &= 1s_a(1)\ 1s_a(2) \\
\chi_2 &= 1s_a(1)\ 1s_b(2) + 1s_b(1)\ 1s_a(2) \\
\chi_3 &= 1s_a(1)\ 2s_a(2) + 2s_a(1)\ 1s_a(2) \\
\chi_4 &= 2s_a(1)\ 2s_a(2) \\
\chi_5 &= 2s_a(1)\ 1s_b(2) + 1s_b(1)\ 2s_a(2) \\
\chi_6 &= 1s_a(1)\ 2s_b(2) + 2s_b(1)\ 1s_a(2) \\
\chi_7 &= 2s_a(1)\ 2s_b(2) + 2s_b(1)\ 2s_a(2)
\end{aligned}
\right\} \qquad \text{(IV-25)}
$$

where the notation is explained by the example: $2s_b(1)$ denotes an atomic orbital with principle quantum number n = 2 for electron 1 centered on nucleus b (taken to be the hydrogen nucleus). See Figure 2.

The electronic Hamiltonian for the system is

$$
H = -\tfrac{1}{2}\nabla_1^2 - \tfrac{1}{2}\nabla_2^2 + \frac{1}{r_{12}} - \frac{2}{r_{a1}} - \frac{2}{r_{a2}} - \frac{1}{r_{b1}} - \frac{1}{r_{b2}} \qquad \text{(IV-26)}
$$

Let

$$
H_{\ell m} = \int \chi_\ell\, H\, \chi_m\, d\tau \qquad \text{(IV-27)}
$$

$$\Delta_{\ell m} = \int \chi_\ell \chi_m \, d\tau \tag{IV-28}$$

be matrices, where the integration is carried out over the coordinates of both electrons.

The expectation value for the electronic energy of an eigenstate corresponding to a trial wave function ψ_i is

$$W_i = \frac{\int \psi_i^* H \psi_i \, d\tau}{\int \psi_i^* \psi_i \, d\tau} \tag{IV-29}$$

where ψ_i is expanded in terms of the elementary wave functions χ_ℓ

$$\psi_i = \sum_{\ell=1}^{N} C_{i\ell} \chi_\ell \quad . \tag{IV-30}$$

Since our trial functions are entirely real, $\psi^* = \psi$. Thus we obtain

$$W_i = \frac{\sum_{\ell}^{N} \sum_{m}^{N} C_{i\ell} C_{im} H_{\ell m}}{\sum_{\ell}^{N} \sum_{m}^{N} C_{i\ell} C_{im} \Delta_{\ell m}} \tag{IV-31}$$

or

$$\sum_{\ell=1}^{N} \sum_{m=1}^{N} C_{i\ell} C_{im} \left[H_{\ell m} - W_i \Delta_{\ell m} \right] = 0 \tag{IV-32}$$

Differentiating with respect to the C_{ik}, we obtain a set of equations

$$\sum_{j}^{N} C_{ij} \left[H_{jk} - W_i \Delta_{jk} \right] = 0$$

$$k = 1, 2, 3, \ldots N \qquad \text{(IV-33)}$$

For this set of N simultaneous homogeneous linear equations to have a non-trivial solution, it is necessary that the determinant of coefficients vanish:

$$\left| H_{jk} - W_i \Delta_{jk} \right| = 0 \qquad \text{(IV-34)}$$

This equation yields a characteristic polynomial for the W_i, which are the approximate expectation values of the true energies of the first N states of the molecule. Pauling and Wilson (34) state that these N expectation values are successively upper limits to the true energies of the lowest N electronic states of the same symmetry. Our procedure is to vary the two nonlinear parameters ζ_a and ζ_b until minimum energies are obtained. Once the minimized roots have been found, we substitute them into equations (IV-29) to obtain the coefficients C_{ij} associated with each state.

The calculation of the matrix elements H_{jk} and Δ_{jk} in equation (IV-30) is described in Appendix A, where it is shown that each element is composed of certain basic one- and two-center molecular integrals. These integrals and their calculation are described in detail in Appendix B. A general procedure would be as follows:

1. A specific basis N = 2, 3, 4, ... 7 is chosen.

2. For a given internuclear separation R, specific values of the non-linear parameters ζ_a and ζ_b are selected. These values are arbitrary so long as they are non-zero and positive.

3. The elementary molecular integrals listed in Appendix B are computed and used to compute the H_{jk} and Δ_{jk} matrices according to Appendix A.

4. The eigenvalues W_i and corresponding eigenvectors C_{ij} are computed from equations (IV-30) and (IV-29).

5. We return to step 2, incrementing the parameters ζ_a and/or ζ_b for the same value of R. The new eigenvalues are tested against the old, and the set of parameters (ζ_a, ζ_b) are chosen which give the lower eigenvalues. Eventually a minimum is found.

A preliminary investigation, using a basis N = 2, revealed two features: 1) at separations R less than about $2a_o$, the sets of non-linear parameters which minimize the different eigenvalues W_i are distinct, such that no one set minimizes all W_i's; 2) at separations R greater than about $2a_o$ the sets become identical in the sense that the ground state becomes nearly independent of ζ_b, while the first excited state is reasonably dependent upon both ζ_a and ζ_b. The physical significance of this behavior (which is a continuous phenomenon) is probably that we have chosen an LCAO approximation, which generally represents the true electronic states better at large internuclear separations than small. Moreover, the second orbital wavefunction in the set (IV-25) is exact at infinite

separations. This point will be discussed in more detail later. Since our primary interest is in electronic transitions between the two lowest states, it seemed necessary that some procedure be adopted that could yield equally reliable wavefunctions for the two lowest states. The arbitrary procedure adopted was to minimize with respect to an algebraic sum of the two lowest eigenvalues.

We must be careful in the application of this procedure, for the "quasi-eigenvalue" $W = W_1 + W_2$ which we are attempting to minimize is a function of ζ_a and ζ_b and may be best visualized as a surface, as may the functions $W_1(\zeta_a, \zeta_b)$ and $W_2(\zeta_a, \zeta_b)$. The last two surfaces are generally found to be quite smooth, with a definite minimum. However, the sum surface $W(\zeta_a, \zeta_b)$ may not be smooth, or in particular, may possess more than one minimum. The nature of this surface should therefore be investigated thoroughly before the decision can be made that a true minimum has been found. A simple procedure for doing this is to use quite different starting locations of the parameters ζ_a and ζ_b, tracing the progress of the minimization and seeing if the same or different final locations are obtained.

It was found that for any basis N up to N = 5, the largest basis used, at separations exceeding R = 2 only one minimum is present. At smaller separations, two minima were found. As we are interested primarily in describing the electronic states at internuclear separations greater than $3a_0$, we consider the calculations to be significant only for $R > 3a_0$.

The optimum procedure would probably be to allow a different set of parameters ζ_a and ζ_b to be associated with each of the elementary wave functions in equations (IV-21). This would, however, give rise to a formidable minimization problem in 11 coordinates.

The preliminary investigation showed that the difference in energy between the two lowest states did not become less than the ionization potential of hydrogen until a separation R greater than about $3a_o$ was reached. As this is appreciably greater than the equilibrium separation $R = 1.4a_o$ found by Anex (14), it is felt that the minimization procedure described above is reasonable.

An additional feature of the two lowest $^1\Sigma^+$ states of HeH^+ should be noted. The excited state dissociates into a hydrogen atom and an ionized helium atom, which are both hydrogenic atoms, and hence the second elementary orbital wave function in equations (IV-25) should yield an exact electronic orbital energy for the excited state at $R = \infty$. The ground state of HeH^+ dissociates into a proton and a normal helium atom in its lowest electronic state. The first wave function in equations (IV-21) is the simplest symmetric representation of the ground state of helium. Thus the chosen wave functions best represent the true states of HeH^+ at large separations R. This is of course guaranteed by the LCAO approach, but we feel that we have improved matters by a judicious choice of the set of orbital wave function. As we have noted, electronic transitions which occur at separations R greater than about $3a_o$ are the only ones which could conceivably contribute significantly

to a stellar opacity, for when the energy difference between the two lowest states of HeH^+ exceeds the ionization potential of hydrogen, photo-ionizations from the ground state of hydrogen will dominate the stellar absorption coefficient.

Accordingly, for different values of internuclear separation R, the best energies for the two lowest states of HeH^+ were computed for different bases N = 2, 3, 4 and 5. Dipole transition integrals $\vec{Q}(R)$, defined by equations (IV-13) and (IV-14) were computed as described in Appendix B. The dipole acceleration form, equation (IV-15), was not used, as the greatest contribution to this integral comes from parts of the wavefunctions close to the nuclei, where the LCAO approximation is least valid.

Results for the two lowest $^1\Sigma^+$ states of HeH^+ as obtained by Evett (13) and Anex (14) are presented in Table I. A comparison of the best potential energies of the ground and excited states of HeH^+ obtained in this investigation at selected internuclear separations R for bases N = 2, 3, 4 and 5 is shown in Table II. The best potential energies obtained in this investigation were computed using a basis N = 5. Final results are shown in Table III.

TABLE I

Published Potential Energies of HeH^+

R (a_o)	Ground State (e^2/a_o)	Excited State (e^2/a_o)	Source
1.0	-2.903		Anex
1.2	-2.956		Evett
1.3	-2.967		Evett
1.4	-2.973	-1.802	Evett
1.4	-2.977		Anex
1.44	-2.972		Evett
1.5	-2.971		Evett
1.6	-2.967		Evett
1.8	-2.967	-2.11 (a)	Anex
2.2	-2.948	-2.24 (a)	Anex
3.272		-2.33 (a)	Anex

a) Private communication from Basil G. Anex describing preliminary results as described on page 1662 of reference (14).

TABLE II

Potential Energies of HeH^+ Obtained in this Investigation

Ground State -- $U_1(R)$ (e^2/a_o)				
R (a_o)	N = 2	N = 3	N = 4	N = 5
2.0	-2.899	-2.900	-2.905	-2.916
3.0	-2.854	-2.861	-2.869	-2.875
4.0	-2.841	-2.849	-2.857	-2.863
5.0	-2.838	-2.847	-2.855	-2.861
10.0	-2.837	-2.846	-2.854	-2.860

Excited State -- $U_2(R)$ (e^2/a_o)				
R (a_o)	N = 2	N = 3	N = 4	N = 5
2.0	-2.194	-2.271	-2.272	-2.275
3.0	-2.417	-2.442	-2.443	-2.448
4.0	-2.466	-2.487	-2.488	-2.490
5.0	-2.476	-2.496	-2.497	-2.498
10.0	-2.478	-2.498	-2.499	-2.500

TABLE III

Results for Transitions between the Two Lowest $^1\Sigma^+$ States of HeH^+

R	$U_1(R)$	$U_2(R)$	E(R)	$\lvert\vec{Q}(R)\rvert$	
	ground	excited	$U_2(R)-U_1(R)$	length	velocity
(a_0)	(e^2/a_0)	(e^2/a_0)	(e^2/a_0)	(a_0)	(a_0)
2.0	-2.9159	-2.2223	0.6936	0.938	2.20
2.5	-2.8898	-2.3301	0.5597	0.845	2.19
3.0	-2.8746	-2.4040	0.4706	0.702	2.01
3.5	-2.8667	-2.4460	0.4207	0.545	1.68
4.0	-2.8631	-2.4706	0.3925	0.399	1.29
4.5	-2.8614	-2.4844	0.3770	0.284	0.960
5.0	-2.8608	-2.4920	0.3688	0.195	0.687
6.0	-2.8604	-2.4977	0.3627	0.0867	0.320
8.0	-2.8603	-2.4994	0.3609	0.0156	0.0639
10.0	-2.8603	-2.4995	0.3608	0.0026	0.0114

Two features of these calculations should be noted. The first is the discrepancy in the dipole transition integral $\vec{Q}(R)$ as computed by the dipole-length and dipole-velocity formulas. This is probably a result of the fact that the wave functions used in this investigation properly represent the true electronic states of HeH^+ only at large separations. As Chandrasekhar (16) has pointed out, the dipole-length formula emphasizes parts of the wave functions at relatively large distances from the nuclei, the main contribution to the dipole-velocity formula comes from intermediate distances, while the dipole-acceleration formula emphasizes regions of the wave function close to the nuclei. As the wavelength region of interest corresponds to large separations R, we place greater confidence in the dipole-length formula. An additional reason for choosing the dipole-length over the dipole-velocity formula is that we wish to determine the minimum effect of absorption by this process in a stellar atmosphere. While the absorption cross-section of a radiative transition between the two lowest $^1\Sigma^+$ states of HeH^+ computed using column 5 of Table III can by no means be considered a lower limit, it will be at least the smallest cross-section we compute in this investigation.

The second feature of Table III is the minimum energy difference at infinite internuclear separation. The best values of the electronic orbital energies of these two states are taken to be -2.90372 Hartrees for the ground state after Hart and Harzberg (15), and -2.4995 Hartrees for the excited state after Evett (13). Thus the best value for the minimum energy difference is

$E(\infty) = 0.4042$ Hartrees

which places the threshold for radiative absorption from the ground state of HeH^+ to the first excited state at

$$1/\lambda = 8.866\ \mu^{-1}$$

or

$$\lambda = 1130\ \text{Å}$$

The minimum energy difference computed in Table III would place the threshold at 1260 Å . A significant amount of the monochromatic flux in the spectra of stars earlier than spectral type A O falls in this wavelength region. Placing the threshold of this reaction at 1260 Å would thus over-emphasize the importance of HeH^+. For this reason the following corrective procedure was used.

In Table III it is seen that the potential energy of the excited state goes to the exact value at large internuclear separation, a reflection of the fact that this electronic state is exactly represented at large internuclear separations by hydrogenic wave functions centered on each nucleus. The ground state potential energy, however, does not go to the exact value, but is about 1.5% too high. The potential energies of the ground state in Table III are shown in Figure 3, where are also plotted the potential energies obtained by Anex and the asymptotic potential energy at infinite separation. The potential energy shown in Table III for the ground state at a separation of 10 a_o is -2.8603 Hartrees and appears to have

approached the asymptotic value which could be obtained from our LCAO approximation. The required energy correction is -0.0434 Hartrees, and if this constant correction is applied to all the potential energies shown in Table III for the ground state, the corrected potential energy curve joins smoothly with the curve of Anex, and is indicated by the dashed line in Figure 3. We adopt the dashed curve as the best potential energy curve for the $^1\Sigma^+$ ground state of HeH^+. Other corrective procedures, such as fitting a simple empirical formula to the upper curve in Figure 3 and then adjusting it to join smoothly with Anex's data and the asymptotic energy, were considered; the elementary correction described, however, seemed best, for it preserves a maximum of the character of the calculations of this investigation.

We refer to equation (IV-16) for the absorption coefficient and write it in the form

$$k(\nu,T) = \frac{32\pi^4 e^2}{3hc}\, g\, G_2 \left|\frac{\nu}{d\nu/dR}\right| R^2 \left|\vec{Q}(R)\right|^2$$

$$\times\ e^{-\frac{U_2(R)}{kT}} \left[e^{h\nu/kT} - 1\right] N_{He}\, N_{H^+} \qquad \text{(IV-35)}$$

where $U_2(R)$ is the potential energy of the excited state shown in Table III, relative to a zero point at $R = \infty$. When the potential energy curve of the ground state is corrected, the factor $\left|\frac{\nu}{d\nu/dR}\right|$ computed from

$$h\nu = \frac{e^2}{a_o} E(R) \qquad \text{(IV-36)}$$

will also be affected.

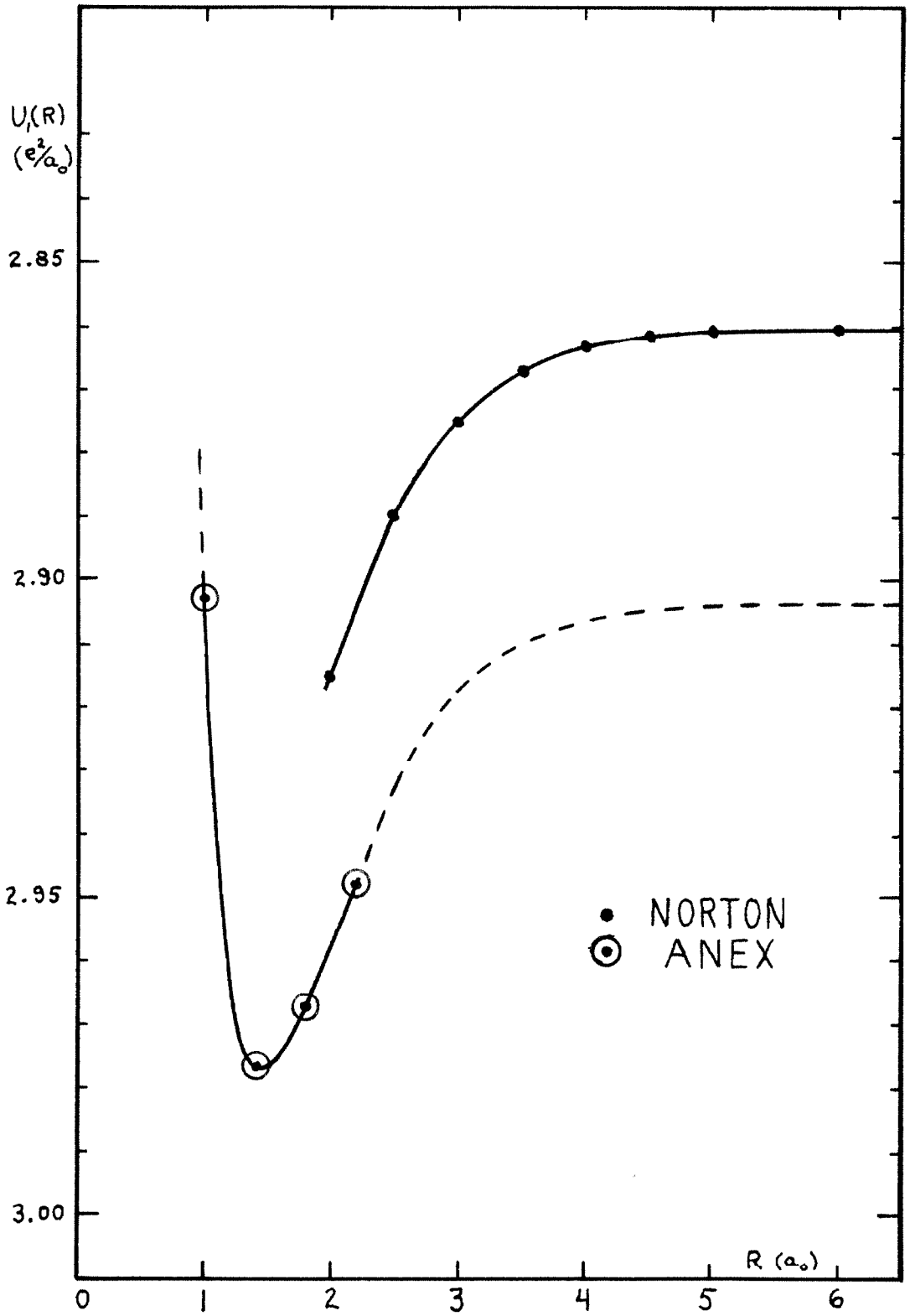

Figure 3. Correction of the Ground State Potential Energy Curve

We assume that all other factors in equation (IV-35) will be unaffected and show the data that enter into equation (IV-35), after correction of the ground state potential energy, in Table IV.

TABLE IV

Corrected Data

R (a_o)	$1/\lambda$ (μ^{-1})	$U_2(R)$ (e^2/a_o)	$\left\lvert \frac{\vec{J}}{dV/dR} \right\rvert$ (a_o)	$\lvert \vec{Q}(R) \rvert$ (a_o)
2.0	16.166	0.2772	1.8	0.938
2.5	13.227	0.1694	2.4	0.845
3.0	11.275	0.0955	3.6	0.702
3.5	10.178	0.0535	6.0	0.545
4.0	9.564	0.0289	10.2	0.399
4.5	9.222	0.0151	19	0.284
5.0	9.040	0.0075	35	0.195
6.0	8.908	0.0018	125	0.0867
8.0	8.867	0.0001	2600	0.0156
10.0	8.866	0.0000	73700	0.0026

The orbital degeneracy factors G_1 and G_2, defined by Mulliken (8), are unity for Σ states. The ratio of statistical weights of the two lowest $^1\Sigma^+$ states of HeH^+ is thus unity. The factor g in equation (IV-35) represents the statistical probability that the atoms will approach each other along a trajectory corresponding to the upper $^1\Sigma^+$ state of HeH^+. Bates (6) assumes that g is given by the ratio of the statistical weight of the upper state to the sum of statistical weights of both states. g thus has the value 1/2.

In equation (IV-35) there is a numerical derivative of a quantity which asymptotically approaches a constant as R increases. The derivative thus vanishes, and the numerical accuracy of this derivative at large R must be investigated. Numerical derivatives were computed by 3 and 4 point Lagrangian formulas given by Kopal (31) and indicated that two significant figures were preserved out to internuclear separations of about $5a_o$. Beyond this R, the derivatives lose all significance. An attempt was made to determine the asymptotic derivative of the energy difference E(R) from the basis wave functions. This failed,however, because it was necessary to evaluate the derivative of an exchange integral (see Appendix B). The asymptotic behavior of the ground state, however, was found to be

$$U_1(R) \underset{R \to \infty}{\sim} \exp(-2 \zeta_a R) \qquad \text{(IV-37)}$$

where ζ_a is the variation parameter centered on the helium nucleus and has an approximate value of 1.7 at large R. The asymptotic behavior of all terms which contribute to the excited state potential

energy curve, except the exchange term, was found to be

$$U_2(R) \underset{R\to\infty}{\sim} \exp(-2\gamma_b R)$$

where $\gamma_b = 1.0$ at large R. The asymptotic form for the dipole length transition integral is easily shown to be

$$|\vec{Q}(R)| \underset{R\to\infty}{\sim} R\, e^{-R}$$

The dominant asymptotic form of the various quantities thus appear to be exp(-2R), and this form was adopted, fitted to the derivatives computed out to $R = 5a_o$ and used to extend the calculations to $R = 10a_o$.

Of interest is a comparison of the reaction rate coefficient $\gamma(R, T)$ for reaction (IV-9) with rate coefficients of other reactions in a stellar atmosphere. In particular, we would like to have a comparison with the rate coefficient for recombination of atomic hydrogen

$$H^+ + e^- \rightarrow H(nS) + h\nu \qquad \text{(IV-38)}$$

and helium

$$He^+ + e^- \rightarrow He(nS) + h\nu \,. \qquad \text{(IV-39)}$$

From equations (IV-7), (IV-11) and (IV-12) we have

$$\gamma(R,T)\,dR = \frac{256\,\pi^5 e^8 a_o^2}{3\,h^4 c^3}\, g\, G_1\, E(R)^3 \times R^2\, |\vec{Q}(R)|^2 \exp\left\{-\frac{e^2 U_2(R)}{a_o kT}\right\} dR$$

$$= 2.0\times 10^{-13}\, E(R)^3\, R^2\, |\vec{Q}(R)|^2 \exp\left\{-\frac{e^2 U_2(R)}{a_o kT}\right\} dR \quad cm^3/sec \qquad \text{(IV-40)}$$

where the units of the various quantities are as indicated in Table III. What is of interest for comparison purposes is the integral of equation (IV-40) over all values of R such that radiative association can occur. We integrate over the limits zero to infinity, introducing an external factor of 2 to cover both the approach and recession halves of the trajectory. Results for different temperatures are shown in Table V. The recombination rate coefficients for hydrogen (to all nS levels) are taken from Bates and Dalgarno (37) and the recombination rate coefficients for helium, again to all nS levels, are taken from Arthurs and Hyslop (11). Also shown are reaction rate coefficients for the sum of free-bound and free-free reactions of H_2^+

$$H + H^+ \rightarrow H_2^+(2p\sigma) \rightarrow H_2^+(1s\sigma) + h\nu$$

$$(H + H^+)(2p\sigma) \rightarrow (H + H^+)(1s\sigma) + h\nu$$

taken from Bates (6), and reaction rate coefficients, free-bound plus free-free, of HeH^{2+}

$$(He^{2+} + H)(2p\sigma) \rightarrow (He^+ + H^+)(1s\sigma) + h\nu$$

taken from Arthurs and Hyslop (11).

TABLE V

Comparison of Rate Coefficients - 10^{-13} cm^3/sec

T (°K)	HeH^+	H	He	HeH^{2+}	H_2^+
10000	0.79	4.2	4.3	1.55	0.004
16000	1.2	2.9	3	1.52	0.009
20000	1.4	2.4	2.7	1.52	0.012

The reaction rate coefficients shown in Table V for HeH^+ and HeH^{2+} are surprisingly high in comparison to the recombination rate coefficients of hydrogen and helium, when we remember that the latter depend essentially upon electron velocities, while the coefficients of the former are determined by nuclear velocities. It follow that the absorption cross sections of HeH^+ and HeH^{2+} are much greater than the photo-ionization cross sections of hydrogen or helium atoms.

V. MODEL STELLAR ATMOSPHERES

A. General Discussion

A comprehensive summary of the basic principles governing the physical processes in a stellar atmosphere has been published by Münch (17), who gives an extensive bibliography on the subject. We follow established principles wherever possible and hence will not discuss in detail the general theory of a model stellar atmosphere. What will be presented in this chapter are the specific computational methods employed and the basic assumptions about these models.

We assume the conditions of hydrostatic and radiative equilibrium. Continuous opacity sources only are considered; absorption line effects are neglected. These models are non-gray in the sense that both thermal and isotropic scattering processes are taken into account; the Milne equation is solved for the monochromatic source function. Local thermodynamic equilibrium is postulated in order that a local temperature may be defined.

B. Computational Methods

1. Chemical composition

The convention will be adopted throughout that chemical composition means the relative abundance by numbers of atoms of a particular chemical element. Let A_i denote this relative abundance; the A_i's will be normalized such that

$$\sum_i A_i = 1 \, . \tag{V-1}$$

2. Ionization and excitation equilibria

The ratio of the number of atoms of the i^{th} element in the $(j + 1)^{st}$ ionization state to the number of atoms in the j^{th} state is given by the Saha equation

$$\frac{N_{i,j+1}}{N_{i,j}} = \frac{(2\pi m)^{3/2} (kT)^{5/2}}{h^3 P_e} \left[2 \frac{B_{i,j+1}}{B_{i,j}} \right] \exp\left(- \frac{I_{i,j}}{kT} \right) \qquad \text{(V-2)}$$

where P_e = electron pressure in dyne/cm^2

I_{ij} = ionization potential, in ev, from j^{th} to $(j + 1)^{st}$ state

$B_{ij}(P_e, T)$ = partition function of element i in state j.

Values for all physical constants are adopted from Cohen, Crowe and Dumond (18). Numerically, equation (V-2) may be written

$$x_{ij} = \frac{N_{i,j+1}}{N_{i,j}} = \frac{1.20222 \times 10^9}{P_e \, \theta^{5/2}} \frac{B_{i,j+1}}{B_{i,j}} \, 10^{-\theta I_{ij}} \qquad \text{(V-3)}$$

where

$$\theta = \frac{5040.17}{T} \quad .$$

Ionizations up to and including the second state are computed for each element. The total number of atoms per cm^3 of a particular element is the sum of the atoms per cm^3 of the atom in ionization states:

$$N_i = N_{i0} + N_{i1} + N_{i2} \tag{V-4}$$

$$= N_{i0}\left[1 + \frac{N_{i1}}{N_{i0}} + \frac{N_{i2}}{N_{i1}}\frac{N_{i1}}{N_{i0}}\right] \tag{V-5}$$

$$= N_{i0}\left[1 + \chi_{i1} + \chi_{i1}\chi_{i2}\right] . \tag{V-6}$$

Hence the fractions of atoms per cm^3 of an element in various ionization states are given by the following ratios:

$$\pi_{i0} = \frac{N_{i0}}{N_i} = \left[1 + \chi_{i1} + \chi_{i1}\chi_{i2}\right]^{-1} \tag{V-7}$$

$$\pi_{i1} = \frac{N_{i1}}{N_i} = \chi_{i1} \cdot \left[1 + \chi_{i1} + \chi_{i1}\chi_{i2}\right]^{-1} \tag{V-8}$$

$$\pi_{i2} = \frac{N_{i2}}{N_i} = \chi_{i1}\chi_{i2} \cdot \left[1 + \chi_{i1} + \chi_{i1}\chi_{i2}\right]^{-1} \tag{V-9}$$

3. The relation between gas pressure and electron pressure

From the equation of state of an ideal gas and the law of partial pressures, we have

$$P_g = P_a + P_e \tag{V-10}$$

$$P_a = N_a kT \tag{V-11}$$

$$P_e = N_e kT \tag{V-12}$$

where

P_g = gas pressure, $dyne/cm^2$

P_a = pressure from atoms, $dyne/cm^2$

P_e = electron pressure, dyne/cm^2

N_a = number of atoms per cm^3 of all elements, in all ionization states

N_e = number of electrons per cm^3

Each singly ionized atom contributes one electron, each doubly ionized atom two electrons etc., so summing over chemical elements and ionization states up to and including the second we have

$$N_e = N_a \sum_i A_i \left(r_{i1} + 2\, r_{i2} \right). \qquad \text{(V-13)}$$

From (V-10), (V-11) and (V-12) we have

$$\frac{P_g}{P_e} = \frac{N_a + N_e}{N_e} = \frac{1 + N_e/N_a}{N_e/N_a} \,. \qquad \text{(V-14)}$$

We may obtain N_e/N_a from equation (V-14), hence we may establish a relation for P_g as

$$P_g = P_e \cdot \left[\frac{1 + \sum_i A_i \left(r_{i1} + 2\, r_{i2} \right)}{\sum_i A_i \left(r_{i1} + 2\, r_{i2} \right)} \right] \qquad \text{(V-15)}$$

or in functional form:

$$P_g = P_g\left(A_i ;\ P_e ,\ T \right) . \qquad \text{(V-16)}$$

Hence it is possible to invert this relationship to obtain

$$P_e = P_e\left(A_i ;\ P_g ,\ T \right) , \qquad \text{(V-17)}$$

however, the inversion is non-analytic through the dependence of the r_{ij}'s and B_{ij}'s on P_e. For a given P_g, T we may obtain P_e through inverse interpolation in a table previously constructed from equation (V-16). It should be noted here that having P_e and T we may compute the mass density of the gas

$$\rho = N_e m_e + N_a \sum_i A_i m_i \qquad \text{(V-18)}$$

$$= \left[m_e + \frac{N_a}{N_e} \sum_i A_i m_i \right] \frac{P_e}{kT} \qquad \text{(V-19)}$$

4. Continuous opacity sources

The sources of continuous absorption of radiative energy in a stellar atmosphere are summarized below

a.	Neutral hydrogen	H I
b.	Neutral helium	He I
c.	Ionized helium	He II
d.	The hydrogen molecule ion	H_2^+
e.	The negative hydrogen ion	H^-
f.	The hydrogen molecule	H_2
g.	Singly ionized helium hydride	HeH^+
h.	Thomson scattering by free electrons	σ
i.	Rayleigh scattering	

Since the principle interest in this thesis is in stars of spectral type earlier than A O, sources (f) and (i) are not included in the computer program at the present time. Source (g) has been discussed at length in Chapter IV, and the remaining sources will be discussed here. The derivation of the atomic absorption coefficients are contained in Appendix C. What are presented here are working equations as used in the computer program.

The continuous atomic absorption coefficient of hydrogen, including both bound-free and free-free transitions and expressed per H I atom in the ground state, is given by equation (C-18) in Appendix C. To obtain the mass absorption coefficient, multiply by $N_{H,1}$, the number per cm^3 of H I atoms in the ground state and divide by the mass density ρ.

The number per cm^3 of H I atoms (all excitation states) plus protons is

$$N_H + N_i = A_H N_a \qquad \text{(V-20)}$$

where A_H is the relative abundance of hydrogen by numbers of atoms, and N_a is the number per cm^3 of all atoms in all ionization and excitation states. From the Boltzmann equation, we compute the ratio of $N_{H,1}$ to N_H as

$$\frac{N_{H,1}}{N_H} = \frac{g_1}{B_H} = \frac{2}{B_H} \qquad \text{(V-21)}$$

where $B_H = B_H(Pe, T)$ is the partition function of hydrogen. From equation (V-7) we have

$$\frac{N_H}{N_H + N_i} = \frac{1}{1 + X_H} \tag{V-22}$$

where $X_H = N_i/N_H$ is computed from the Saha equation, equation (V-3). We thus have

$$N_{H,1} = \frac{2}{B_H} \frac{A_H}{1 + X_H} N_a \tag{V-23}$$

We use the definition of the mass density ρ as given in equation (V-18) and neglect the mass of the electron:

$$\rho = N_a \sum_i A_i m_i \tag{V-24}$$

The quantity

$$AM = \sum_i A_i m_i \tag{V-25}$$

depends only upon the chemical composition of the model, hence is treated as a constant in the program. We express the masses of the chemical elements in terms of atomic weights, and thus absorb a factor of one atomic mass unit into the constant which appears in the expressions for each of the atomic absorption coefficients. This helps to avoid the possibility of encountering numbers which exceed the numerical range allowed by the computer. We obtain finally the following program equations for the monochromatic mass absorption coefficient of hydrogen.

$$k_1 = \frac{\lambda^3}{e^{a_1}} \left[\sum_{n^2 > \frac{\lambda}{\lambda_1}}^{15} \frac{e^{a_n}}{n^3} g_I(\lambda, n) + \frac{1.10\left(e^{a_{16}} - 1\right) + g_{II}(\lambda, T)}{2 a_1} \right] \qquad \text{(V-27)}$$

$$K(\nu, T)_{H\,I} = 1.25935 \times 10^{10} \frac{A_H}{B_H\, AM} \frac{k_1}{1 + X_H} \left(1 - e^{-\frac{hc}{R\lambda T}}\right) \qquad \text{(V-28)}$$

$$a_n = 31.30932 \frac{\theta}{n^2} \qquad \theta = \frac{5040.17}{T}$$

where λ is expressed in microns, $g_I(\nu, n)$ and $g_{II}(\nu, T)$ are the bound-free and free-free Gaunt factors respectively and the factor $\left(1 - e^{-\frac{hc}{R\lambda T}}\right)$ is included to allow for stimulated transitions.

The continuous atomic absorption coefficient of neutral helium, is given in Appendix C by equation (C-36). We convert this to a mass absorption coefficient by multiplying by the number of He I atoms in the ground state $N_{He,\,1}$ and dividing by the density ρ. We proceed in the same manner as for hydrogen, except that in this case we have three possible ionization states instead of two. The result is

$$\frac{N_{He,1}}{\rho} = \frac{A_{He}}{B_{He}\, AM} \frac{1}{1 + X_2 + X_2 X_3} \qquad \text{(V-29)}$$

where A_{He} is the abundance by number of helium, B_{He} is the partition function of neutral helium, and X_2 and X_3 are ionization ratios defined by

$$X_2 = \frac{N_{He^+}}{N_{He}}$$

$$X_3 = \frac{N_{He^{2+}}}{N_{He^+}}$$

and are computed through the Saha equation, equation (V-3).

The continuous atomic absorption coefficient of ionized helium, given in Appendix C by equation (C-22), is converted to a mass absorption coefficient by multiplying by the number of He^+ atoms in the ground state and dividing by the density ρ. Specifically, we obtain

$$\frac{N_{He^+,1}}{\rho} = \frac{A_{He}}{B_{He^+} AM} \frac{X_2}{1 + X_2 + X_2 X_3} \qquad \text{(V-30)}$$

where B_{He^+} is the partition function of singly ionized helium. We of course include the stimulated emission factor for both neutral and ionized helium.

The continuous absorption coefficient of the hydrogen molecule ion, H_2^+, has been calculated by Bates (6, 7, 19), and his semi-classical procedure has been described in Chapter IV. Specifically, we write

$$k_4 = \left| \frac{\nu}{d\nu/dR} \right| R^2 \left| \vec{Q}(R) \right|^2 \times \left[e^{-\frac{U_1(R)}{kT}} - e^{-\frac{U_2(R)}{kT}} \right] \qquad \text{(V-31)}$$

$$K(\nu,T)_{H_2^+} = 5.007 \times 10^{-42} g G_1 k_4 \frac{N_H N_{H^+}}{\rho} \quad cm^2/gm \qquad \text{(V-32)}$$

the factor $\frac{N_H N_{H^+}}{\rho}$ may be written

$$\frac{N_H N_{H^+}}{\rho} = \pi_H (1 - \pi_H) \left(\frac{A_H}{AM} \right)^2 \rho \qquad \text{(V-33)}$$

where π_H is the fraction of neutral hydrogen, defined in equation (V-7). And since we are defining AM in terms of atomic weights, we absorb a factor of one atomic mass unit squared into the constant in equation (V-31). The quantities appearing in the right hand side of equation (V-31) are given in Table VI , where in column 7 is listed the quantity

$$Y = R^2 \left| \frac{v}{dv/dR} \right| \left| \vec{Q}(R) \right|^2 \qquad \text{(V-34)}$$

The orbital degeneracy factor G_1 appearing in equation (V-32) has the value 1 for the $1s\sigma - 2p\sigma$ transition of H_2^+, and the statistical weight ratio g has the value 1/2. Thus we may write for the continuous mass absorption coefficient of H_2^+:

$$K(\nu, T)_{H_2^+} = 9.088 \times 10^5 \; Y \left(e^{-\frac{u_1}{RT}} - e^{-\frac{u_2}{RT}} \right)$$

$$\times \; \pi_H (1 - \pi_H) \rho \left(\frac{A_H}{AM} \right)^2 \quad \text{cm}^2/\text{gm} . \qquad \text{(V-35)}$$

This expression includes the stimulated emission factor.

TABLE VI

R (a_o)	$1/\lambda$ (μ^{-1})	$\left\|\frac{\partial}{\partial v/\partial R}\right\|$ (a_o)	$\|\vec{Q}(R)\|$ (a_o)	U1(R) (e^2/a_o)	U2(R) (e^2/a_o)	Y (a_o^5)
0.0	32.9033	6.987	0.3728	∞	∞	0.0
0.2	31.2807	2.716	0.3972	3.57130	4.99733	0.0171
0.4	28.2967	1.851	0.4511	1.19922	2.48921	0.0603
0.6	25.1644	1.649	0.5203	0.49516	1.64236	0.1607
0.8	22.1929	1.555	0.5966	0.19553	1.20726	0.3543
1.0	19.4561	1.490	0.6745	0.04822	0.93519	0.6781
1.2	16.9714	1.441	0.7525	-0.02897	0.74472	1.175
1.4	14.7448	1.405	0.8305	-0.06998	0.60221	1.899
1.6	12.7736	1.381	0.9035	-0.09093	0.49140	2.887
1.8	11.0463	1.368	0.9779	-0.10025	0.40333	4.239
2.0	9.54392	1.362	1.0487	-0.10263	0.33247	5.992
2.2	8.24380	1.361	1.1213	-0.10083	0.27499	8.282
2.4	7.12104	1.362	1.1968	-0.09654	0.22809	11.24
2.6	6.15280	1.364	1.2750	-0.09083	0.18966	14.99
2.8	5.31684	1.365	1.3557	-0.08435	0.15803	19.67
3.0	4.59472	1.365	1.4386	-0.07756	0.13191	25.43
3.2	3.97077	1.365	1.5260	-0.07073	0.11029	32.54
3.4	3.43082	1.361	1.6122	-0.06408	0.09233	40.90
3.6	2.96272	1.357	1.7023	-0.05771	0.07736	50.95
3.8	2.55735	1.350	1.7934	-0.05170	0.06489	62.71
4.0	2.20518	1.341	1.8843	-0.04608	0.05445	76.20
4.2	1.89973	1.332	1.9785	-0.04090	0.04571	92.00
4.4	1.63485	1.322	2.0702	-0.03615	0.03838	109.7
4.6	1.40519	1.311	2.1696	-0.03183	0.03223	130.6
4.8	1.20612	1.299	2.2643	-0.02793	0.02706	153.5
5.0	1.03382	1.281	2.3600	-0.02442	0.02271	178.4
5.5	0.698756	1.234	2.6040	-0.01723	0.01462	253.2
6.0	0.467665	1.205	2.8564	-0.01196	0.00936	353.8
6.5	0.310497	1.180	3.1036	-0.00821	0.00594	480.1
7.0	0.204439	1.157	3.3517	-0.00559	0.00373	636.9
7.5	0.133807	1.139	3.6018	-0.00380	0.00230	831.3
8.0	0.086974	1.122	3.8509	-0.00257	0.00140	1065.
8.5	0.056265	1.108	4.1039	-0.00174	0.00082	1348.
9.0	0.036194	1.092	4.3589	-0.00119	0.00046	1888.

Gingerich (20) has given a polynomial approximation for the absorption cross-section of H^-, including the stimulated emission factor, after the values computed by Chandrasekhar and Breen (21). This cross-section is expressed per neutral hydrogen atom per unit electron pressure. In their calculations, Chandrasekhar and Breen took the partition function B_H of hydrogen to be 2; hence we must multiply their values by the ratio $2/B_H$. Remembering our definition of AM in terms of atomic weights, we multiply Gingerich's expression by Avogadro's number. We have then to multiply this cross-section by the number of hydrogen atoms per cm^3 and divide by the density. We obtain

$$\frac{N_H}{\rho} = \frac{\pi_H A_H}{AM} \quad . \tag{V-36}$$

We compute, with λ in microns and $\theta = 5040.17/T$

$$A = -3.00633 - 7.53475\lambda + 8.74112\lambda^2 - 3.90694\lambda^3$$

$$B = -14.3126 + 105.678\lambda - 148.916\lambda^2 + 92.6638\lambda^3 - 21.2049\lambda^4$$

$$C = 26.9706 - 139.117\lambda + 199.280\lambda^2 - 124.719\lambda^3 + 28.6145\lambda^4$$

$$D = -15.3323 + 74.2823\lambda - 107.612\lambda^2 + 67.6839\lambda^3 - 15.5738\lambda^4$$

$$E = 2.9937 - 14.1345\lambda + 20.5901\lambda^2 - 13.0050\lambda^3 + 3.000878\lambda^4$$

$$T1 = -3.65704 + 10.4608\theta - 5.45925\theta^2 + 1.9351\theta^3 - 0.278743\theta^4$$

$$T2 = 0.432655 + 0.045334\theta - 0.0147151\theta^2$$

$$T3 = 0.0379403 + 0.326858\theta - 0.354844\theta^2$$

$$T4 = -0.410321 + 6.71408\theta - 0.975664\theta^2 + 0.186518\theta^3$$

and

$$k_\lambda = k_b + k_f \tag{V-37}$$

where for $\lambda < 0.65\,\mu$

$$k_b + k_f = 6.02486 \times 10^{-3} \exp\left[T1 - \frac{T2}{\lambda}\right] \tag{V-38}$$

and for $0.65 < \lambda < 1.65\,\mu$

$$k_b = 6.02486 \times 10^{-3} \exp\left[A + B\theta + C\theta^2 + D\theta^3 + E\theta^4\right] \tag{V-39}$$

$$k_f = 6.02486 \times 10^{-4} \left[\frac{T4}{\lambda^2} + \frac{T3}{\lambda}\right] \tag{V-40}$$

and for $\lambda > 1.65\,\mu$, k_f is given by equation (V 40) and

$$k_b = 0 \tag{V-41}$$

We then have

$$K(\nu, T)_{H^-} = \frac{2 n_H A_H}{B_H AM} P_e k_\lambda . \tag{V-42}$$

The cross-section for Thomson scattering by free electrons is given by

$$\sigma_T = \frac{8\pi e^4}{3 m^2 c^4} = 6.65208 \times 10^{-25} \text{ cm}^2 \tag{V-43}$$

To convert this to a scattering coefficient per unit mass, multiply by the number of electrons per cm^3 and divide by the density. Thus

$$\sigma = 6.65208 \times 10^{-25} \frac{N_e}{\rho} \quad cm^2/gm \tag{V-44}$$

or in terms of the ratio of gas pressure to electron pressure

$$\sigma = \frac{0.400778}{AM\left(\frac{P_g}{P_e} - 1\right)} \tag{V-45}$$

The continuous absorption coefficients of HeH^+ was described in Chapter IV. We form the total continuous monochromatic mass absorption coefficient by summing over the different sources:

$$K_\nu(T) = K(\nu,T)_H + K(\nu,T)_{He} + K(\nu,T)_{He^+} + K(\nu,T)_{H_2^+} + K(\nu,T)_{H^-} + K(\nu,T)_{HeH^+} \tag{V-46}$$

The total monochromatic opacity is

$$K'_\nu(T) = K_\nu(T) + \sigma \tag{V-47}$$

5. The Equation of Hydrostatic Equilibrium

Assuming a plane-parallel stratified atmosphere with the z-direction pointing outwards along the direction of gravity, we have, in a state of mechanical equilibrium:

$$\frac{dP}{dz} = -g\rho \tag{V-48}$$

where P is the total pressure, gas plus radiation.

We introduce the characteristic optical depth, defined by

$$d\tau = -(\kappa + \sigma)\rho\, dz \qquad \text{(V-49)}$$

Here κ is a mass absorption coefficient defined at some particular frequency. For hot stars an opacity defined at λ 4000 Å has been found suitable; for cooler stars one should define the characteristic opacity at a longer wavelength.

Hereafter, when we mean to specify the characteristic opacity and optical depth, we shall write κ and τ respectively. κ_ν and τ_ν will denote for a different frequency the monochromatic mass absorption coefficient and associated optical depth. The total opacity is the sum of the mass absorption coefficient and the mass scattering coefficient. Thus equation (V-48) becomes

$$\frac{dP_g}{d\tau} = \frac{g}{\kappa + \sigma} - \frac{dP_R}{d\tau} \qquad \text{(V-50)}$$

Under an assumed temperature distribution $T(\tau)$ equation (V-50) is integrated numerically, with the physical boundary condition

$$P_g = 0 \qquad \text{at} \qquad \tau = 0 \qquad \text{(V-51)}$$

This physical boundary condition is an unsatisfactory condition to impose, because the ionization equilibria and other relations are not defined at zero pressure. Hence it is necessary to adopt a gas pressure at some non-vanishing optical depth.

The procedure followed in this computer program is to assume that at sufficiently small optical depths, the mass scattering coefficient σ dominates over the mass absorption coefficient κ. The gas pressure gradient is then expected to be reasonably constant, and a linear dependence of $P_{g_0}(\tau)$ can be assumed. We assume an arbitrary trial electron pressure, for example 10^{-2} dyne/cm^2. With this Pe and boundary T(o) from the assumed T(τ) distribution, we compute κ and τ . We compute from (V-50) a value for the gas pressure gradient $\left(\frac{dP_g}{d\tau}\right)_0$. The gas pressure at a small optical depth $\Delta\tau$ is

$$P_{g_0}(\Delta\tau) = \left(\frac{dP_g}{d\tau}\right)_0 \Delta\tau \qquad \text{(V-52)}$$

The gas pressure at $\frac{\Delta\tau}{2}$ is

$$P_{g_0}\left(\frac{\Delta\tau}{2}\right) = \frac{1}{2} P_{g_0}(\tau) \qquad \text{(V-53)}$$

and the temperature $T(\frac{\Delta\tau}{2})$ and radiation pressure gradient $\left(\frac{dP_R}{d\tau}\right)_{\Delta\tau/2}$ are found by interpolation in the assumed distributions. From the gas pressure tables we then find $P_e(\frac{\Delta\tau}{2})$. We compute κ, σ and $\frac{dP_g}{d\tau}$ for $\frac{\Delta\tau}{2}$ and then obtain an improved value of $P_g(\Delta\tau)$. This process thus becomes iterative, and has proved to be quickly convergent; most important, it provides a systematic method of defining the boundary conditions from model to model.

Once the starting values have been computed, integration of equation (V-50) is performed by standard procedures. At any depth τ_j values of the independent variable and derivatives up to the

fourth are used to predict values at the next integration step. Third-order Lagrangian interpolation is used to obtain current values of electron pressure, temperature and radiation pressure gradient; the absorption and scattering coefficients are computed. Round-off and truncation errors can be kept below a specified amount by the numerical integrator. A typical computing time on an IBM 7094 computer for integration to an optical depth of 250 is 40^{sec}.

6. Monochromatic Optical Depths

After the equation of hydrostatic equilibrium has been integrated, a table of monochromatic mass absorption coefficients $\kappa_\nu(\tau)$ is computed for all optical depths and frequencies. Monochromatic optical depths $\tau_\nu(\tau)$ are defined in terms of the characteristic optical depth τ by

$$\tau_\nu(\tau) = \int_0^\tau \frac{\kappa_\nu(\tau) + \sigma(\tau)}{\kappa(\tau) + \sigma(\tau)} \, d\tau \quad . \tag{V-54}$$

The characteristic τ -scale is chosen such that integration of equation (V-54) can be done by Simson's rule, which is quite efficient, yet is accurate to third order. Typical computing times on an IBM 7094 computer for 40 optical depths and 26 frequencies are 30 seconds for the $\kappa_\nu(\tau)$ table and 10 seconds for the $\tau_\nu(\tau)$ table.

7. The Equation of Radiative Transfer

We assume a semi-infinite, plane-parallel atmosphere; we may then write the equation of radiative transfer for a ray of ν-radiation in the form

$$\mu \frac{\partial I_\nu(\tau_\nu, \mu)}{\partial \tau_\nu} = I_\nu(\tau_\nu, \mu) - S_\nu(\tau_\nu) \tag{V-55}$$

where μ is the cosine of the angle between the ray and the outward normal to the atmosphere. $I_\nu(\tau_\nu, \mu)$ is the specific intensity of the ray, or the amount of radiative energy crossing a unit area at a monochromatic optical depth τ_ν per second per unit solid angle in the direction μ. $S_\nu(\tau_\nu)$ is the source function, defined as the ratio of the coefficient of spontaneous emission to the coefficient of absorption. In strict thermodynamic equilibrium, $S_\nu(\tau_\nu)$ is the Planck function $B_\nu(\tau)$. As a boundary condition, we require that at $\tau_\nu = 0$, the radiation field is all directed outwards:

$$I_\nu(0, \mu) = 0 \qquad \text{for } \mu < 0 . \tag{V-56}$$

We note that a formal solution to equation (V-55) exists:

$$I_\nu(\tau_\nu, \mu<0) = -\int_0^{\tau_\nu} S_\nu(x_\nu)\, e^{\frac{\tau_\nu - x_\nu}{\mu}} \frac{dx_\nu}{\mu} \tag{V-57}$$

$$I_\nu(\tau_\nu, \mu>0) = \int_{\tau_\nu}^{\infty} S_\nu(x_\nu)\, e^{-\frac{x_\nu - \tau_\nu}{\mu}} \frac{dx_\nu}{\mu} . \tag{V-58}$$

Following Eddington (12) we define the mean intensity

$$J_\nu(\tau_\nu) = \frac{1}{2} \int_{-1}^{+1} I_\nu(\tau_\nu, \mu)\, d\mu \tag{V-59}$$

and the monochromatic flux

$$\pi F_\nu(\tau_\nu) = 2\pi \int_{-1}^{+1} I_\nu(\tau_\nu, \mu)\, \mu\, d\mu . \tag{V-60}$$

We introduce the formal solution into equations (V-59) and (V-60) and obtain

$$J_\nu(\tau_\nu) = \frac{1}{2}\int_{\tau_\nu}^{\infty} S_\nu(x_\nu)\, E_1(x_\nu - \tau_\nu)\, dx_\nu + \frac{1}{2}\int_0^{\tau_\nu} S_\nu(x_\nu)\, E_1(\tau_\nu - x_\nu)\, dx_\nu \qquad \text{(V-61)}$$

$$\pi F_\nu(\tau_\nu) = 2\pi\int_{\tau_\nu}^{\infty} S_\nu(x_\nu)\, E_2(x_\nu - \tau_\nu)\, dx_\nu - 2\pi\int_0^{\tau_\nu} S_\nu(x_\nu)\, E_2(\tau_\nu - x_\nu)\, dx_\nu \qquad \text{(V-62)}$$

where $E_n(X)$ is the n^{th} exponential integral, defined as

$$E_n(x) = \int_1^{\infty} \frac{e^{-xt}}{t^n}\, dt\ . \qquad \text{(V-63)}$$

We define the general Λ -operator to be

$$\Lambda_\tau^{(n)}(f) = \int_\tau^{\infty} f(x)\, E_n(x-\tau)\, dx - (-1)^n\int_0^{\tau} f(x)\, E_n(\tau - x)\, dx\ . \qquad \text{(V-64)}$$

Equations (V-61) and (V-62) are then rewritten

$$J_\nu(\tau_\nu) = \frac{1}{2}\,\Lambda_{\tau_\nu}^{(1)}(S_\nu) \qquad \text{(V-65)}$$

$$\pi F_\nu(\tau_\nu) = 2\pi\,\Lambda_{\tau_\nu}^{(2)}(S_\nu) \qquad \text{(V-66)}$$

In the previous section, the monochromatic optical depth τ_ν was defined in terms of the characteristic optical depth τ by

$$d\tau_\nu = \frac{\kappa_\nu(\tau) + \sigma(\tau)}{\kappa(\tau) + \sigma(\tau)} \, d\tau \, . \qquad \text{(V-67)}$$

We define

$$\eta_\nu(\tau) = \frac{d\tau_\nu}{d\tau} = \frac{\kappa_\nu(\tau) + \sigma(\tau)}{\kappa(\tau) + \sigma(\tau)} \, . \qquad \text{(V-68)}$$

The equation of transfer, equation (V-55), may then be written in terms of the characteristic optical depth τ :

$$\mu \frac{\partial I_\nu(\tau,\mu)}{\partial \tau} = \eta_\nu(\tau) \left[I_\nu(\tau,\mu) - S_\nu(\tau) \right] \qquad \text{(V-69)}$$

We must now investigate the form of the monochromatic source function $S_\nu(\tau)$. We postulate that both continuous absorption and scattering occur, and that free electrons dominate the scattering processes because of their high velocities. Moreover, we assume the radiation field to be unpolarized; the cross section of a free electron for scattering is then given by Thomson's classical formula, equation (V-43). We confine our attention to a cylinder of unit cross-section and length ds, located at a height z and oriented at an angle θ to the outward direction. The loss of beam intensity in passing through this cylinder will be

$$-(\kappa_\nu + \sigma) \rho \, I_\nu(\gamma,\theta) \, da \, d\omega \qquad \text{(V-70)}$$

where κ_ν and σ denote the mass absorption and scattering coefficients,

ρ is the mass density and $d\omega$ is a unit solid angle about the direction θ. The energy returned to the beam will consist of a contribution from thermal emission

$$j_\nu \rho \, ds \, \frac{d\omega}{4\pi} \tag{V-71}$$

where j_ν denotes the coefficient of thermal emission. We are assuming local thermodynamic equilibrium, and hence invoke Kirchhoff's law

$$j_\nu = 4\pi \kappa_\nu B_\nu(T) \, . \tag{V-72}$$

Thus the energy returned to the beam from thermal emission is

$$\kappa_\nu \rho B_\nu(T) \, ds \, d\omega \, . \tag{V-73}$$

Energy is also simply scattered into the beam from all other directions, and this contribution is

$$\sigma \rho \, ds \, d\omega \int p(\cos\theta) \, I_\nu(z,\theta) \, \frac{d\omega}{4\pi} \tag{V-74}$$

where $p(\cos\theta)$ is the phase function of the scattered light. For isotropic scattering, $p(\cos\theta) = 1$, and using the definition of J_ν in expression (V-74), the contribution to the beam from light scattered from all other directions is

$$\sigma \rho \, J_\nu(z) \, ds \, d\omega \tag{V-75}$$

Adding up the gains and losses, the equation of radiative transfer becomes

$$\mu \frac{\partial I_\nu(z,\mu)}{\partial z} = -(\kappa_\nu + \sigma)\rho\, I_\nu(z,\mu) + \kappa_\nu \rho\, B_\nu(T) + \sigma\rho\, J_\nu(z) \,. \tag{V-76}$$

Since

$$dz = \cos\theta\, ds = \mu\, ds \tag{V-77}$$

and the monochromatic optical depth is defined by

$$d\tau_\nu = -(\kappa_\nu + \sigma)\rho\, dz \tag{V-78}$$

equation (V-76) is written

$$\mu \frac{\partial I_\nu(\tau_\nu,\mu)}{\partial \tau_\nu} = I_\nu(\tau_\nu,\mu) - \left[\frac{\kappa_\nu}{\kappa_\nu+\sigma} B_\nu(T) + \frac{\sigma}{\kappa_\nu+\sigma} J_\nu(\tau_\nu)\right] . \tag{V-79}$$

We now define the source function $S_\nu(\tau_\nu)$ to be

$$S_\nu(\tau_\nu) = \frac{\kappa_\nu}{\kappa_\nu+\sigma} B_\nu(T) + \frac{\sigma}{\kappa_\nu+\sigma} J_\nu(\tau_\nu) . \tag{V-80}$$

When we introduce the formal solution to the equation of transfer, we have the Milne integral equation for both scattering and continuous thermal absorption

$$S_\nu(\tau_\nu) = \frac{\kappa_\nu}{\kappa_\nu+\sigma} B_\nu(T) + \frac{1}{2}\frac{\sigma}{\kappa_\nu+\sigma} \Lambda^{(1)}_{\tau_\nu}(S_\nu) . \tag{V-81}$$

We solve this equation for S_ν and substitute into equations (V-65) and (V-66) to obtain the mean intensity J_ν and monochromatic flux πF_ν. In the computer program, this constitutes the solution of the equation of radiative transfer.

Equation (V-81) may be solved in several manners, the simplest of which is iteration, since our procedures are geared to numerical methods. A trial function for S_ν is inserted into the right hand side of equation (V-81), and an improved S_ν is obtained. This is then used as the trial function on the next iteration. In regions of the spectrum where thermal absorption dominates over scattering, this procedure converges rapidly. However, convergence is slow when scattering dominates; this dictates an improved procedure.

We write the Milne equation in the form

$$S_\nu = (1-\lambda_\nu)\, B_\nu + \lambda_\nu\, J_\nu \qquad \text{(V-82)}$$

where

$$\lambda_\nu = \frac{\sigma}{\kappa_\nu + \sigma} \qquad \text{(V-83)}$$

and

$$J_\nu = \frac{1}{2}\, \Lambda^{(1)}_{\tau_\nu}(S_\nu) \quad .$$

The straightforward iteration procedure may then be formulated as

$$S_\nu^{(i)} = (1-\lambda_\nu)\, B_\nu + \lambda_\nu\, J_\nu^{(i-1)} \qquad \text{(V-84)}$$

$$S_\nu^{(i+1)} = (1-\lambda_\nu)\, B_\nu + \lambda_\nu\, J_\nu^{(i)} \qquad \text{(V-85)}$$

where

$$J_\nu^{(i)} = \frac{1}{2}\, \Lambda^{(1)}_{\tau_\nu}\left(S_\nu^{(i)}\right) \qquad \text{(V-86)}$$

and

$$S_\nu^{(0)} = B_\nu \quad . \qquad \text{(V-87)}$$

The change in the source function is

$$\begin{aligned} \Delta_\nu^{(i)} &= S_\nu^{(i+1)} - S_\nu^{(i)} \\ &= \lambda_\nu \left[J_\nu^{(i)} - J_\nu^{(i-1)} \right] \\ &= \frac{1}{2}\, \lambda_\nu \left[\Lambda^{(1)}_{\tau_\nu}(S_\nu^{(i)}) - \Lambda^{(1)}_{\tau_\nu}(S_\nu^{(i-1)}) \right] \end{aligned} \qquad \text{(V-88)}$$

or

$$\Delta_\nu^{(i)} = \frac{1}{2}\, \lambda_\nu\, \Lambda^{(1)}_{\tau_\nu}\left(\Delta_\nu^{(i-1)}\right) \qquad \text{(V-89)}$$

Since the first exponential operator is singular at $x_\nu = \tau_\nu$, we expand $\Delta_\nu^{(i-1)}$ in a Taylor series about $x_\nu = \tau_\nu$ and keep only the zero-th order term.

$$\begin{aligned} \Delta_\nu^{(i)} &\approx \frac{1}{2}\, \lambda_\nu\, \Delta_\nu^{(i-1)}\, \Lambda^{(1)}_{\tau_\nu}(1) \\ &\approx \lambda_\nu\, \Delta_\nu^{(i-1)} \left[1 - \frac{1}{2}\, E_2(\tau_\nu) \right] . \end{aligned} \qquad \text{(V-90)}$$

Our iteration procedure is then to compute

$$S_\nu^{(i)} = (1-\lambda_\nu) B_\nu + \tfrac{1}{2} \lambda_\nu \Lambda_{\tau_\nu}^{(1)} (S_\nu^{(i-1)}) \tag{V-91}$$

and

$$\Delta_\nu^{(i)} = \lambda_\nu \left[1 - \tfrac{1}{2} E_2(\tau_\nu) \right] \left[S_\nu^{(i)} - S_\nu^{(i-1)} \right] \tag{V-92}$$

and for our next trial source function, take

$$S_\nu^{(i+1)} = S_\nu^{(i)} + \Delta_\nu^{(i)} \quad . \tag{V-93}$$

This procedure has proven to converge roughly twice as quickly as the straightforward iteration method.

However, in extreme cases where scattering dominates over thermal absorption by several orders of magnitude, convergence is extremely slow whatever iteration method is used. Two procedures seemed worthwhile investigating. The first was to keep higher order terms in the expansion of $\Delta_\nu^{(i-1)}$, but this involves numerical derivatives of $S_\nu^{(i)}$ and $S_\nu^{(i-1)}$. Enough significant figures were lost that this method failed in nearly every case in which it was tried. The second procedure is to attempt to provide an initial $S_\nu^{(0)}$ that is closer to the final S_ν than the approximation $S_\nu^{(0)} = B_\nu$. The assumption made here is that at those frequencies and optical depths where the scattering dominates over absorption, the monochromatic source function will resemble a gray-body source function.

The monochromatic absorption coefficient is small near the surface of the star; at large depths κ_ν dominates over σ. Thus we can expect the source function S_ν to look like the Planck function B_ν at large depths, but near the surface to look like a gray-body source function with some scaling factor so that the two limiting solutions will join. We write for large optical depths

$$S_\nu^{(0)} = B_\nu$$

and at small optical depths

$$S_\nu^{(0)} = c^* \left[\tau_\nu + q(\tau_\nu) \right]$$

where $q(\tau_\nu)$ is the Hopf function, discussed in Appendix D. The mean intensities J_ν associated with these limiting cases are

$$J_\nu^{(0)} = \frac{1}{2} \Lambda_{\tau_\nu}^{(1)} (B_\nu) \tag{V-94}$$

$$J_\nu^{(0)} = c^* \left[\tau_\nu + q(\tau_\nu) \right] . \tag{V-95}$$

We join these solutions by the λ_ν function, defined in equation (V-83). Thus

$$J_\nu^{(0)} = \frac{1}{2} (1-\lambda_\nu) \Lambda_{\tau_\nu}^{(1)} (B_\nu) + \lambda_\nu c^* \left[\tau_\nu + q(\tau_\nu) \right] . \tag{V-96}$$

Inserting this into the Milne equation we obtain

$$S_\nu^{(0)} = (1-\lambda_\nu) \left[B_\nu + \frac{1}{2} \lambda_\nu \Lambda_{\tau_\nu}^{(1)} (B_\nu) \right] + c^* \lambda_\nu^2 \left[\tau_\nu + q(\tau_\nu) \right] \tag{V-97}$$

Our fitting procedure for the best determination of C* is the following. We find the smallest optical depth τ_ν^* where $\lambda_\nu \leq 0.9$ and compute the quantity

$$J_\nu^* = \frac{1}{2} \Lambda^{(1)}_{\tau_\nu^*}(B_\nu) \tag{V-98}$$

for the one optical depth τ_ν^*. Then an initial value of C* is given by

$$C^* = \frac{J_\nu^*}{\tau_\nu^* + q(\tau_\nu^*)} \quad . \tag{V-99}$$

We compute an initial source function $S_\nu^{(0)}$ for all optical depths from equation (V-97) and use this to obtain a better value of J_ν^* :

$$J_\nu^* = \frac{1}{2} \Lambda^{(1)}_{\tau_\nu^*}(S_\nu^{(0)}) \quad . \tag{V-100}$$

Now an improved value of C* may be determined

$$C^* = \frac{J_\nu^* - \frac{1}{2}(1-\lambda_\nu^*)\Lambda^{(1)}_{\tau_\nu^*}(B_\nu)}{\lambda_\nu^* \left[\tau_\nu^* + q(\tau_\nu^*)\right]} \quad . \tag{V-101}$$

This in turn leads to a better initial source function, and the process becomes iterative. The value of a procedure such as this may be realized from the fact that the lambda-operator is evaluated at one optical depth τ_ν^* only. Once the initial source function $S_\nu^{(0)}$ has been determined, we proceed with the iteration-prediction procedure described above.

Now we need to evaluate the lambda-operator at every optical depth, and this is what takes up most of the computing time.

The evaluation of the first two lambda-operators is discussed in Appendix E, where some efficient and accurate quadrature formulae are given.

Once a final source function has been found that satisfies the Milne equation at all optical depths to within some prescribed accuracy, we integrate equations (V-65) and (V-66) to obtain the monochromatic mean intensity J_ν and monochromatic flux πF_ν. We integrate the monochromatic flux over all frequencies to obtain the total flux at each characteristic optical depth

$$\pi F(\tau) = \pi \int_0^\infty F_\nu(\tau)\, d\nu \quad . \tag{V-102}$$

Quadrature formulae for all frequency integrations such as this are given in Appendix E.

The condition of radiative equilibrium requires that the total flux be constant with depth; in other words, the tau-gradient of the integrated flux must vanish. The tau-gradient of the integrated flux is most accurately computed by first integrating the transfer equation over all μ to obtain

$$\frac{1}{4}\,\frac{d}{d\tau_\nu} F_\nu(\tau_\nu) = \frac{\kappa_\nu}{\kappa_\nu+\sigma}\left[\, J_\nu(\tau_\nu) - B_\nu(T) \right] . \tag{V-103}$$

Transforming to the τ -scale and integrating over frequency yields

$$\frac{d}{d\tau}\,\pi F(\tau) \;=\; \frac{4\pi}{\kappa+\sigma}\int_0^\infty \kappa_\nu\left[J_\nu(\tau)-B_\nu(T)\right]d\nu \qquad \text{(V-104)}$$

so that the condition of radiative equilibrium may be written

$$\int_0^\infty \kappa_\nu(\tau)\left[J_\nu(\tau)-B_\nu(T)\right]d\nu \;=\; 0 \qquad \text{(V-105)}$$

8. Radiation Pressure

The amount of radiative energy crossing a unit area dS in a direction $\mu=\cos\theta$ with its normal within a unit solid angle $d\omega$ in a unit of time dt and in the frequency range ν to $\nu+d\nu$ is

$$dE_\nu \;=\; I_\nu(z,\mu)\,\mu\; d\omega\, d\nu\, dS\, dt. \qquad \text{(V-106)}$$

The momentum carries is dE_ν/c , and the net rate of transfer of the normal component of this momentum, $\mu\, dE_\nu/c$, across dS, expressed per unit area per unit time and per unit frequency interval is

$$2\pi\int_{-1}^{+1}\mu\,\frac{dE_\nu}{c}\,d\mu \;=\; \frac{2\pi}{c}\int_{-1}^{+1} I_\nu(z,\mu)\,\mu^2\,d\mu \qquad \text{(V-107)}$$

This is the definition of the radiation pressure $p_R(\nu,z)$ of ν-radiation, and by using the definition of $K_\nu(z)$ after Eddington (12)

$$K_\nu(z) \;=\; \frac{1}{2}\int_{-1}^{+1} I_\nu(z,\mu)\,\mu^2\,d\mu \qquad \text{(V-108)}$$

we have

$$P_R(\nu, z) = \frac{4\pi}{c} K_\nu(z) \quad . \tag{V-109}$$

We note that if the equation of radiative transfer, equation (V-69), is multiplied by μ and integrated over all μ, we obtain

$$\frac{d}{dt} K_\nu(t) = \frac{1}{4} \frac{\kappa_\nu + \sigma}{\kappa + \sigma} F_\nu(t) \, . \tag{V-110}$$

Thus the tau-gradient of the total radiation pressure $P_R(\tau)$ is

$$\frac{d}{d\tau} P_R(\tau) = \frac{\pi}{c} \int_0^\infty \frac{\kappa_\nu + \sigma}{\kappa + \sigma} F_\nu(\tau) \, d\nu \tag{V-111}$$

or

$$\frac{d P_R(\tau)}{d\tau} = \frac{\pi}{c} \int_0^\infty \frac{d\tau_\nu(\tau)}{d\tau} F_\nu(\tau) \, d\nu \, . \tag{V-112}$$

For a gray atmosphere where $\frac{d\tau_\nu(\tau)}{d\tau} = 1$, we have

$$\left.\frac{d P_R(\tau)}{d\tau}\right|_{Gray} = \frac{\pi}{c} F(\tau) = \frac{\sigma_R}{c} T_e^4 \tag{V-113}$$

where σ_R is the Stefan-Boltzmann constant. For an initial model of a star, where no knowledge of the true temperature distribution is known, the gray body value of the radiation pressure gradient is used in the equation of hydrostatic equilibrium, equation (V-50).

Once the equation of radiative transfer has been solved by the methods of the preceding section, all the quantities appearing in the right hand side of equation (V-112) are known, and an improved table of the radiation pressure gradient may be computed for use in the next iteration of the model as we strive for radiative equilibrium.

9. The Temperature Correction Procedure

The temperature correction procedure used in this non-gray stellar atmospheres computer program is the perturbation method developed by Krook (22) and Avrett and Krook (23). In this method a perturbation is applied to the independent variable τ as well as to the dependent variables. Slight modifications of the method as published will be described here. These modifications allow for coherent isotropic scattering.

We write the equation of radiative transfer in terms of the characteristic optical depth

$$\mu \frac{\partial}{\partial \tau} I_\nu(\tau,\mu) = \eta_\nu \Big[I_\nu(\tau,\mu) - (1-\lambda_\nu) B_\nu\{T(\tau)\} - \lambda_\nu J_\nu(\tau) \Big] \qquad \text{(V-114)}$$

where as before

$$\eta_\nu = \frac{K_\nu(\tau) + \sigma(\tau)}{K(\tau) + \sigma(\tau)}$$

$$\lambda_\nu = \frac{\sigma(\tau)}{K_\nu(\tau) + \sigma(\tau)}$$

We introduce the following perturbations

$$\tau = t + \lambda\, \tau^{(1)}(t)$$

$$T(\tau) = T^{(0)}(t) + \lambda T^{(1)}(t)$$

Thus

$$\frac{d\tau}{dt} = 1 + \lambda \frac{d}{dt}\tau^{(1)}(t)$$

$$I_\nu(\tau,\mu) = I_\nu^{(0)}(t,\mu) + \lambda I_\nu^{(1)}(t,\mu)$$

$$J_\nu(\tau) = J_\nu^{(0)}(t) + \lambda J_\nu^{(1)}(t)$$

$$F_\nu(\tau) = F_\nu^{(0)}(t) + \lambda F_\nu^{(1)}(t)$$

$$\eta_\nu(\tau) = \eta_\nu(t) + \lambda\, \tau^{(1)}(t)\, \eta_\nu'(t)$$

$$\lambda_\nu(\tau) = \lambda_\nu(t) + \lambda\, \tau^{(1)}(t)\, \lambda_\nu'(t)$$

$$B_\nu(T) = B_\nu(T^{(0)}) + \lambda\, T^{(1)}(t)\, \dot{B}_\nu(T^{(0)})$$

where λ is a disposable parameter, and the prime and dot refer to differentiation with respect to t and $T^{(0)}$ respectively. We introduce these expansions into the equation of transfer, group terms according to powers of λ, and obtain the zero-order equation:

$$\mu \frac{\partial}{\partial t} I_\nu^{(0)} = \eta_\nu \left[I_\nu^{(0)} - (1-\lambda_\nu) B_\nu - \lambda_\nu J_\nu^{(0)} \right] \qquad \text{(V-115)}$$

and the first-order equation, cancelling the λ :

$$\mu \frac{\partial}{\partial t} I_\nu^{(1)} = \eta_\nu \left[I_\nu^{(1)} - \lambda_\nu J_\nu^{(1)} - (1-\lambda_\nu) T^{(1)} \dot{B}_\nu + \tau^{(1)} \lambda_\nu' \left(B_\nu - J_\nu^{(0)} \right) \right]$$
$$+ \left(\eta_\nu \tau^{(1)} + \tau^{(1)} \eta_\nu' \right) \left[I_\nu^{(0)} - (1-\lambda_\nu) B_\nu - \lambda_\nu J_\nu^{(0)} \right] \qquad \text{(V-116)}$$

We integrate the zero-order equation over all μ and obtain

$$\frac{d}{d\tau} F_\nu^{(0)} = 4\,\eta_\nu (1-\lambda_\nu)(J_\nu^{(0)} - B_\nu) \tag{V-117}$$

and by first multiplying by μ and then integrating over all μ, we obtain the first moment of the zero-order equation

$$\frac{d}{d\tau} K_\nu^{(0)} = \frac{1}{4}\,\eta_\nu F_\nu^{(0)} \quad . \tag{V-118}$$

The corresponding moments of the first order equation are

$$\begin{aligned} \frac{d}{d\tau} F_\nu^{(1)} = {} & 4\,\eta_\nu \Big[(1-\lambda_\nu)(J_\nu^{(1)} - T^{(1)} \dot{B}_\nu) \\ & - \tau^{(1)} \lambda_\nu' (J_\nu^{(0)} - B_\nu) \Big] \\ & + 4(\eta_\nu \tau^{(1)\prime} + \tau^{(1)} \eta_\nu') \Big[(1-\lambda_\nu)(J_\nu^{(0)} - B_\nu) \Big] \end{aligned} \tag{V-119}$$

and

$$\frac{d}{d\tau} K_\nu^{(1)} = \frac{1}{4}\,\eta_\nu F_\nu^{(1)} + \frac{1}{4}(\eta_\nu \tau^{(1)\prime} + \tau^{(1)} \eta_\nu') F_\nu^{(0)} . \tag{V-120}$$

We assume the Eddington approximation in the form

$$\frac{d}{d\tau} K_\nu^{(1)} = \frac{1}{3} \frac{d}{d\tau} J_\nu^{(1)}$$

and integrate equations (V-119) and (V-120) over all frequencies to obtain

$$\frac{1}{4}\frac{d}{dt}F^{(1)} = \int_0^\infty \eta_\nu(1-\lambda_\nu)\left(J_\nu^{(1)} - T^{(1)}\dot{B}_\nu\right)d\nu$$

$$+ \tau^{(1)'}\int_0^\infty \eta_\nu(1-\lambda_\nu)\left(J_\nu^{(0)} - B_\nu\right)d\nu$$

$$- \tau^{(1)}\int_0^\infty \left[\eta_\nu\lambda_\nu' - \eta_\nu' + \eta_\nu'\lambda_\nu\right]\left(J_\nu^{(0)} - B_\nu\right)d\nu \qquad \text{(V-121)}$$

and

$$\frac{4}{3}\frac{d}{dt}J^{(1)} = \int_0^\infty \eta_\nu F_\nu^{(1)}\,d\nu$$

$$+ \tau^{(1)'}\int_0^\infty \eta_\nu F_\nu^{(0)}\,d\nu + \tau^{(1)}\int_0^\infty \eta_\nu' F_\nu^{(0)}\,d\nu \quad . \qquad \text{(V-122)}$$

The function $\tau^{(1)}$ is chosen for convenience so that the $J^{(1)}$ terms vanish. $\tau^{(1)}(t)$ is then defined by the differential equation

$$\frac{d}{dt}\tau^{(1)}(t) = -\frac{F^{(1)}}{F^{(0)}} - \frac{\tau^{(1)}}{F^{(0)}}\int_0^\infty \frac{\eta_\nu'}{\eta_\nu}F_\nu^{(0)}\,d\nu \qquad \text{(V-123)}$$

and since

$$F = F^{(0)} + F^{(1)}$$

where F is the desired flux, we have

$$\frac{d}{dt}\tau^{(1)}(t) = \left[1 - \frac{F}{F^{(0)}(t)}\right] - \frac{\tau^{(1)}}{F^{(0)}}\int_0^\infty \frac{\eta_\nu'}{\eta_\nu}F_\nu^{(0)}\,d\nu \; . \qquad \text{(V-124)}$$

Equation (V-124) is numerically integrated under the boundary condition

$$\tau^{(1)}(0) = 0 \quad . \tag{V-125}$$

Now that $\tau^{(1)}$ and $\tau^{(1)\prime}$ are know, an expression for $T^{(1)}$ may be derived from equation (V-121). We assume the boundary condition for a gray atmosphere

$$F_\nu^{(1)}(0) = \frac{4}{\sqrt{3}} J_\nu^{(1)}(0) \tag{V-126}$$

and our choice of $\tau^{(1)}(t)$ implies that

$$\int_0^\infty \frac{1}{\eta_\nu} \frac{d}{dt} J_\nu^{(1)} \, d\nu = 0 \quad . \tag{V-127}$$

In view of this equation and in order that we may eliminate the $J_\nu^{(1)}$ term from equation (V-121) we require that

$$\frac{d}{dt} J_\nu^{(1)}(t) = 0 \quad . \tag{V-128}$$

We then may write

$$J_\nu^{(1)}(t) = J_\nu^{(1)}(0) = \frac{\sqrt{3}}{4} F_\nu^{(1)}(0)$$

$$= \frac{\sqrt{3}}{4} \left(\frac{F}{F^{(0)}(0)} - 1 \right) F_\nu^{(0)}(0) \tag{V-129}$$

The expression for $T^{(1)}(t)$ then becomes

$$T^{(1)}(t) = \Bigg[\frac{1}{4} \frac{d}{dt} F^{(1)}(t) - \frac{\sqrt{3}}{4} \left(\frac{F}{F^{(0)}(0)} - 1 \right) \int_0^\infty \eta_\nu (1-\lambda_\nu) F_\nu^{(0)}(0)\, d\nu$$

$$+ \tau^{(1)\prime} \int_0^\infty \eta_\nu (1-\lambda_\nu) \left(J_\nu^{(0)} - B_\nu \right) d\nu$$

$$- \tau^{(1)} \int_0^\infty \left[\eta_\nu \lambda_\nu' - \eta_\nu' - \lambda_\nu \eta_\nu' \right] (J_\nu^{(0)} - B_\nu) d\nu \Bigg]$$

$$\Big/ \int_0^\infty \eta_\nu (1-\lambda_\nu) \dot{B}_\nu \, d\nu$$

Now from the identities

$$F = F^{(0)}(t) + F^{(1)}(t)$$

$$\frac{d}{dt} F^{(0)}(t) = - \frac{d}{dt} F^{(1)}(t)$$

$$\frac{d}{dt} F^{(0)}(t) = 4 \int_0^\infty \eta_\nu (1-\lambda_\nu) \left(J_\nu^{(0)} - B_\nu \right) d\nu$$

we may write

$$T^{(1)}(t) = Q_1 / Q_2$$

$$Q_1 = (1 + \tau^{(1)\prime}) \int_0^\infty \eta_\nu (1-\lambda_\nu) \left(J_\nu^{(0)} - B_\nu \right) d\nu$$

$$+ \frac{\sqrt{3}}{4} \left(\frac{F}{F^{(0)}(0)} - 1 \right) \int_0^\infty \eta_\nu (1-\lambda_\nu) F_\nu^{(0)}(0)\, d\nu$$

$$+ \tau^{(1)} \int_0^\infty \left[\eta_\nu' (1-\lambda_\nu) - \eta_\nu \lambda_\nu' \right] \left(J_\nu^{(0)} - B_\nu \right) d\nu$$

$$Q_2 = \int_0^\infty \eta_\nu (1-\lambda_\nu) \dot{B}_\nu \, d\nu$$

The development of the temperature correction procedure is now complete. To summarize, we assume an initial temperature distribution $T^{(0)}(t)$, solve the equation of transfer and obtain $J_\nu^{(0)}(t)$, $F_\nu^{(0)}(t)$, and $F^{(0)}(t)$. The perturbations $\tau^{(1)}(t)$ and $T^{(1)}(t)$ follow from equations (V-124) and (V-130). An improved temperature distribution is then computed from the relations

$$\tau = t + \tau^{(1)}(t)$$

$$T(\tau) = T^{(0)}(t) + T^{(1)}(t)$$

and the process become iterative.

10. Adiabatic and Radiative Temperature Gradients

Schwarzschild (24) established that the condition of instability of a stellar atmosphere against convection is

$$\left| \frac{d \ln T}{d \ln P_g} \right|_{ad} < \left| \frac{d \ln T}{d \ln P_g} \right|_{rad} \qquad \text{(V-131)}$$

where ad and rad specify adiabatic and radiative respectively. In other words, whenever the radiative temperature gradient exceeds the adiabatic temperature gradient, convection sets in.

We write the radiative temperature gradient in the form

$$\left| \frac{d \ln T}{d \ln P_g} \right|_{rad} = \frac{P_g}{T} \left| \frac{dT/d\tau}{dP_g/d\tau} \right| \qquad \text{(V-132)}$$

Thus the radiative temperature is computed by numerically differentiating the assumed $T(\tau)$ relation and obtaining $dP_g/d\tau$ from the equation of hydrostatic equilibrium, equation (V-50).

The adiabatic temperature gradient is computed using an expression derived by Krishna Swamy (25), for an ensemble of atoms of different elements in varying degrees of ionization; radiation pressure is also taken into account, and only first ionizations are considered. We write

$$\left| \frac{d \ln T}{d \ln P_g} \right|_{ad} = \left| \frac{F_1}{F_2} \right| \tag{V-133}$$

where

$$F_1 = (1+\bar{x}) + \frac{\bar{x} + \bar{x}^2}{2\bar{x} + \bar{x}^2 - \langle x^2 \rangle} \sum_i A_i x_i (1-x_i)\left(\frac{5}{2} + \frac{\chi_i}{kT}\right)$$

$$+4 \frac{P_R}{P_g}\left[(1+\bar{x}) + \frac{\bar{x} + \bar{x}^2}{2\bar{x} + \bar{x}^2 - \langle x^2 \rangle} \sum_i A_i x_i (1-x_i)\right] \tag{V-134}$$

$$F_2 = \frac{5}{2}(1+\bar{x}) + \sum_i A_i x_i (1-x_i)\left(\frac{5}{2} + \frac{\chi_i}{kT}\right)^2$$

$$- \frac{\left[\sum_i A_i x_i (1-x_i)\left(\frac{5}{2} + \frac{\chi_i}{kT}\right)\right]^2}{2\bar{x} + \bar{x}^2 - \langle x^2 \rangle}$$

$$+ 4 \frac{P_R}{P_g}\left[4(1+\bar{x})\right.$$

$$\left. + \frac{\bar{x} + \bar{x}^2}{2\bar{x} + \bar{x}^2 - \langle x^2 \rangle} \sum_i A_i x_i (1-x_i)\left(\frac{5}{2} + \frac{\chi_i}{kT}\right)\right] \tag{V-135}$$

and

$$\bar{x} = \sum_i A_i x_i$$

$$\langle x^2 \rangle = \sum_i A_i x_i^2$$

A_i is the relative abundance of the element by numbers of atoms, and x_i is the degree of ionization, or the fraction of atoms of element i that are at least singly ionized.

No attempt is made to allow for the effects of convection in the computer program. The adiabatic and radiative temperature gradients are merely computed as the equation of hydrostatic equilibrium is being solved.

VI HeH^+ IN MODEL STELLAR ATMOSPHERES

Eight model stellar atmospheres were computed with the program outlined in Chapter V. The chemical composition chosen for this set of models was the abundance table of the elements given by Aller (41), and the adopted surface gravity was

$$\log_{10} g = 4.0$$

Thus the only parameter which varies among the models is the effective temperature T_e; the models cover the range

$$9500^{\circ} \text{ K.} \leq T_e \leq 30000^{\circ} \text{ K.}$$

Radiative equilibrium within $\pm$ 1% was attained for these models first without the helium hydride molecule ion. To determine the effect of HeH^+ upon these models, the final model for each effective temperature was recomputed, using the same initial conditions, except that the absorption of HeH^+ was now taken into account.

One of the more obvious criteria for judging the importance of a new opacity in a stellar atmosphere is the degree to which radiative equilibrium is destroyed when the opacity source is introduced. Figure 4 shows as a function of effective temperature the departure in per cent from the previous radiative equilibrium of the models. Two curves are shown, for the surface, at $\tau = 0$, and for somewhat deeper layers, at $\tau = 1$. Figure 4 can also be interpreted as showing the relative amount of total flux that has been removed by the opacity of HeH^+ and must be redistributed in order that radiative equilibrium be re-established.

A more detailed comparison between the models is given in Figure 5, where is shown the per cent change in total flux due to HeH^+ opacity as a function of the standard optical depth τ_{4000}. An inspection of this graph shows the atmospheric layers of different models which are most affected by the opacity of HeH^+. Note that at the lowest effective temperatures investigated the effect of the opacity of HeH^+ is appreciable, especially in the deeper layers of the atmosphere.

Radiative equilibrium was re-established for the T_e = 16000° K. model, which showed the maximum departure from radiative equilibrium at the surface when the HeH^+ opacity was introduced. The 16000° K. model computed without HeH^+ is shown in Table VII, while Table VIII shows the same model including HeH^+. The columns labeled "Partition Functions" give the logarithm to base ten of the partition functions.

The general effect of the HeH^+ opacity is to make the atmosphere hotter; pressures are increased. The striking feature between the models is the introduction of a convective zone, between τ = 0.008 and τ = 0.192. The degree to which flux constancy with depth was achieved for these two models is shown in Figure 6. The change in the temperature distribution $T(\tau)$ is shown in Figure 7, where we plot the ratio $T_{with}/T_{without}$ as a function of standard optical depth. In Figure 8 are shown the emergent monochromatic fluxes of the two models; shown as short vertical lines are the centers of the Lyman α, β and γ lines of hydrogen.

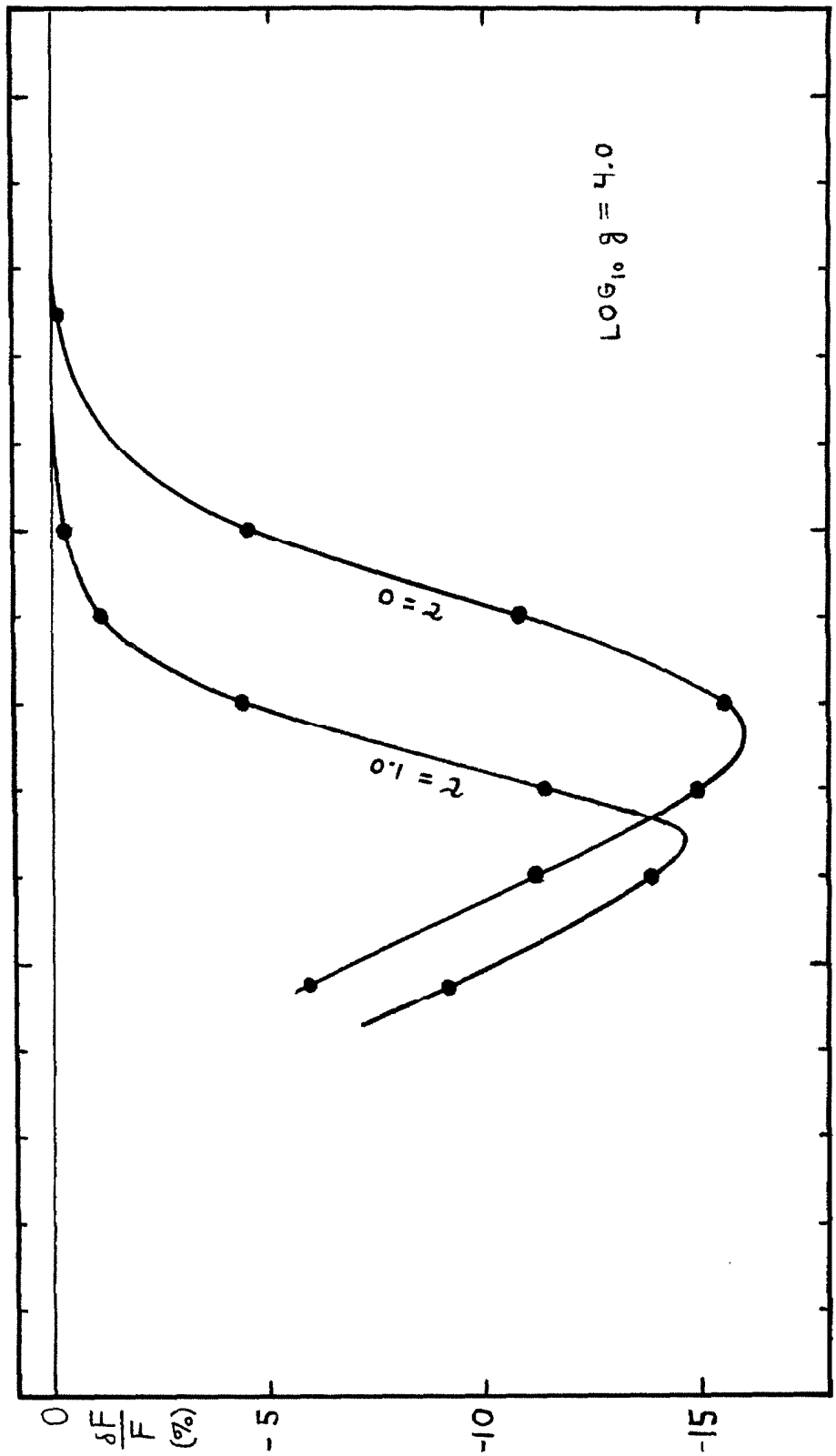

Figure 4. Flux Changes in Models due to HeH^+. $\delta F/F$ measures in per cent the departure from flux constancy when HeH^+ opacity is introduced into the models.

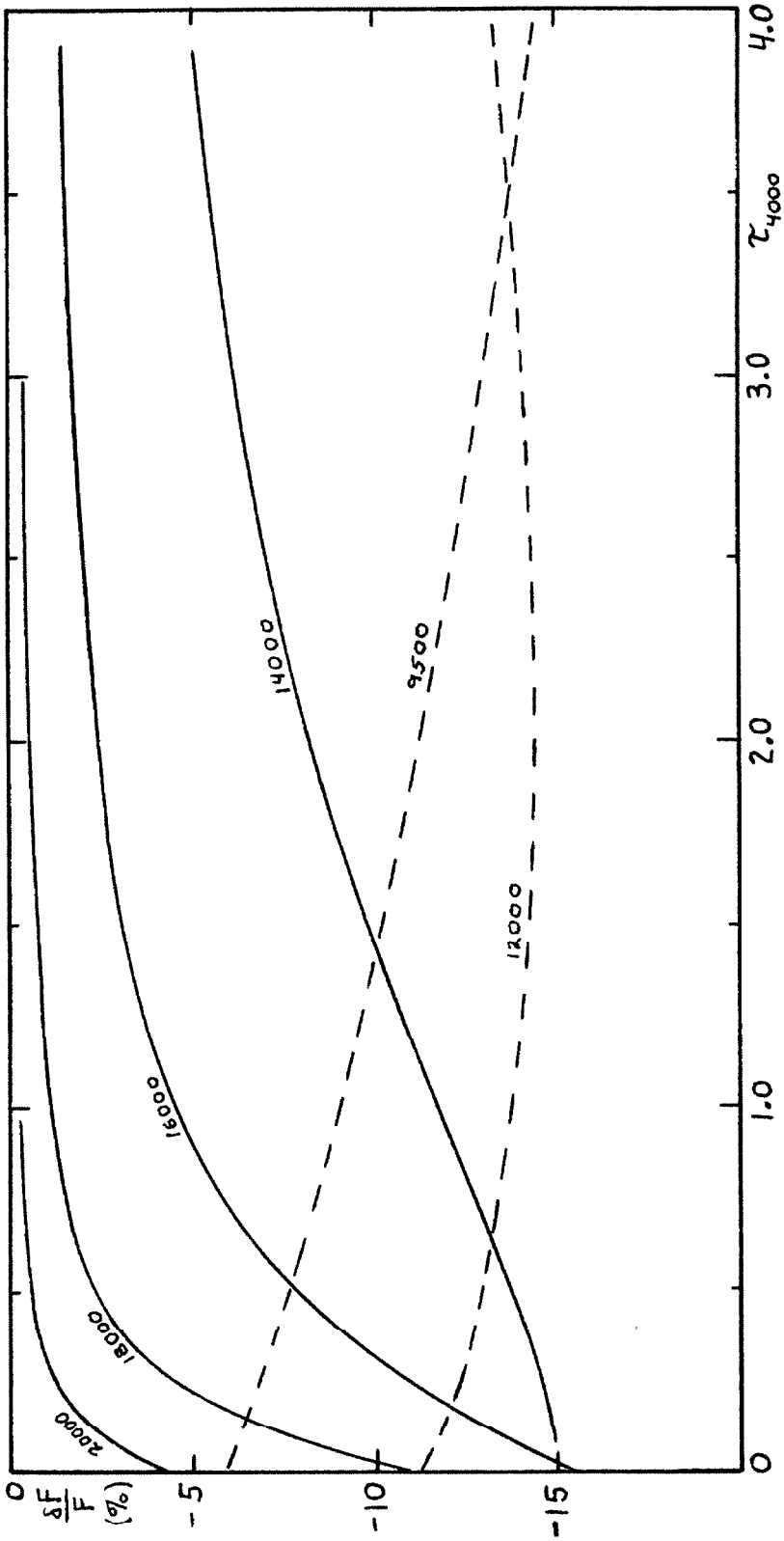

Figure 5. Flux Changes due to HeH^+ as a Function of Depth. The effective temperature of each model is shown above each curve.

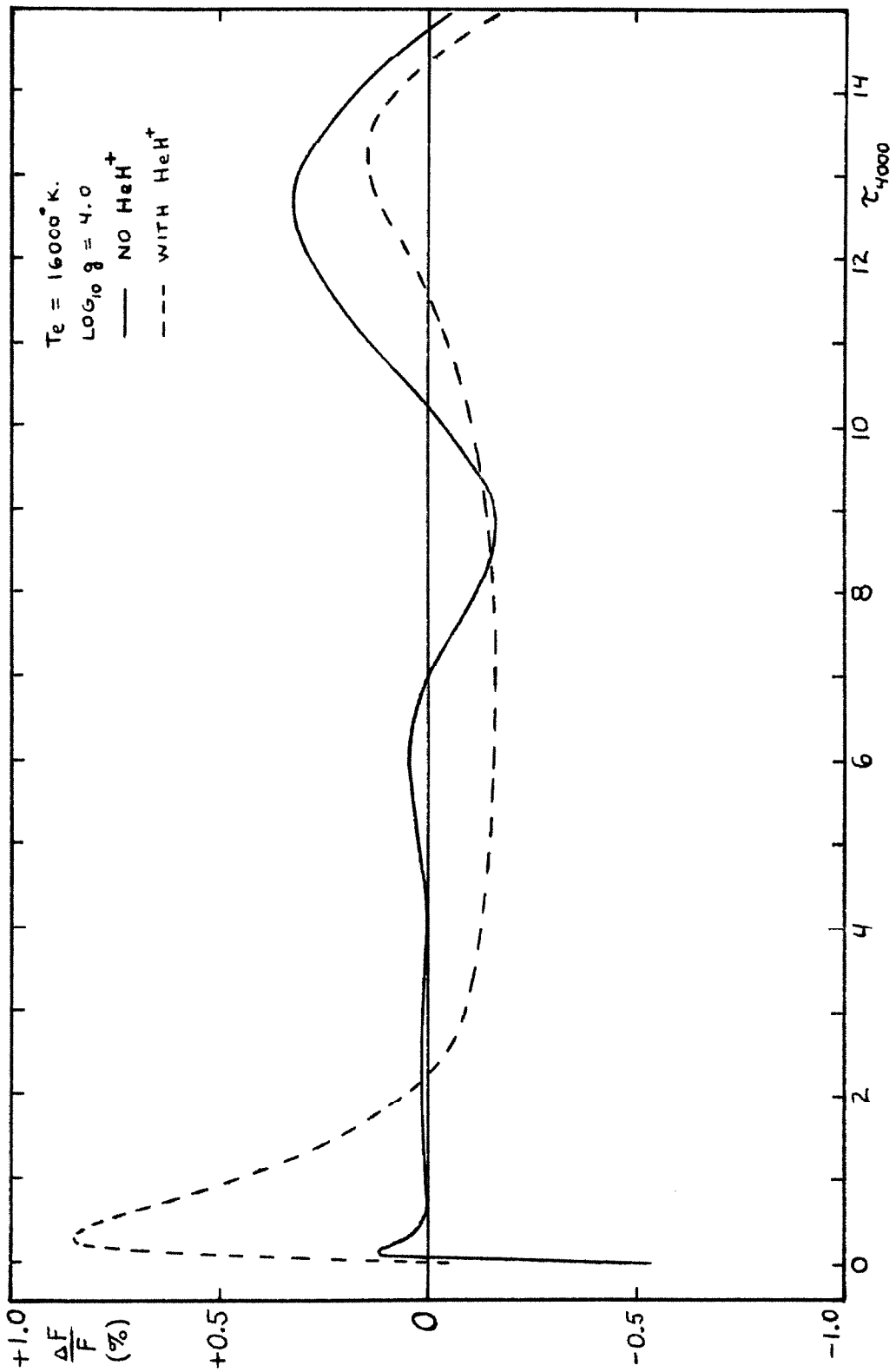

Figure 6. Flux Constancy with Depth for the Models

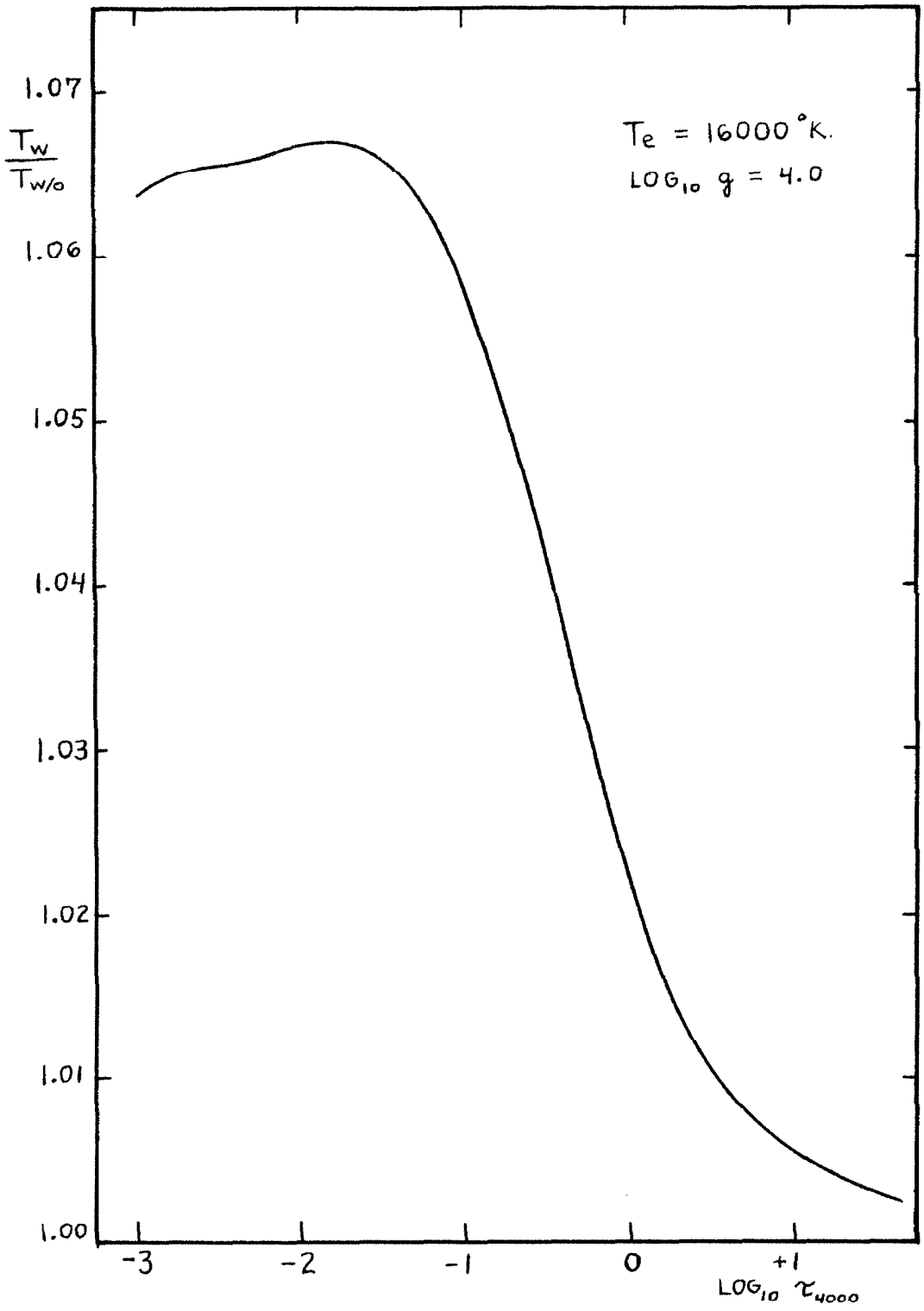

Figure 7. Change in Temperature Distribution. The ordinate gives the ratio T(with HeH^+) / T (without HeH^+) for the models in radiative equilibrium.

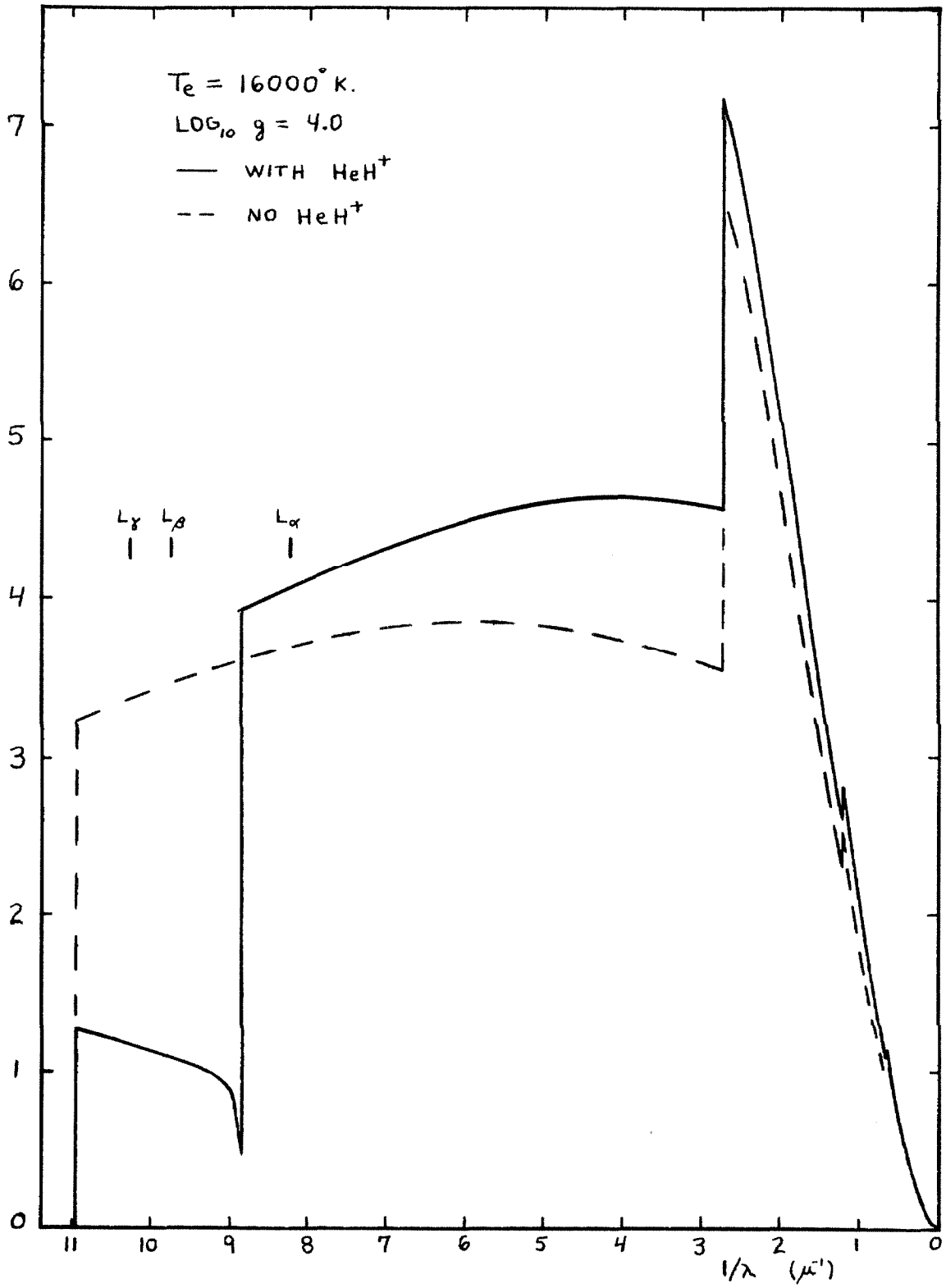

Figure 8. Emergent Monochromatic Fluxes of the Models. Ordinate in units of 10^{-4} erg/cm^2/sec/sec^{-1}.

The inescapable conclusion is that the wings of Lyman β and all higher members of the Lyman series of hydrogen are weaker than they would be if the HeH^+ opacity were not present. Lyman α must still be a strong line, since most of it will be formed in the highly transparent spectral region to the red of the HeH^+ threshold at 1130 A. Moreover, the increased temperature leads to an increase in the ionization of hydrogen, such that the mass absorption coefficient to the red of the HeH^+ threshold is reduced. Hence we have the phenomenon that the center and red wing of Lyman α are formed in a spectral region that has become more transparent with the introduction of HeH^+, while part of the violet wing of Lyman α is formed in an opaque spectral region.

We turn now to the question of how the effect of HeH^+ on a stellar atmosphere might be observed. The obvious feature is of course the discontinuity at 1130 A. Observations of this feature would have to be made from above the atmosphere and hence present technological problems. A feature that could possibly be observed from the ground is the slope of the spectral energy distribution at wavelengths just to the violet of the Balmer discontinuity. Note that in Figure 8 the slopes of the two energy distributions at 3000 A are markedly different to the eye.

What are needed are careful comparisons of the observed and theoretical ultraviolet continua. It would be best to perform this comparison differentially, say between stars of spectral type A 0 and B 7. Possibly a binary system with both stars unevolved could be used to detect this color difference. The unevolved main

sequence of the Hyades might also provide observational material. The ultraviolet continuum would have to be observed quite accurately, for the difference in color between the two distributions in Figure 8 is only 0.04 mag ($1/\lambda$ scale) over the portion of the Balmer continuum that can be observed. In any event a grid of standard models at closely spaced intervals is needed.

From an inspection of Figure 5, we can see that it is quite possible that the 16000° K. model might not exhibit the most marked difference in slope of the Balmer continuum, for the effect of absorption by HeH^+ is concentrated to the surface layers. A model more like the 14000° K. or 12000° K. model could very well show a greater difference in the slope of the ultraviolet continuum around 3300 - 3400 A.

The most direct observational test would be to observe the line profile of Lyman α, which should show a very pronounced asymmetry; in particular, the depth and narrowness of the HeH^+ absorption just to the violet of 1130 A should be a striking feature.

It should be emphasized once more that the calculations of Chapter IV have been made in a rather pessimistic manner, in the sense that we have chosen, whenever a decision was made, the set of numbers which would result in the smallest absorption coefficient of HeH^+. It is possible that the effects upon the model atmospheres by the opacity of HeH^+ found in this investigation underestimate the true effects by a significant amount. At the present time, however, all that can be said is that the effects of HeH^+ upon a model stellar atmosphere are probably no smaller

than the effects reported here.

TABLE VII

T_e = 16000°K. LOG G = 4.0 MODEL ATMOSPHERE INTEGRATION HeH^+ NOT INCLUDED

STEP	TAU	LOG PE	LOG PG	THETA	TEMP	KAPPA	SIGMA	TEMPERATURE GRADIENTS ADIABATIC	RADIATIVE	AD-RAD
0	0.	-1.0268	-0.6968	0.53380	9442.1	0.002764	0.245096	3.967E-01	2.354E-03	3.943E-01
11	0.0005	0.8656	1.1967	0.46227	10903.0	0.125110	0.244334	2.836E-01	6.791E-02	2.157E-01
20	0.0010	1.1126	1.4442	0.45869	10988.2	0.214345	0.243763	2.565E-01	4.990E-02	2.066E-01
27	0.0015	1.2456	1.5777	0.45862	10989.8	0.290368	0.243211	2.321E-01	2.709E-03	2.294E-01
31	0.0020	1.3356	1.6681	0.45791	11007.0	0.354721	0.242835	2.177E-01	1.086E-02	2.068E-01
39	0.0030	1.4575	1.7905	0.45643	11042.5	0.463203	0.242281	2.000E-01	1.417E-02	1.858E-01
46	0.0040	1.5408	1.8742	0.45502	11076.8	0.554147	0.241890	1.897E-01	1.842E-02	1.713E-01
53	0.0060	1.6548	1.9887	0.45236	11141.9	0.703960	0.241380	1.790E-01	2.642E-02	1.526E-01
59	0.0080	1.7335	2.0679	0.44992	11202.5	0.826362	0.240846	1.745E-01	3.333E-02	1.412E-01
66	0.0120	1.8426	2.1773	0.44550	11313.4	1.024167	0.240518	1.727E-01	4.527E-02	1.274E-01
72	0.0160	1.9190	2.2539	0.44158	11413.8	1.182801	0.240437	1.750E-01	5.510E-02	1.199E-01
79	0.0240	2.0261	2.3608	0.43481	11591.8	1.432830	0.240587	1.835E-01	7.059E-02	1.129E-01
84	0.0320	2.1017	2.4364	0.42904	11747.7	1.628066	0.240603	1.933E-01	8.243E-02	1.109E-01
91	0.0480	2.2091	2.5432	0.41947	12015.4	1.930402	0.241212	2.120E-01	9.996E-02	1.120E-01
97	0.0640	2.2860	2.6195	0.41167	12243.1	2.162980	0.241820	2.280E-01	1.124E-01	1.156E-01
104	0.0960	2.3955	2.7282	0.39930	12622.6	2.514669	0.242590	2.529E-01	1.293E-01	1.236E-01
109	0.1280	2.4742	2.8064	0.38961	12936.6	2.781872	0.243174	2.710E-01	1.407E-01	1.303E-01
116	0.1920	2.5877	2.9184	0.37485	13445.9	3.192514	0.244757	2.948E-01	1.551E-01	1.397E-01
122	0.2560	2.6694	2.9990	0.36374	13856.5	3.510162	0.245865	3.098E-01	1.643E-01	1.455E-01
129	0.3840	2.7871	3.1141	0.34744	14506.7	4.019367	0.248715	3.272E-01	1.761E-01	1.511E-01
134	0.5120	2.8721	3.1963	0.33559	15018.8	4.439934	0.251749	3.364E-01	1.839E-01	1.525E-01
141	0.7680	2.9933	3.3123	0.31876	15811.9	5.135541	0.257560	3.455E-01	1.934E-01	1.520E-01
147	1.0240	3.0799	3.3943	0.30688	16423.8	5.702797	0.262830	3.497E-01	1.993E-01	1.504E-01
154	1.5360	3.2005	3.5102	0.29042	17355.0	6.545767	0.268573	3.535E-01	2.036E-01	1.499E-01
158	2.0480	3.2865	3.5929	0.27901	18064.3	7.173132	0.272435	3.553E-01	2.053E-01	1.500E-01
166	3.0720	3.4074	3.7114	0.26343	19132.7	8.082605	0.275542	3.570E-01	2.047E-01	1.523E-01
173	4.0960	3.4940	3.7967	0.25272	19943.3	8.770609	0.277149	3.579E-01	2.055E-01	1.524E-01
180	6.1440	3.6169	3.9189	0.23810	21168.4	9.813470	0.278143	3.590E-01	2.069E-01	1.521E-01
186	8.1920	3.7049	4.0066	0.22797	22109.3	10.611120	0.278519	3.596E-01	2.111E-01	1.485E-01
194	12.2880	3.8304	4.1316	0.21401	23551.2	11.832429	0.279074	3.602E-01	2.178E-01	1.425E-01
198	16.3840	3.9201	4.2212	0.20405	24701.2	12.716112	0.279237	3.606E-01	2.287E-01	1.319E-01
206	24.5760	4.0476	4.3485	0.19087	26406.7	14.150661	0.279488	3.607E-01	2.301E-01	1.306E-01
210	32.7680	4.1394	4.4401	0.18026	27961.2	14.924735	0.279680	3.608E-01	2.728E-01	8.795E-02
220	49.1520	4.2696	4.5702	0.16913	29801.2	16.926895	0.279884	3.606E-01	1.779E-01	1.827E-01
228	65.5360	4.3602	4.6606	0.16180	31150.3	18.508762	0.280036	3.602E-01	2.069E-01	1.533E-01
238	98.3040	4.4871	4.7872	0.15133	33306.8	20.780931	0.280423	3.595E-01	2.298E-01	1.297E-01
245	131.0720	4.5769	4.8766	0.14432	34924.2	22.546393	0.280828	3.590E-01	2.232E-01	1.358E-01
252	196.6080	4.7032	5.0017	0.13498	37339.5	25.816077	0.282491	3.580E-01	2.264E-01	1.316E-01
259	262.1440	4.7921	5.0889	0.12873	39153.9	28.526230	0.284935	3.572E-01	2.344E-01	1.227E-01

MODEL ATMOSPHERE INTEGRATION

	IONIZATION STATES			PARTITION FUNCTIONS					
TAU	H+/ALL H	HE+/ALL HE	HE++/ALL HE	HYDROGEN	HELIUM I	HELIUM II	DENSITY	DPG/DTAU	DPR/DTAU
0.	0.999399	0.009165	0.000000	0.3091	-0.	0.3013	1.9583E-13	40204.028	141.472
0.0005	0.996515	0.009641	0.000000	0.3101	-0.	0.3013	1.3281E-11	26876.273	191.416
0.0010	0.994632	0.006839	0.000000	0.3088	0.	0.3013	2.3325E-11	21657.388	171.529
0.0015	0.992758	0.005065	0.000000	0.3077	-0.	0.3013	3.1746E-11	18564.320	177.057
0.0020	0.991344	0.004307	0.000000	0.3072	0.	0.3013	3.9058E-11	16553.039	181.787
0.0030	0.989181	0.003567	0.000000	0.3067	-0.	0.3013	5.1663E-11	13987.780	186.886
0.0040	0.987583	0.003216	0.000000	0.3064	0.	0.3013	6.2506E-11	12372.604	189.628
0.0060	0.985401	0.002918	0.000000	0.3062	-0.	0.3013	8.0964E-11	10386.041	192.156
0.0080	0.984040	0.002835	0.000000	0.3060	0.	0.3013	9.6726E-11	9177.295	192.951
0.0120	0.982585	0.002901	0.000000	0.3061	-0.	0.3013	1.2330E-10	7714.565	192.545
0.0160	0.982032	0.003104	0.000000	0.3064	0.	0.3013	1.4579E-10	6835.118	191.110
0.0240	0.982084	0.003699	0.000000	0.3070	0.	0.3013	1.8358E-10	5788.349	187.448
0.0320	0.982755	0.004451	0.000000	0.3075	-0.	0.3013	2.1558E-10	5167.713	183.691
0.0480	0.984446	0.006307	0.000000	0.3090	-0.	0.3013	2.6924E-10	4428.100	176.771
0.0640	0.986053	0.008592	0.000000	0.3105	0.	0.3013	3.1460E-10	3987.566	170.784
0.0960	0.988612	0.014437	0.000000	0.3133	-0.	0.3013	3.9138E-10	3465.861	160.928
0.1280	0.990444	0.021992	0.000000	0.3160	0.	0.3012	4.5672E-10	3152.673	153.063
0.1920	0.992774	0.042121	0.000000	0.3228	0.	0.3012	5.6696E-10	2768.305	140.960
0.2560	0.994196	0.068600	0.000000	0.3289	-0.0000	0.3012	6.6108E-10	2530.451	131.936
0.3840	0.995798	0.136831	0.000000	0.3417	-0.0000	0.3012	8.1859E-10	2224.127	118.846
0.5120	0.996659	0.217513	0.000000	0.3556	-0.0000	0.3012	9.5008E-10	2021.806	109.625
0.7680	0.997567	0.382748	0.000000	0.3809	0.0001	0.3012	1.1659E-09	1757.285	96.935
1.0240	0.998035	0.522409	0.000000	0.4042	0.0002	0.3012	1.3429E-09	1587.917	88.352
1.5360	0.998501	0.707107	0.000000	0.4495	0.0004	0.3012	1.6420E-09	1390.572	76.922
2.0480	0.998738	0.806626	0.000000	0.4874	0.0008	0.3012	1.8956E-09	1273.561	69.520
3.0720	0.998971	0.897859	0.000000	0.5520	0.0016	0.3012	2.3378E-09	1136.214	60.223
4.0960	0.999085	0.935875	0.000000	0.6048	0.0031	0.3012	2.7222E-09	1050.617	54.629
6.1440	0.999200	0.966677	0.000001	0.6870	0.0062	0.3012	3.3919E-09	942.897	48.025
8.1920	0.999258	0.978988	0.000002	0.7514	0.0087	0.3012	3.9721E-09	874.067	44.237
12.2880	0.999319	0.988721	0.000009	0.8468	0.0201	0.3012	4.9681E-09	785.633	40.048
16.3840	0.999353	0.992782	0.000030	0.9221	0.0299	0.3011	5.8208E-09	731.540	37.966
24.5760	0.999385	0.995741	0.000139	1.0244	0.0559	0.3011	7.2972E-09	657.755	35.239
32.7680	0.999417	0.996884	0.000492	1.1160	0.0907	0.3011	8.5086E-09	624.280	33.424
49.1520	0.999422	0.996466	0.001724	1.2025	0.1424	0.3011	1.0768E-08	550.143	31.023
65.5360	0.999422	0.994634	0.003905	1.2592	0.1876	0.3011	1.2685E-08	502.807	29.425
98.3040	0.999428	0.986202	0.012695	1.3433	0.2728	0.3011	1.5871E-08	447.492	27.312
131.0720	0.999429	0.971519	0.027543	1.3990	0.3427	0.3011	1.8590E-08	410.258	25.905
196.6080	0.999430	0.924645	0.074591	1.4716	0.4509	0.3011	2.3121E-08	359.119	24.044
262.1440	0.999430	0.860033	0.139313	1.5192	0.5312	0.3012	2.6835E-08	323.082	22.806

TABLE VIII

T_e = 16000°K. LOG G = 4.0 MODEL ATMOSPHERE INTEGRATION HeH^+ INCLUDED

								TEMPERATURE GRADIENTS		
SILP	TAU	LOG PE	LOG PG	THETA	TEMP	KAPPA	SIGMA	ADIABATIC	RADIATIVE	AD-RAD
0	0.	-1.0301	-0.7048	0.48491	10394.0	0.061961	0.250531	3.967E-01	1.640E-03	3.951E-01
11	0.0005	0.8820	1.2114	0.43735	11524.3	0.107371	0.246153	5.124E-02	5.522E-02	-3.972E-03
20	0.0010	1.1327	1.4624	0.43130	11686.0	0.181682	0.245772	4.686E-02	1.572E-02	3.114E-02
27	0.0015	1.2695	1.5997	0.43078	11700.1	0.247309	0.245272	4.074E-02	2.727E-03	3.802E-02
31	0.0020	1.3620	1.6927	0.42995	11722.7	0.303576	0.244782	3.799E-02	1.141E-02	2.658E-02
39	0.0030	1.4874	1.8184	0.42841	11764.7	0.399548	0.244434	3.530E-02	1.480E-02	2.050E-02
46	0.0040	1.5731	1.9043	0.42697	11804.6	0.480423	0.244219	3.411E-02	1.948E-02	1.463E-02
54	0.0060	1.6898	2.0212	0.42430	11878.7	0.614245	0.243963	3.325E-02	2.742E-02	5.829E-03
59	0.0080	1.7704	2.1019	0.42188	11947.0	0.724284	0.243829	3.317E-02	3.436E-02	-1.190E-03
66	0.0120	1.8814	2.2130	0.41761	12069.2	0.902214	0.243731	3.382E-02	4.548E-02	-1.165E-02
72	0.0160	1.9589	2.2906	0.41390	12177.4	1.045501	0.243731	3.492E-02	5.440E-02	-1.948E-02
79	0.0240	2.0669	2.3986	0.40764	12364.3	1.272235	0.243619	3.770E-02	6.776E-02	-3.005E-02
85	0.0320	2.1432	2.4748	0.40246	12523.3	1.452673	0.243826	4.089E-02	7.734E-02	-3.646E-02
92	0.0480	2.2508	2.5819	0.39413	12788.0	1.735752	0.244302	4.801E-02	9.112E-02	-4.311E-02
98	0.0640	2.3271	2.6581	0.38750	13007.0	1.957035	0.244459	5.589E-02	1.009E-01	-4.498E-02
105	0.0960	2.4359	2.7659	0.37718	13362.9	2.305070	0.245443	7.304E-02	1.143E-01	-4.129E-02
110	0.1280	2.5134	2.8429	0.36920	13651.8	2.576907	0.246030	9.137E-02	1.239E-01	-3.253E-02
117	0.1920	2.6246	2.9523	0.35713	14113.0	3.008864	0.247902	1.282E-01	1.366E-01	-8.413E-03
123	0.2560	2.7042	3.0304	0.34803	14481.9	3.353219	0.249593	1.624E-01	1.459E-01	1.648E-02
130	0.3840	2.8181	3.1411	0.33460	15063.3	3.908709	0.252987	2.171E-01	1.578E-01	5.921E-02
135	0.5120	2.9000	3.2199	0.32473	15521.2	4.363865	0.256528	2.545E-01	1.663E-01	8.821E-02
142	0.7680	3.0156	3.3313	0.31049	16232.7	5.083066	0.261387	2.973E-01	1.767E-01	1.206E-01
148	1.0240	3.0986	3.4105	0.30020	16789.2	5.651035	0.265864	3.186E-01	1.846E-01	1.340E-01
156	1.5360	3.2155	3.5233	0.28557	17649.6	6.493036	0.270848	3.376E-01	1.920E-01	1.456E-01
160	2.0480	3.2969	3.6044	0.27515	18318.0	7.112131	0.273603	3.456E-01	1.966E-01	1.490E-01
167	3.0720	3.4174	3.7209	0.26061	19340.2	8.025572	0.276115	3.522E-01	1.989E-01	1.532E-01
172	4.0960	3.5026	3.8051	0.25044	20125.1	8.718282	0.277446	3.549E-01	2.012E-01	1.537E-01
179	6.1440	3.6239	3.9257	0.23642	21316.3	9.772691	0.278287	3.574E-01	2.039E-01	1.535E-01
185	8.1920	3.7109	4.0125	0.22655	22247.3	10.568507	0.278594	3.585E-01	2.100E-01	1.485E-01
193	12.2880	3.8351	4.1363	0.21312	23648.9	11.822079	0.279106	3.596E-01	2.135E-01	1.461E-01
197	16.3840	3.9241	4.2251	0.20315	24810.2	12.675143	0.279262	3.601E-01	2.339E-01	1.262E-01
204	24.5760	4.0507	4.3515	0.19049	26459.4	14.172038	0.279495	3.604E-01	2.222E-01	1.381E-01
208	32.7680	4.1418	4.4426	0.17977	28037.4	14.898064	0.279691	3.605E-01	2.813E-01	7.920E-02
216	49.1520	4.2716	4.5721	0.16893	29836.5	16.948719	0.279889	3.604E-01	1.693E-01	1.911E-01
222	65.5360	4.3616	4.6620	0.16182	31147.6	18.572085	0.280034	3.601E-01	2.023E-01	1.578E-01
230	98.3040	4.4876	4.7878	0.15151	33266.1	20.873087	0.280405	3.594E-01	2.285E-01	1.309E-01
238	131.0720	4.5770	4.8768	0.14462	34852.1	22.763165	0.280782	3.589E-01	2.204E-01	1.385E-01
245	196.6080	4.7028	5.0012	0.13542	37218.4	25.975710	0.282695	3.579E-01	2.235E-01	1.344E-01
252	262.1440	4.7910	5.0880	0.12926	38993.9	28.774513	0.284616	3.571E-01	2.310E-01	1.261E-01

MODEL ATMOSPHERE INTEGRATION

	IONIZATION STATES			PARTITION FUNCTIONS					
TAU	H+/ALL H	HE+/ALL HE	HE++/ALL HE	HYDROGEN	HELIUM I	HELIUM II	DENSITY	OPG/DTAU	OPR/DTAU
0.	0.999891	0.158679	0.000000	0.3382	0.	0.3013	1.7274E-13	39468.455	136.780
0.0005	0.998516	0.042274	0.000000	0.3210	-0.	0.3013	1.2953E-11	28040.044	246.581
0.0010	0.997897	0.034884	0.000000	0.3194	-0.	0.3013	2.2784E-11	23197.900	196.414
0.0015	0.997192	0.026530	0.000000	0.3171	0.	0.3013	3.1245E-11	20096.360	204.836
0.0020	0.996645	0.022669	0.000000	0.3154	-0.	0.3013	3.8667E-11	18023.499	212.716
0.0030	0.995786	0.018764	0.000000	0.3141	0.	0.3013	5.1504E-11	15306.869	221.518
0.0040	0.995146	0.016896	0.000000	0.3135	-0.	0.3013	6.2573E-11	13573.579	226.341
0.0060	0.994260	0.015278	0.000000	0.3130	0.	0.3013	8.1446E-11	11421.370	230.826
0.0080	0.993691	0.014776	0.000000	0.3129	-0.	0.3013	9.7534E-11	10097.106	232.271
0.0120	0.993052	0.014946	0.000000	0.3132	-0.	0.3013	1.2473E-10	8494.622	231.860
0.0160	0.992762	0.015760	0.000000	0.3137	-0.	0.3013	1.4778E-10	7526.867	229.668
0.0240	0.992647	0.018154	0.000000	0.3143	-0.	0.3013	1.8670E-10	6372.566	224.375
0.0320	0.992756	0.021010	0.000000	0.3156	0.	0.3013	2.1958E-10	5675.495	218.996
0.0480	0.993172	0.027508	0.000000	0.3181	0.	0.3013	2.7496E-10	4841.057	209.310
0.0640	0.993633	0.034788	0.000000	0.3200	-0.	0.3012	3.2204E-10	4341.229	201.141
0.0960	0.994399	0.051078	0.000000	0.3248	-0.	0.3012	4.0107E-10	3732.903	187.876
0.1280	0.995010	0.069446	0.000000	0.3286	-0.0000	0.3012	4.6822E-10	3364.988	177.421
0.1920	0.995848	0.110564	0.000000	0.3374	0.0000	0.3012	5.8058E-10	2909.182	161.349
0.2560	0.996421	0.155914	0.000000	0.3447	-0.0000	0.3012	6.7515E-10	2626.372	149.238
0.3840	0.997127	0.251199	0.000000	0.3606	0.0000	0.3012	8.3232E-10	2271.277	131.590
0.5120	0.997561	0.343555	0.000000	0.3740	0.0001	0.3012	9.6213E-10	2045.235	119.052
0.7680	0.998059	0.500986	0.000000	0.4013	0.0002	0.3012	1.1782E-09	1768.822	102.277
1.0240	0.998348	0.617630	0.000000	0.4244	0.0003	0.3012	1.3560E-09	1598.629	91.446
1.5360	0.998668	0.761882	0.000000	0.4672	0.0005	0.3012	1.6574E-09	1400.317	78.124
2.0480	0.998841	0.839267	0.000000	0.5054	0.0011	0.3012	1.9154E-09	1283.896	70.136
3.0720	0.999026	0.911681	0.000000	0.5680	0.0020	0.3012	2.3617E-09	1144.077	60.498
4.0960	0.999121	0.943316	0.000000	0.6195	0.0035	0.3012	2.7485E-09	1056.830	54.809
6.1440	0.999221	0.969600	0.000001	0.6993	0.0068	0.3012	3.4206E-09	946.692	48.236
8.1920	0.999273	0.980569	0.000002	0.7627	0.0096	0.3012	4.0009E-09	877.645	44.260
12.2880	0.999326	0.989235	0.000011	0.8543	0.0211	0.3012	5.0010E-09	786.122	40.243
16.3840	0.999360	0.993119	0.000034	0.9305	0.0316	0.3011	5.8479E-09	733.811	38.127
24.5760	0.999386	0.995804	0.000146	1.0277	0.0569	0.3011	7.3340E-09	656.637	35.352
32.7680	0.999420	0.996914	0.000524	1.1211	0.0929	0.3011	8.5335E-09	625.365	33.474
49.1520	0.999422	0.996437	0.001765	1.2042	0.1436	0.3011	1.0804E-08	549.410	31.019
65.5360	0.999421	0.994649	0.003885	1.2584	0.1872	0.3011	1.2727E-08	501.056	29.388
98.3040	0.999426	0.986532	0.012354	1.3406	0.2705	0.3011	1.5912E-08	445.501	27.234
131.0720	0.999427	0.972625	0.026424	1.3949	0.3385	0.3011	1.8633E-08	408.152	25.802
196.6080	0.999426	0.928816	0.070406	1.4655	0.4431	0.3011	2.3159E-08	356.920	23.910
262.1440	0.999426	0.868638	0.130690	1.5122	0.5220	0.3012	2.6908E-08	321.473	22.653

APPENDIX A

HAMILTONIAN AND OVERLAP MATRICES

The Hamiltonian for the system HeH^{+}, without the nuclear Coulomb repulsion term $\frac{2}{R}$ is

$$H = -\frac{1}{2}\nabla_1^2 - \frac{1}{2}\nabla_2^2 + \frac{1}{r_{12}} - \frac{2}{r_{a1}} - \frac{2}{r_{a2}} - \frac{1}{r_{b1}} - \frac{1}{r_{b2}} \qquad (A-1)$$

where we follow the notation of Chapter IV. Subscripts 1 and 2 denote electrons, and subscripts a and b denote the helium and hydrogen nuclei respectively. See figure 2 .

The Hamiltonian matrix H_{ij} and overlap matrix Δ_{ij} are defined to be

$$H_{ij} = \iint \chi_i \, H \, \chi_j \, d\tau_1 \, d\tau_2 \qquad (A-2)$$

$$\Delta_{ij} = \iint \chi_i \, \chi_j \, d\tau_1 \, d\tau_2 \qquad (A-3)$$

where χ_i and χ_j are members of the set of expansion wavefunctions defined in equations (IV-25), Chapter IV. The integrations are carried out over the coordinates of both electrons.

We can see that the substitution of equation (A-1) into (A-2) gives seven integrals of the general form

$$(\chi_i | O | \chi_j) = \iint \chi_i \, O \, \chi_j \, d\tau_1 \, d\tau_2 \qquad (A-4)$$

where the operator O is 1, $-\frac{1}{2}\nabla^2$ or $\frac{1}{r}$.

Every integral of this general form can be expressed in terms of the basic molecular integrals which are treated individually in Appendix B. Recognizing that our set of expansion wavefunctions, equations (IV-25) of Chapter IV, are comprised only of s-type atomic orbital wavefunctions, we anticipate the notation of Appendix B and define the following basic two-center integrals. Our notation here will be to use parentheses to indicate integrals involving one electron and brackets to denote two-electron integrals.

1. Overlap integrals

$$(n s_a \mid m s_b)$$

2. Kinetic energy integrals

$$\left(n s_a \left| -\tfrac{1}{2}\nabla^2 \right| m s_b\right)$$

3. Nuclear attraction integrals (Type I)

$$\left(n s_a \left| \frac{Z}{r_a} \right| m s_b\right)$$

$$\left(n s_a \left| \frac{1}{r_b} \right| m s_b\right)$$

4. Nuclear attraction integrals (Type II)

$$\left(n s_a \left| \frac{1}{r_b} \right| m s_a\right)$$

$$\left(n s_b \left| \frac{Z}{r_a} \right| m s_b\right)$$

5. Coulomb integrals

$$\left[n s_a(1)\, n' s_a(1) \left| \frac{1}{r_{12}} \right| m s_b(2)\, m' s_b(2)\right]$$

6. Hybrid integrals

$$\left[n s_a(1)\, n' s_a(1) \left| \frac{1}{r_{12}} \right| n'' s_a(2)\, m s_b(2)\right]$$

7. Exchange integrals

$$\left[n s_a(1)\, m s_b(1) \left| \frac{1}{r_{12}} \right| n' s_a(2)\, m' s_b(2)\right]$$

It is noted that certain one-center integrals will arise in equation (A-4) and that these integrals are treated as limiting cases of the basic integrals above when the internuclear separation R is reduced to zero.

Rather than present the detailed derivations of the expressions for each element of the H_{ij} and Δ_{ij} matrices, we give the example of the H_{12} and Δ_{12} elements for illustration. Our wavefunctions in this case are

$$\chi_1 = |\lambda_a(1)\ \lambda_a(2)|$$
$$\chi_2 = |\lambda_a(1)\ \lambda_b(2)| + |\lambda_b(1)\ \lambda_a(2)| \qquad \text{(A-5)}$$

following the notation of Chapter IV. Our general integral is then

$$I = \left[|\lambda_a(1)\ \lambda_a(2)| \,O\, |\lambda_a(1)\ \lambda_b(2)| + |\lambda_b(1)\ \lambda_a(2)| \right] \qquad \text{(A-6)}$$

Our wavefunctions are symmetric with respect to an interchange of electron indices; hence

$$I = 2 \left[|\lambda_a(1)\ \lambda_a(2)| \,O\, |\lambda_a(1)\ \lambda_b(2)| \right] \qquad \text{(A-7)}$$

We have for H_{12}

$$\begin{aligned}
\tfrac{1}{2} H_{12} = &\left[|\lambda_a(1)\ \lambda_a(2)| -\tfrac{1}{2}\nabla_1^2 - \tfrac{1}{2}\nabla_2^2 | \lambda_a(1)\ \lambda_b(2)| \right] \\
&+ \left[|\lambda_a(1)\ \lambda_a(2)| \ \frac{1}{r_{12}}\ | \lambda_a(1)\ \lambda_b(2)| \right] \\
&+ \left[|\lambda_a(1)\ \lambda_a(2)| -\frac{2}{r_{a1}} - \frac{2}{r_{a2}} | \lambda_a(1)\ \lambda_b(2)| \right] \\
&+ \left[|\lambda_a(1)\ \lambda_a(2)| -\frac{1}{r_{b1}} - \frac{1}{r_{b2}} | \lambda_a(1)\ \lambda_b(2)| \right]
\end{aligned}$$

which can be written, suppressing the electron indices in all one-electron integrals, as

$$\begin{aligned}\frac{1}{2} H_{12} = {} & (1s_a|-\tfrac{1}{2}\nabla^2|1s_a)(1s_a|1s_b) + (1s_a|1s_a)(1s_a|-\tfrac{1}{2}\nabla^2|1s_b) \\ & + \left[1s_a(1)\,1s_a(1)\left|\frac{1}{r_{12}}\right|1s_a(2)\,1s_b(2)\right] \\ & - (1s_a|\frac{2}{r_a}|1s_a)(1s_a|1s_b) - (1s_a|1s_a)(1s_a|\frac{2}{r_a}|1s_b) \\ & - (1s_a|\frac{1}{r_b}|1s_a)(1s_a|1s_b) - (1s_a|1s_a)(1s_a|\frac{1}{r_b}|1s_a) \end{aligned} \tag{A-8}$$

Since our s-type atomic orbital wavefunctions are normalized

$$(1s_a|1s_a) = 1$$

and we can group terms in equation (A-8) as follows

$$\begin{aligned}\frac{1}{2} H_{12} = {} & (1s_a|1s_b)\left\{(1s_a|-\tfrac{1}{2}\nabla^2|1s_a) - (1s_a|\frac{2}{r_a}|1s_a)\right. \\ & \left. - (1s_a|\frac{1}{r_b}|1s_a)\right\} + (1s_a|-\tfrac{1}{2}\nabla^2|1s_b) \\ & - (1s_a|\frac{2}{r_a}|1s_b) - (1s_a|\frac{1}{r_b}|1s_b) \\ & + \left[1s_a(1)\,1s_a(1)\left|\frac{1}{r_{12}}\right|1s_a(2)\,1s_b(2)\right] \end{aligned} \tag{A-9}$$

The Δ_{12} element is considerably simpler and is written

$$\begin{aligned}\Delta_{12} &= 2\left[1s_a(1)\,1s_a(2)\,|\,1\,|\,1s_a(1)\,1s_b(2)\right] \\ &= 2\,(1s_a|1s_a)(1s_a|1s_b) \\ &= 2\,(1s_a|1s_b)\end{aligned} \tag{A-10}$$

As is shown in Appendix B, the expressions for the H_{ij} elements are further reduced because the kinetic energy integrals and the nuclear

attraction integrals (Type 1) can be expressed as simple combinations of overlap integrals.

Only the elements lying on or above the principle diagonals of the H_{ij} and Δ_{ij} matrices need be computed. This is so because the operators $1, -\frac{1}{2}\nabla^2$ and $\frac{1}{r}$ are symmetric operators, such that

$$(n\Lambda_a \mid O \mid m\Lambda_b) = (m\Lambda_b \mid O \mid n\Lambda_a)$$

Hence H_{ij} and Δ_{ij} are symmetric matrices.

APPENDIX B

BASIC TWO-CENTER MOLECULAR INTEGRALS

As described in Chapter IV, our basic one-electron atomic orbital wave functions are normalized Slater s-type orbitals, defined in spherical coordinates by

$$n_A = \frac{(2\zeta)^{n+\frac{1}{2}}}{[4\pi(2n)!]^{1/2}} r^{n-1} \exp(-\zeta r) \tag{B-1}$$

For a two-center problem such as the HeH^+ molecule, confocal elliptic coordinates are useful. These coordinates are defined by:

$$\xi = \frac{r_a + r_b}{R} \qquad 1 \le \xi \le \infty \tag{B-2}$$

$$\eta = \frac{r_a - r_b}{R} \qquad -1 \le \eta \le +1 \tag{B-3}$$

$$\nabla^2 = \frac{4}{R^2(\xi^2-\eta^2)} \left[\frac{\partial}{\partial\xi}\left\{(\xi^2-1)\frac{\partial}{\partial\xi}\right\} + \frac{\partial}{\partial\eta}\left\{(1-\eta^2)\frac{\partial}{\partial\eta}\right\} + \frac{\xi^2-\eta^2}{(\xi^2-1)(1-\eta^2)}\frac{\partial^2}{\partial\phi^2} \right] \tag{B-4}$$

and the volume element is

$$d\tau = \frac{R^3}{8}(\xi^2-\eta^2)\, d\xi\, d\eta\, d\phi \tag{B-5}$$

Lower case subscripts denote the nuclei a and b, while R denotes the internuclear separation following the notation shown in figure 2 . In this coordinate system, our basic a- and b-centered atomic orbitals are

$$n_{A_a} = \frac{(2\zeta_a)^{n+\frac{1}{2}}}{[4\pi(2n)!]^{1/2}} \left(\frac{R}{2}\right)^{n-1} (\xi+\eta)^{n-1} \exp\left\{-\frac{\zeta_a R}{2}(\xi+\eta)\right\} \tag{B-6}$$

$$n\Delta_b = \frac{(2J_b)^{n+\frac{1}{2}}}{[4\pi(2n)!]^{1/2}} \left(\frac{R}{2}\right)^{n-1} (\xi-\eta)^{n-1} \exp\left\{-\frac{J_b R}{2}(\xi-\eta)\right\} \tag{B-7}$$

We consider the following one-electron, two-center basic integrals:

Overlap integrals

$$(n\Delta_a | m\Delta_b) = \int (n\Delta_a)(m\Delta_b)\, d\tau \tag{B-8}$$

Kinetic energy integrals

$$(n\Delta_a | -\tfrac{1}{2}\nabla^2 | m\Delta_b) = -\tfrac{1}{2}\int (n\Delta_a)\nabla^2(m\Delta_b)\, d\tau \tag{B-9}$$

Nuclear attraction integrals

$$\text{I.} \quad (n\Delta_a | \frac{Z_a}{r_a} | m\Delta_b) = Z_a \int (n\Delta_a)\frac{1}{r_a}(m\Delta_b)\, d\tau \tag{B-10}$$

$$\text{II.} \quad (n\Delta_b | \frac{Z_a}{r_a} | m\Delta_b) = Z_a \int (n\Delta_b)\frac{1}{r_a}(m\Delta_b)\, d\tau \tag{B-11}$$

In addition, the following two-electron, two-center basic integrals are encountered:

Coulomb integrals

$$\left[n\Delta_a(1)\, n'\Delta_a(1) \left| \frac{1}{r_{12}} \right| m\Delta_b(2)\, m'\Delta_b(2)\right]$$

$$= \iint n\Delta_a(1)\, m'\Delta_a(1)\frac{1}{r_{12}} m\Delta_b(2)\, m'\Delta_b(2)\, d\tau_1 d\tau_2 \tag{B-12}$$

Hybrid integrals

$$\left[n\mathcal{A}_a(1)\, n'\mathcal{A}_a(1) \mid \frac{1}{r_{12}} \mid n''\mathcal{A}_a(2)\, m\mathcal{A}_b(2) \right]$$

$$= \iint n\mathcal{A}_a(1)\, n'\mathcal{A}_a(1)\, \frac{1}{r_{12}}\, n''\mathcal{A}_a(2)\, m\mathcal{A}_b(2)\, d\tau_1 d\tau_2 \qquad \text{(B-13)}$$

Exchange integrals

$$\left[n\mathcal{A}_a(1)\, m\mathcal{A}_b(1) \mid \frac{1}{r_{12}} \mid n'\mathcal{A}_a(2)\, m'\mathcal{A}_b(2) \right]$$

$$= \iint n\mathcal{A}_a(1)\, m\mathcal{A}_b(1)\, \frac{1}{r_{12}}\, n'\mathcal{A}_a(2)\, m'\mathcal{A}_b(2)\, d\tau_1 d\tau_2 \qquad \text{(B-14)}$$

where r_{12} denotes the inter-electronic distance.

All these basic integrals except the exchange integral may be evaluated in terms of two auxiliary functions, defined by

$$C_n(\rho) = \rho^{n+1} e^{\rho} \int_1^{\infty} x^n e^{-\rho x}\, dx \qquad (\rho > 0) \qquad \text{(B-15)}$$

$$= n! \sum_{\ell=0}^{n} \frac{\rho^{\ell}}{\ell!} \qquad (\text{all } \rho) \qquad \text{(B-16)}$$

$$B_n(\gamma) = \int_{-1}^{+1} x^n e^{-\gamma x}\, dx \qquad \text{(B-17)}$$

The computation of the functions $C_n(\rho)$ presents no problem; the set $n = o(1)N$ may be computed from the upward recursion relation

$$C_o(\rho) = 1 \qquad \text{(B-18)}$$

$$C_n(\rho) = \rho^n + n\, C_{n-1}(\rho) \qquad \text{(B-19)}$$

For small values of the argument y, we may expand the integrand for the functions $B_n(y)$:

$$B_n(y) = \sum_{i=0}^{\infty} \frac{(-1)^i}{i!} y^i \int_{-1}^{+1} x^{n+i} dx \tag{B-20}$$

We obtain two expressions:

n even

$$B_n(y) = 2 \sum_{i=0}^{\infty} \frac{y^{2i}}{(n+2i+1)\cdot(2i)!} \tag{B-21}$$

n odd

$$B_n(y) = -2 \sum_{i=1}^{\infty} \frac{y^{2i-1}}{(n+2i)\cdot(2i-1)!} \tag{B-22}$$

In addition it should be noted that for all n:

$$B_n(-|y|) = (-1)^n B_n(|y|) \tag{B-23}$$

The expansion described above proves to be quickly convergent for values of y up to approximately y = 5. For larger values of y, we follow the formulation of Corbato (1), expanding x^n in Legendre polynomials:

$$x^n = \sum_{\ell=0,1}^{n}{}' a_{n\ell} P_\ell(x) \tag{B-24}$$

where

$$a_{n\ell} = n!\,(2\ell+1)\cdot\left[(n-\ell)!!\,(n+\ell+1)!!\right]^{-1}$$

$\sum'$ = sum over: ℓ even if n even ; ℓ odd if n odd

$$n!! = n(n-2)(n-4)\cdots(2 \text{ or } 1)$$

and using the integral representation of the spherical hyperbolic Bessel function of the first kind.

$$i_n(x) = \left(\frac{\pi}{2x}\right)^{1/2} I_{n+\frac{1}{2}}(x)$$

$$= \frac{1}{2}(-1)^n \int_{-1}^{+1} P_n(t)\, e^{-xt}\, dt \qquad \text{(B-25)}$$

where $I_{n+\frac{1}{2}}(x)$ is the ordinary modified Bessel function. It follows that

$$B_n(y) = 2(-1)^n \sum_{\ell=0,1}^{n}{}' a_{n\ell}\, i_\ell(y) \qquad \text{(B-26)}$$

The $i_\ell(y)$ are computed by the following technique. First a set of ratios

$$\pi_\ell(y) = i_{\ell+1}(y) \Big/ i_\ell(y) \qquad \text{(B-27)}$$

are computed using the recursion relation

$$\pi_{\ell-1}(y) = y \cdot \left[2\ell + 1 + y\,\pi_\ell(y)\right]^{-1} \qquad \text{(B-28)}$$

in the numerically accurate downward direction starting from $l = M$, where π_M is made zero. M is chosen to be

$$M \geq n + 5 + 10\,|y| \cdot \left(n+\tfrac{1}{2}\right)^{-1} \qquad \text{(B-29)}$$

which retains seven significant figure accuracy in the ratios for $\ell \leq n$. The function $i_0(y)$ is found from

$$i_0(y) = e^{|y|} \cdot \left[1 + |y| \left\{ 1 + r_0(y) \right\} \right]^{-1} \qquad \text{(B-30)}$$

The general one-electron overlap integral is

$$(n s_a \mid m s_b) = G_{nm} \rho^{n+m+1} \int_1^{\infty} d\xi \int_{-1}^{+1} d\eta$$

$$\times \; (\xi+\eta)^n (\xi-\eta)^m e^{-\rho\xi} e^{-\tau\eta} \qquad \text{(B-31)}$$

where we define

$$\rho = \tfrac{1}{2} (\zeta_a + \zeta_b) R$$

$$\tau = \tfrac{1}{2} (\zeta_a - \zeta_b) R$$

$$\bar{\zeta} = \tfrac{1}{2} (\zeta_a + \zeta_b)$$

$$G_{nm} = \frac{1}{2} \frac{\zeta_a^{n+\frac{1}{2}} \; \zeta_b^{m+\frac{1}{2}}}{\left[(2n)! \; (2m)! \right]^{1/2}} \quad \frac{1}{(\bar{\zeta})^{n+m+1}}$$

Upon multiplying out the polynomials appearing in the integrand of equation (B-31), it is seen that the integral is expressible in terms of the auxiliary functions $C_n(\rho)$ and $B_n(\tau)$.

Kinetic energy integrals, equation (B-9) may be expressed in terms of overlap integrals, since

$$-\frac{1}{2}\nabla^2(n\lambda) = -\frac{1}{2}\zeta^2\left[(n\lambda) - 2\left(\frac{2n}{2n-1}\right)^{1/2}((n-1)\lambda) + \left(\frac{4n(n-1)}{(2n-1)(2n-3)}\right)^{1/2}((n-2)\lambda)\right] \quad \text{(B-32)}$$

Thus

$$(n\lambda_a|-\tfrac{1}{2}\nabla^2|m\lambda_b) = (m\lambda_b|-\tfrac{1}{2}\nabla^2|n\lambda_a)$$

$$= -\frac{1}{2}\zeta_a^2\left[(n\lambda_a|m\lambda_b) - 2\left(\frac{2n}{2n-1}\right)^{1/2}((n-1)\lambda_a|m\lambda_b) + \left(\frac{4n(n-1)}{(2n-1)(2n-3)}\right)^{1/2}((n-2)\lambda_a|m\lambda_b)\right] \quad \text{(B-33)}$$

Nuclear attraction integrals of type I in equation (A-10) may also be expressed in terms of overlap integrals, since

$$\frac{Z_a}{r_a}(n\lambda_a) = 2Z_a\zeta_a\left(2n(2n-1)\right)^{-1/2}((n-1)\lambda_a) \quad \text{(B-34)}$$

and

$$\frac{Z_b}{r_b}(m\lambda_b) = 2Z_b\zeta_b\left(2m(2m-1)\right)^{-1/2}((m-1)\lambda_b) \quad \text{(B-35)}$$

Thus

$$(n\lambda_a|\frac{Z_a}{r_a}|m\lambda_b) = 2Z_a\zeta_a\left[2n(2n-1)\right]^{-1/2}((n-1)\lambda_a|m\lambda_b) \quad \text{(B-36)}$$

$$(n\lambda_a|\frac{Z_b}{r_b}|m\lambda_b) = 2Z_b\zeta_b\left[2m(2m-1)\right]^{-1/2}(n\lambda_a|(m-1)\lambda_b) \quad \text{(B-37)}$$

The nuclear attraction integral defined in equation (B-11) is evaluated by means of the auxiliary functions $C_n(\rho)$ and $B_n(y)$

$$\left(n\mathcal{A}_b \left| \frac{Z_a}{r_a} \right| m\mathcal{A}_b\right) = \frac{Z_a}{2} \frac{(2\zeta_b)^{n+\frac{1}{2}} (2\zeta_b')^{m+\frac{1}{2}}}{(\zeta_b+\zeta_b')^{n+m} [(2n)!\,(2m)!]^{1/2}}$$

$$\times \rho_b^{n+m} \int_1^{\infty} d\xi \int_{-1}^{+1} d\eta\, e^{-\rho_b \xi} e^{+\rho_b \eta} (\xi-\eta)^{n+m-1} \tag{B-38}$$

where, as before,

$$\rho_b = \tfrac{1}{2}(\zeta_b + \zeta_b')R$$

and

$$\rho_a = \tfrac{1}{2}(\zeta_a + \zeta_a')R$$

In this analysis, only one non-linear variation parameter is allowed per nucleus:

$$\zeta_a' = \zeta_a$$

$$\zeta_b' = \zeta_b$$

Thus

$$\left(n\mathcal{A}_b \left| \frac{Z_a}{r_a} \right| m\mathcal{A}_b\right) = \frac{Z_a \zeta_b}{[(2n)!\,(2m)!]^{1/2}} \rho_b^{n+m}$$

$$\times \int_1^{\infty} d\xi \int_{-1}^{+1} d\eta\, e^{-\rho_b \xi} e^{+\rho_b \eta} (\xi-\eta)^{n+m-1} \tag{B-39}$$

and

$$(n s_a \left| \frac{Z_b}{r_b} \right| m s_a) = \frac{Z_b \, J_a}{\left[(2n)!\,(2m)!\right]^{1/2}} \rho_a^{n+m}$$

$$\times \int_1^{\infty} d\xi \int_{-1}^{+1} d\eta \; e^{-\rho_a \xi} e^{-\rho_a \eta} (\xi - \eta)^{n+m-1} \tag{B-40}$$

As before, the polynomials in the integrands of (B-40) and (B-41) are multiplied out and the result is then expressible in terms of the $C_n(\rho)$ and $B_n(y)$.

Coulomb integrals, equation (B-12), and hybrid integrals, equation (B-13), are evaluated by means of the tables of Ruedenberg, Roothaan and Jaunzemis (2). We first define basic charge distributions on atoms, remembering that the non-linear parameters J_a and J_b are the same for all ns_a and ms_b orbitals respectively:

$$(n s_a)(n' s_a) = \frac{(n+n')!}{\left[(2n)!\,(2n')!\right]^{1/2}} \left[N S_a \right] \tag{B-41}$$

where

$$N = n + n' - 1 \tag{B-42}$$

Thus our general coulomb integral will become, ordering the atomic orbitals to identify the electrons

$$\left[n s_a \; n' s_a \left| \frac{1}{r_{12}} \right| m s_b \; m' s_b \right]$$

$$= \frac{(n+n')!\,(m+m')!}{\left[(2n)!\,(2n')!\,(2m)!\,(2m')!\right]^{1/2}} \left[N S_a \middle| M S_b \right] \tag{B-43}$$

We define

$$\left.\begin{aligned} \rho_a &= 2\zeta_a R \\ \rho_b &= 2\zeta_b R \\ \mu &= \zeta_a/2\zeta_b \end{aligned}\right\} \qquad \text{(B-44)}$$

The six basic Coulomb integrals comprised only of s-orbitals then become:

$$\left.\begin{aligned}
[1S_a|1S_b] &= \frac{\zeta_b}{2}\left\{G_{01}(0,\rho_b) - G_{01}(\rho_a,\rho_b) - \mu\, G_{11}(\rho_a,\rho_b)\right\} \\
[1S_a|2S_b] &= \frac{\zeta_b}{6}\left\{G_{02}(0,\rho_b) - G_{02}(\rho_a,\rho_b) - \mu\, G_{12}(\rho_a,\rho_b)\right\} \\
[1S_a|3S_b] &= \frac{\zeta_b}{24}\left\{G_{03}(0,\rho_b) - G_{03}(\rho_a,\rho_b) - \mu\, G_{13}(\rho_a,\rho_b)\right\} \\
[2S_a|2S_b] &= \frac{\zeta_b}{18}\left\{3\,G_{02}(0,\rho_b) - 3\,G_{02}(\rho_a,\rho_b)\right. \\
&\qquad \left. -4\mu\, G_{12}(\rho_a,\rho_b) - 2\mu^2 G_{22}(\rho_a,\rho_b)\right\} \\
[2S_a|3S_b] &= \frac{\zeta_b}{72}\left\{3\,G_{03}(0,\rho_b) - 3\,G_{03}(\rho_a,\rho_b)\right. \\
&\qquad \left. -4\mu\, G_{13}(\rho_a,\rho_b) - 2\mu^2 G_{23}(\rho_a,\rho_b)\right\} \\
[3S_a|3S_b] &= \frac{\zeta_b}{144}\left\{6\,G_{03}(0,\rho_b) - 6\,G_{03}(\rho_a,\rho_b)\right. \\
&\qquad \left. -9\mu\, G_{13}(\rho_a,\rho_b) - 6\mu^2 G_{23}(\rho_a,\rho_b) - 2\mu^3 G_{33}(\rho_a,\rho_b)\right\}
\end{aligned}\right\} \qquad \text{(B-45)}$$

where

$$G_{\alpha\beta}(x,y) = \left(\frac{y}{2}\right)^{\alpha+\beta+1} \int_1^{\infty} d\xi \int_{-1}^{+1} d\eta$$

$$\times\, e^{-\left(\frac{x+y}{2}\right)\xi}\, e^{-\left(\frac{x-y}{2}\right)\eta}\, (\xi+\eta)^{\alpha}\, (\xi-\eta)^{\beta} \qquad \text{(B-46)}$$

It is to be noted that by multiplying out the polynomials in the integrand of (B-46), the $G_{\alpha\beta}(x,y)$ functions are expressible in terms of the $C_n(\rho)$ and $B_n(y)$ functions already defined, and that $[NS_a|MS_b]$ is obtained from $[MS_a|NS_b]$ by interchanging subscripts a and b for the arguments of the $G_{\alpha\beta}$ functions in equations (B-45).

Hybrid integrals involving only s-type orbitals may be represented as

$$\left[n\mathcal{A}_a(1)\, n'\mathcal{A}_a(1)\left|\frac{1}{r_{12}}\right|n''\mathcal{A}_a(2)\, m\mathcal{A}_b(2)\right] = \left[\Omega_a|\Omega_{ab}\right] \qquad \text{(B-47)}$$

where Ω_a and Ω_{ab} represent basic charge distributions. The Ω_a are S-type charge distributions, given by equation (B-42). The basic charge distributions Ω_{ab} arising from s-orbitals are given in equation (B-48).

$$(n\mathcal{A}_a)(m\mathcal{A}_b) = \frac{2}{\pi}\frac{\int_a^{n+\frac{1}{2}}\int_b^{m+\frac{1}{2}}}{[(2n)!\,(2m)!]^{1/2}} R^{n+m-2}(\xi+\eta)^{n-1}(\xi-\eta)^{m-1} e^{-\rho\xi} e^{-\tau\eta} \qquad \text{(B-48)}$$

where

$$\rho = \tfrac{1}{2}(\zeta_a+\zeta_b)R$$

$$\tau = \tfrac{1}{2}(\zeta_a-\zeta_b)R$$

In terms of these basic charge distributions Ω_a and Ω_{ab}, Ruedenberg, Roothaan and Jaunzemis (2) show that there are 12 basic hybrid integrals comprised of s-orbitals with atomic orbital quantum numbers less than 3. We define

$$\rho_a = \zeta_a R \;; \qquad \rho_b = \zeta_b R \;; \qquad \mu = \zeta_a/\zeta_b$$

The twelve basic hybrid integrals are

$$\left[1A_a\,1A_a\,|\,1A_a\,1A_b\right] = 2\,\zeta_a^{3/2}\,\zeta_b^{-1/2}\left[G_{01}(\rho_a,\rho_b) - G_{01}(3\rho_a,\rho_b) - \mu\, G_{11}(3\rho_a,\rho_b)\right]$$

$$\left[1A_a\,1A_a\,|\,1A_a\,2A_b\right] = \frac{2}{\sqrt{3}}\,\zeta_a^{3/2}\,\zeta_b^{-3/2}\left[G_{02}(\rho_a,\rho_b) - G_{02}(3\rho_a,\rho_b) - \mu\, G_{12}(3\rho_a,\rho_b)\right]$$

$$\left[1A_a\,1A_a\,|\,2A_a\,1A_b\right] = \frac{2}{\sqrt{3}}\,\zeta_a^{5/2}\,\zeta_b^{-1/2}\left[G_{11}(\rho_a,\rho_b) - G_{11}(3\rho_a,\rho_b) - \mu\, G_{21}(3\rho_a,\rho_b)\right]$$

$$\left[1A_a\,1A_a\,|\,2A_a\,2A_b\right] = \frac{2}{3}\,\zeta_a^{5/2}\,\zeta_b^{-3/2}\left[G_{12}(\rho_a,\rho_b) - G_{12}(3\rho_a,\rho_b) - \mu\, G_{22}(3\rho_a,\rho_b)\right]$$

$$\left[1A_a\,2A_a\,|\,1A_a\,1A_b\right] = \frac{1}{\sqrt{3}}\,\zeta_a^{3/2}\,\zeta_b^{-1/2}\left[3\,G_{01}(\rho_a,\rho_b) - 3\,G_{01}(3\rho_a,\rho_b) - 4\mu\, G_{11}(3\rho_a,\rho_b) - 2\mu^2\, G_{21}(3\rho_a,\rho_b)\right]$$

$$\left[1A_a\,2A_a\,|\,1A_a\,2A_b\right] = \frac{1}{3}\,\zeta_a^{3/2}\,\zeta_b^{-3/2}\left[3\,G_{02}(\rho_a,\rho_b) - 3\,G_{02}(3\rho_a,\rho_b) - 4\mu\, G_{12}(3\rho_a,\rho_b) - 2\mu^2\, G_{22}(3\rho_a,\rho_b)\right]$$

$$\left[1A_a\,2A_a\,|\,2A_a\,1A_b\right] = \frac{1}{3}\,\zeta_a^{5/2}\,\zeta_b^{-1/2}\left[3\,G_{11}(\rho_a,\rho_b) - 3\,G_{11}(3\rho_a,\rho_b) - 4\mu\, G_{21}(3\rho_a,\rho_b) - 2\mu^2\, G_{31}(3\rho_a,\rho_b)\right] \qquad \text{(B-49)}$$

$$\left[1A_a\,2A_a\,|\,2A_a\,2A_b\right] = \frac{1}{3\sqrt{3}}\,\zeta_a^{5/2}\,\zeta_b^{-3/2}\left[3\,G_{12}(\rho_a,\rho_b) - 3\,G_{12}(3\rho_a,\rho_b) - 4\mu\, G_{22}(3\rho_a,\rho_b) - 2\mu^2\, G_{32}(3\rho_a,\rho_b)\right]$$

$$\left[2A_a\,2A_a\,|\,1A_a\,1A_b\right] = \frac{1}{3}\,\zeta_a^{3/2}\,\zeta_b^{-1/2}\left[6\,G_{01}(\rho_a,\rho_b) - 6\,G_{01}(3\rho_a,\rho_b) - 9\mu\, G_{11}(3\rho_a,\rho_b) - 6\mu^2\, G_{21}(3\rho_a,\rho_b) - 2\mu^3\, G_{31}(3\rho_a,\rho_b)\right]$$

$$\left[2A_a\,2A_a\,|\,1A_a\,2A_b\right] = \frac{1}{3\sqrt{3}}\,\zeta_a^{3/2}\,\zeta_b^{-3/2}\left[6\,G_{02}(\rho_a,\rho_b) - 6\,G_{02}(3\rho_a,\rho_b) - 9\mu\, G_{12}(3\rho_a,\rho_b) - 6\mu^2\, G_{22}(3\rho_a,\rho_b) - 2\mu^3\, G_{32}(3\rho_a,\rho_b)\right]$$

$$\left[2A_a\,2A_a\,|\,2A_a\,1A_b\right] = \frac{1}{3\sqrt{3}}\,\zeta_a^{5/2}\,\zeta_b^{-1/2}\left[6\,G_{11}(\rho_a,\rho_b) - 6\,G_{11}(3\rho_a,\rho_b) - 9\mu\, G_{21}(3\rho_a,\rho_b) - 6\mu^2\, G_{31}(3\rho_a,\rho_b) - 2\mu^3\, G_{41}(3\rho_a,\rho_b)\right]$$

$$\left[2A_a\,2A_a\,|\,2A_a\,2A_b\right] = \frac{1}{9}\,\zeta_a^{5/2}\,\zeta_b^{-3/2}\left[6\,G_{12}(\rho_a,\rho_b) - 6\,G_{12}(3\rho_a,\rho_b) - 9\mu\, G_{22}(3\rho_a,\rho_b) - 6\mu^2\, G_{32}(3\rho_a,\rho_b) - 2\mu^3\, G_{42}(3\rho_a,\rho_b)\right]$$

where the $G_{\alpha\beta}(x,y)$ are defined in equation (B-46) and

$$\left[n\lambda_a n'\lambda_a \middle| n''\lambda_a m\lambda_b \right] = \left[n'\lambda_a n\lambda_a \middle| n''\lambda_a m\lambda_b \right] . \qquad \text{(B-50)}$$

We write for the general exchange integral

$$I = \left[n\lambda_a(1)\, m\lambda_b(1) \left| \frac{1}{r_{12}} \right| n'\lambda_a(2)\, m'\lambda_b(2) \right] . \qquad \text{(B-51)}$$

Following Rudenberg (3) we write equation (B-51) in terms of the basic charge distributions introduced in equation (B-48):

$$I = \left[\Omega_{nm}(1) \mid \Omega_{n'm'}(2) \right] . \qquad \text{(B-52)}$$

Upon introducing the Neumann expansion for $1/r_{12}$ in confocal elliptic coordinates

$$\frac{R}{r_{12}} = 4 \sum_{\ell=0}^{\infty} \sum_{m=-\ell}^{\ell} (-1)^m \frac{(\ell-|m|)!}{(\ell+|m|)!} P_\ell^{|m|}(\xi_1) Q_\ell^{|m|}(\xi_2) P_\ell^{|m|}(\eta_1)$$

$$\times P_\ell^{|m|}(\eta_2)\, e^{im\phi_1}\, e^{-im\phi_2} \qquad (\xi_1 < \xi_2)$$

with a similar expression for $\xi_1 > \xi_2$ obtained by interchanging all indices, Rudenberg is able to write equation (B-52) in terms of certain auxiliary functions. He obtains

$$I = \frac{1}{R} (R\mathcal{J}_a)^{n+n'+1} (R\mathcal{J}_b)^{m+m'+1} \sum_{\ell=0}^{\infty} I_\ell \qquad \text{(B-53)}$$

$$I_\ell = \sum_{p=0}^{N} \sum_{q=0}^{N} \omega_p^\ell(\tau)\, \omega_q^\ell(\tau)\, \phi_{pq}^\ell(\rho) \qquad \text{(B-54)}$$

where

$$\rho = \frac{1}{2}(\tau_a + \tau_b) R$$

$$\tau = \frac{1}{2}(\tau_a - \tau_b) R$$

$$N = n + m$$

$$\omega_p^{\ell}(\tau) = \sum_{i=0}^{N} \alpha_{pi} \, \mathbb{B}_i^{\ell}(\tau) \tag{B-55}$$

$$\mathbb{B}_i^{\ell}(\tau) = \left[\frac{2\ell+1}{2}\right]^{1/2} \int_{-1}^{+1} e^{\tau x} P_{\ell}(x) \, x^i \, dx \tag{B-56}$$

$$\phi_{pq}^{\ell}(\rho) = \int_1^{\infty} \frac{f_p^{\ell}(y,\rho) \, f_q^{\ell}(y,\rho)}{y^2 - 1} \, dy \tag{B-57}$$

$$f_p^{\ell}(y,\rho) = \frac{1}{P_{\ell}(y)} \int_1^{y} e^{-\rho x} P_{\ell}(x) \, x^p \, dx \tag{B-58}$$

and the $P_{\ell}(x)$ are the unnormalized Legendre functions of the first kind.

The $\mathbb{B}_i^{\ell}(\tau)$ functions are explicit and easy to treat; we write the unnormalized Legendre functions in the form

$$P_{\ell}(x) = \sum_{j=0}^{\ell} C_{\ell j} \, x^j \tag{B-59}$$

where the C_{lj} are the Legendre coefficients. The $\mathbb{B}_i^{\ell}$ may then be written

$$\mathbb{B}_i^{\ell}(\tau) = \left[\frac{2\ell+1}{2}\right]^{1/2} \sum_{j=0}^{\ell} C_{\ell j} \int_{-1}^{+1} e^{\tau x} \, x^{i+j} \, dx \tag{B-60}$$

$$\mathbb{B}_i^{\ell}(\tau) = \left[\frac{2\ell+1}{2}\right]^{1/2} \sum_{j=0}^{\ell} C_{\ell j} (-1)^{i+j} B_{i+j}(|\tau|) \tag{B-61}$$

where the $B_{i+j}(|\tau|)$ functions are the same $B_n(y)$ functions introduced in equation (B-17). Equation (B-61) can be somewhat reduced by the identity

$$(-1)^j C_{\ell j} = (-1)^{\ell} C_{\ell j} \tag{B-62}$$

which comes about because Legendre functions of even or odd order contain only even or odd terms respectively. Thus

$$\mathbb{B}_i^{\ell}(\tau) = \left[\frac{2\ell+1}{2}\right]^{1/2} (-1)^{\ell+i} \sum_{j=0}^{\ell} C_{\ell j} B_{i+j}(|\tau|) \ . \tag{B-63}$$

The coefficients α_{pi} in equation (B-55) are defined as follows. The basic charge distributions defined in equation (B-48) can be written

$$(n s_a)(m s_b) = k \ w(\xi,\eta) \ e^{-\rho\xi} \ e^{-\tau\eta} \tag{B-64}$$

where $w(\xi,\eta)$ is a polynomial defined as

$$w(\xi,\eta) = (\xi+\eta)^{n-1} (\xi-\eta)^{m-1} \ . \tag{B-65}$$

The coefficients α_{pi} are then defined in terms of these polynomials:

$$(\xi^2-\eta^2) w(\xi,\eta) = \sum_p \sum_i \alpha_{pi} \xi^p \eta^i \tag{B-66}$$

or

$$\sum_{p=0}^{n+m} \sum_{i=0}^{n+m} \alpha_{pi} \xi^p \eta^i = (\xi+\eta)^n (\xi-\eta)^m \tag{B-67}$$

where n and m are the quantum numbers of the atomic orbitals making up the charge distribution. Thus from equations (B-67) and (B-63) one can compute the functions $\omega_p^\ell(\tau)$ defined in equation (B-55).

The functions $\phi_{pq}^\ell(\rho)$ defined by equations (B-57) and (B-58) are seen to be double integrals; however, they can be reduced to single integrals in the following manner. We introduce into equation (B-58) the form of the Legendre function given in equation (B-59):

$$f_p^\ell(y,\rho) = \frac{1}{P_\ell(y)} \sum_{i=0}^{\ell} C_{\ell i} \int_1^y e^{-\rho x} x^{p+i} dx \tag{B-68}$$

$$= \frac{1}{P_\ell(y)} \sum_{i=0}^{\ell} C_{\ell i} \left[\int_1^\infty e^{-\rho x} x^{p+i} dx - \int_y^\infty e^{-\rho x} x^{p+i} dx \right] \tag{B-69}$$

In the second integral of equation (B-69) substitute

$$u = \frac{x}{y}$$

and note that

$$\int_1^\infty e^{-tx} x^n dx = \frac{e^{-t}}{t^{n+1}} C_n(t) \tag{B-70}$$

where the $C_n(t)$ are defined in equation (B-16). We thus obtain

$$f_p^{\ell}(y,\rho) = \frac{1}{P_\ell(y)} \sum_{i=0}^{\ell} C_{\ell i} \left[\frac{e^{-\rho}}{\rho^{p+i}} C_{p+i}(\rho) - \frac{e^{-\rho y}}{(\rho y)^{p+i}} C_{p+i}(\rho y) \right] \tag{B-71}$$

The functions $\phi_{pq}^{\ell}(\rho)$ are now computed by numerical integration over the single variable y.

It is found that only a few terms in equation (B-53) for the exchange integral provide high accuracy; in cases where convergence is not rapid, corresponding to large values of the internuclear separation R, the integral as a whole is small.

In addition to the molecular integrals described so far, there are two more integrals defining the dipole transition integral for an electronic transition between the two lowest states of the molecule. These two transition integrals are defined in terms of the dipole-length formula

$$\vec{Q}_L = \iint \psi_f^* (\vec{r}_1 + \vec{r}_2) \, d\tau_1 \, d\tau_2 \, \psi_i \tag{B-72}$$

and the dipole-velocity formula

$$\vec{Q}_V = \iint \psi_f^* \left[(\vec{\nabla}_1 + \vec{\nabla}_2) \psi_i \right] d\tau_1 \, d\tau_2 \Big/ E(R) \tag{B-73}$$

where ψ_f and ψ_i are the final and initial electronic wave functions respectively, and E(R) is the difference in energy between the two electronic states at an internuclear separation R. As our trial wave functions consist only of s-orbitals, the x- and y-components of the position vector $\vec{\pi}$ vanish for symmetry reasons. Thus the dipole-length formula becomes

$$\vec{Q}_L = \vec{e}_z \iint \psi_f^* (z_1 + z_2) \psi_i \, d\tau_1 \, d\tau_2 \qquad \text{(B-74)}$$

where $\vec{e}_z$ denotes a unit vector in the z-direction (along the line connecting the nuclei). From the definition of the electronic wave functions given in Chapter IV, equation (IV-30), we write

$$\vec{Q}_L = \vec{e}_z \sum_m \sum_n C_{im} C_{fn} \iint \chi_m (z_1 + z_2) \chi_n \, d\tau_1 \, d\tau_2 \qquad \text{(B-75)}$$

where C_{im} and C_{fn} are the coefficients in the expansion of our initial state and final state trial electronic wave functions, and the χ_m, χ_n are the set of 2-electron wave functions defined in Chapter IV, equations (IV-25). It can be seen that we require basic one-electron integrals of the form

$$\left.\begin{aligned} &(n s_a \,|\, z \,|\, m s_a) \\ &(n s_a \,|\, z \,|\, m s_b) \\ &(n s_b \,|\, z \,|\, m s_b) \end{aligned}\right\} \qquad \text{(B-76)}$$

We evaluate these integrals in the same confocal elliptic coordinate system that we have been using; in this system

$$z = \frac{R}{2}\,\xi\,\eta \tag{B-77}$$

From the definition of atomic orbitals in equations (B-6) and (B-7) we may write for the integrals in equation (B-76).

$$(n\Lambda_a|z|m\Lambda_a) = \frac{R\,(\zeta_a R)^{n+m+1}}{4\left[(2n)!\,(2m)!\right]^{1/2}} \times \int_1^{\infty} d\xi \int_{-1}^{+1} d\eta\; e^{-\zeta_a R(\xi+\eta)}\,\xi\eta\,(\xi+\eta)^{n+m-1}\,(\xi-\eta) \tag{B-78}$$

$$(n\Lambda_a|z|m\Lambda_b) = \frac{R\,(\zeta_a R)^{n+\frac{1}{2}}\,(\zeta_b R)^{m+\frac{1}{2}}}{4\left[(2n)!\,(2m)!\right]^{1/2}} \times \int_1^{\infty} d\xi \int_{-1}^{+1} d\eta\; e^{-\frac{1}{2}(\zeta_a+\zeta_b)R\xi}\,e^{-\frac{1}{2}(\zeta_a-\zeta_b)R\eta}\,\xi\eta\,(\xi+\eta)^{n}\,(\xi-\eta)^{m} \tag{B-79}$$

$$(n\Lambda_b|z|m\Lambda_b) = \frac{R\,(\zeta_b R)^{n+m+1}}{4\left[(2n)!\,(2m)!\right]^{1/2}} \times \int_1^{\infty} d\xi \int_{-1}^{+1} d\eta\; e^{-\zeta_b R(\xi-\eta)}\,\xi\eta\,(\xi-\eta)^{n+m-1}\,(\xi+\eta) \tag{B-80}$$

By multiplying out the polynomials in the integrands of equations (B-78), (B-79) and (B-80) it is clear that these basic integrals are expressible in terms of the $C_n(x)$ and $B_n(y)$ functions introduced and defined in equations (B-15) and (B-17).

Turning our attention now to the dipole-velocity formula, equation (B-73), we expand our trial electronic wave functions as before and note that since our set of basic wave functions consist only of s-orbitals, the x- and y-components vanish for symmetry reasons. We thus must evaluate basic one-electron integrals of the form

$$\left.\begin{aligned}&(n\mathcal{A}_a \mid \vec{\nabla}\, m\mathcal{A}_a)\\&(n\mathcal{A}_a \mid \vec{\nabla}\, m\mathcal{A}_b)\\&(n\mathcal{A}_b \mid \vec{\nabla}\, m\mathcal{A}_a)\\&(n\mathcal{A}_b \mid \vec{\nabla}\, m\mathcal{A}_b)\end{aligned}\right\} \qquad \text{(B-81)}$$

By symmetry arguments, it can be shown that

$$\left.\begin{aligned}&(n\mathcal{A}_a \mid \vec{\nabla}\, m\mathcal{A}_a) = 0\\&(n\mathcal{A}_b \mid \vec{\nabla}\, m\mathcal{A}_b) = 0\end{aligned}\right\} \qquad \text{(B-82)}$$

The only non-vanishing components of the dipole velocity integrals are the z-components; from the definition of the s-orbitals in spherical coordinates centered on nucleus a and b in turn, we have

$$\vec{\nabla}\, n\mathcal{A}_a = \vec{e}_z \frac{\partial}{\partial z}\, n\mathcal{A}_a$$

$$= \vec{e}_z \left(\frac{n-1}{r_a} - \zeta_a\right)\left(\frac{z-\frac{R}{2}}{r_a}\right) n\mathcal{A}_a \qquad \text{(B-83)}$$

and

$$\vec{\nabla}\, m\mathcal{A}_b = \vec{e}_z \frac{\partial}{\partial z}\, m\mathcal{A}_b$$

$$= \vec{e}_z \left(\frac{m-1}{r_b} - \zeta_b\right)\left(\frac{z+\frac{R}{2}}{r_b}\right) m\mathcal{A}_b \qquad \text{(B-84)}$$

where

$$r_a = \left[x^2 + y^2 + \left(z - \frac{R}{2}\right)^2 \right]^{1/2}$$

$$r_b = \left[x^2 + y^2 + \left(z + \frac{R}{2}\right)^2 \right]^{1/2}$$

We introduce equations (B-83) and (B-84) into the two non-vanishing integrals of equations (B-82) and transform to confocal elliptic coordinates

$$(n s_b | \vec{\nabla} m s_a) = \vec{e}_z \frac{(\xi_b)^{n+\frac{1}{2}} (\xi_a)^{m+\frac{1}{2}}}{[(2n)!\,(2m)!]^{1/2}} R^{n+m}$$

$$\times \left[(m-1) \int_1^{\infty} d\xi \int_{-1}^{+1} d\eta \; e^{-\rho\xi} e^{-\tau\eta} (\xi\eta - 1)(\xi - \eta)^n (\xi + \eta)^{m-2} \right.$$

$$\left. - \frac{\xi_a R}{2} \int_1^{\infty} d\xi \int_{-1}^{+1} d\eta \; e^{-\rho\xi} e^{-\tau\eta} (\xi\eta - 1)(\xi - \eta)^n (\xi + \eta)^{m-1} \right] \qquad \text{(B-85)}$$

and

$$(m s_a | \vec{\nabla} n s_b) = \vec{e}_z \frac{(\xi_b)^{n+\frac{1}{2}} (\xi_a)^{m+\frac{1}{2}}}{[(2n)!\,(2m)!]^{1/2}} R^{n+m}$$

$$\times \left[(n-1) \int_1^{\infty} d\xi \int_{-1}^{+1} d\eta \; e^{-\rho\xi} e^{-\tau\eta} (\xi\eta + 1)(\xi + \eta)^m (\xi - \eta)^{n-2} \right.$$

$$\left. - \frac{\xi_b R}{2} \int_1^{\infty} d\xi \int_{-1}^{+1} d\eta \; e^{-\rho\xi} e^{-\tau\eta} (\xi\eta + 1)(\xi + \eta)^m (\xi - \eta)^{n-1} \right] \qquad \text{(B-86)}$$

where

$$\rho = \frac{1}{2}(\zeta_a + \zeta_b)R$$

$$\tau = \frac{1}{2}(\zeta_a - \zeta_b)R$$

Once again, by multiplying out the various polynomials appearing in the integrands of equation (B-85) and (B-86), it is clear that our two basic non-vanishing dipole-velocity transition integrals are expressible in terms of the $C_n(x)$ and $B_n(y)$ functions.

APPENDIX C

THE ATOMIC ABSORPTION COEFFICIENTS OF HYDROGEN AND HELIUM

The following general notation is adopted.

a_ν - atomic absorption coefficient - cm^2/atom

k_ν - absorption coefficient per unit volume - cm^{-1}

κ_ν - absorption coefficient per unit mass - cm^2/gm

thus

$$\kappa_\nu = \frac{k_\nu}{\rho}$$

ρ - mass density - gm/cm^3

N_e - number of electrons per cm^3

N_a - number of atoms of all kinds per cm^3

N - number of particles per cm^3

thus

$$N = N_e + N_a$$

P_g - gas pressure - $dyne/cm^2$

P_e - electron pressure - $dyne/cm^2$

A_i - relative abundance of element i by number of atoms

thus

$$\rho = N_e m_e + N_a \sum_i A_i m_i$$

but for practical purposes

$$\rho = N_a \sum_i A_i m_i$$

1. Neutral Hydrogen - H I

The cross section of one hydrogen-like atom in quantum state n, for $\nu \geq \nu_n$ is

$$a_{\nu n} = \frac{64 \pi^4 m e^{10} Z^4}{3\sqrt{3}\, c\, h^6} \frac{1}{\nu^3} \frac{1}{n^5} g_I(\nu, n) \qquad \text{(C-1)}$$

$$\nu_n = \frac{2 \pi^2 m_e e^4 Z^2}{h^3 n^2} = \frac{\nu_1}{n^2} \qquad \text{(C-2)}$$

$g_I(\nu, n)$ is the Gaunt factor for bound-free transitions. We multiply (1) by N_n, the number of H-atoms in level n, and sum over levels such that $\nu_n \leq \nu$: From the Boltzmann distribution, we have

$$N_n = \frac{g_n}{g_1} e^{-\frac{\chi_n}{kT}} N_1 \qquad \text{(C-3)}$$

where

N_1 = number H-atoms in ground state

g_n = $2n^2$ for hydrogen

g_1 = 2

χ_n = excitation energy of level n above ground level

We thus have

$$a_\nu(T) = \frac{64 \pi^4 m_e e^{10}}{3\sqrt{3}\, c\, h^6 \nu^3} \sum_{n^2 \geq \frac{\nu_1}{\nu}}^{\infty} \frac{e^{-\frac{\chi_n}{kT}}}{n^3} g_I(\nu, n) \,. \qquad \text{(C-4)}$$

Karzas and Latter (26) have computed $g_I(\nu,n)$ for a wide range of ν and for n up to n = 15. We therefore sum terms up to n = 15 in equation (C-4), and replace the remainder of the sum, $n>15$, by an integral. In doing this, a mean value of g_I is adopted:

$$g_I(\nu, n>15) = \overline{g_I} = 1.10 . \tag{C-5}$$

We have

$$\sum_{n=16}^{\infty} \frac{e^{-\chi_n/kT}}{n^3} g_I(\nu,n) = \overline{g_I} \int_{16}^{\infty} \frac{e^{-\frac{\chi_n}{kT}}}{n^3} dn \tag{C-6}$$

$$\frac{\chi_n}{kT} = \frac{h(\nu_1-\nu_n)}{kT} = a_1 - a_n \tag{C-7}$$

$$a_n = \frac{a_1}{n^2} \tag{C-8}$$

Thus

$$\sum_{n=16}^{\infty} \frac{e^{-\frac{\chi_n}{kT}}}{n^3} g_I(\nu,n) = \overline{g_I}\, e^{-a_1} \int_{16}^{\infty} e^{a_1/n^2} \frac{dn}{n^3}$$

$$= \frac{e^{-a_1}\,\overline{g_I}}{2a_1} \int_0^{a_{16}} e^x dx$$

$$= e^{-a_1}\left[\frac{e^{a_{16}}-1}{2a_1}\right]\overline{g_I} \tag{C-9}$$

Thus the total bound-free atomic absorption coefficient of hydrogen per H-atom in the ground state is

$$a_\nu(T) = \frac{64\pi^4 m_e e^{10}}{3\sqrt{3}\, c h^6} \frac{e^{-a_1}}{\nu^3} \left[\sum_{n^2 \geq \frac{\nu_1}{\nu}}^{15} \frac{e^{a_1/n^2}}{n^3} g_I(\nu, n) + \frac{e^{\frac{a_1}{256}} - 1}{2a_1} \overline{g_I} \right] \quad \text{(C-10)}$$

To this is added the contribution from free-free interactions between protons and electrons. The continuous free-free absorption coefficient between a proton and an electron with velocity between v and $v+dv$ is:

$$a_{\nu K} = \frac{4\pi e^6}{3\sqrt{3}\, m_e^2 c h} \frac{1}{\nu^3} \frac{1}{v} g_{II}(\nu, T) \quad \text{(C-11)}$$

Where $g_{II}(\nu, T)$ is the free-free Gaunt factor, also computed by Karzas and Latter (26). The number of electrons per cm^3 with velocities between v and $v+dv$ is given by the Maxwellian velocity distribution:

$$N_e(v)\, dv = 4\pi N_e \left(\frac{m_e}{2\pi k T}\right)^{3/2} v^2 e^{-\frac{m_e v^2}{2kT}} dv. \quad \text{(C-12)}$$

We multiply equation (C-11) by (C-12) and N_i, the number of protons per cm^3, and integrate over all velocities, ν being held fixed.

$$a_\nu(T) = \frac{16\pi^2 e^6}{3\sqrt{3}\, c h} \left(\frac{1}{2\pi m_e k T}\right)^{3/2} \frac{kT\, N_i N_e}{\nu^3} g_{II}(\nu, T). \quad \text{(C-13)}$$

We may express the product $N_i N_e$ in terms of N_1, the number of H-atoms in the ground state by the combined Saha and Boltzmann equations:

$$N_i N_e = \frac{(2\pi m_e kT)^{3/2}}{h^3} e^{-a_1} N_1 \tag{C-14}$$

also, from the definition of a_n, we have:

$$a_1 = \frac{h\nu_1}{kT} = \frac{2\pi^2 m_e e^4}{h^2 kT} \tag{C-15}$$

Thus

$$kT\, N_i N_e = \frac{(2\pi m_e kT)^{3/2}\, 2\pi^2 m_e e^4}{h^5 a_1} N_1 \tag{C-16}$$

and

$$a_\nu(T) = \frac{64\pi^4 m_e e^{10}}{3\sqrt{3}\, c\, h^6} \frac{e^{-a_1}}{\nu^3} \frac{g_{II}(\nu,T)}{2a_1} N_1 \tag{C-17}$$

We add equations (C-17) and (C-10) to obtain the total continuous atomic absorption coefficient of hydrogen per H-atom in the ground state:

$$a_\nu(T) = \frac{64\pi^4 m_e e^{10}}{3\sqrt{3}\, c h^6} \frac{e^{-a_1}}{\nu^3} \left[\sum_{n^2 \geq \frac{\nu_1}{\nu}}^{15} \frac{e^{a_1/n^2}}{n^3} g_I(\nu, n) + \frac{\left(e^{a_1/256} - 1\right) \overline{g_I} + g_{II}(\nu,T)}{2a_1} \right] \tag{C-18}$$

Numerically, we write for the total continuous atomic absorption coefficient of hydrogen:

$$\alpha_\nu(T) = 1.0448792 \times 10^{-14} \frac{\lambda^3}{e^{a_1}} \left[\sum_{n^2 \geq \frac{\nu_1}{\nu}}^{15} \frac{e^{a_1/n^2}}{n^3} g_I(\nu, n) + \frac{1.10\left(e^{a_1/256} - 1\right) + g_{II}(\nu, T)}{2a_1} \right] \quad \text{(C-19)}$$

λ in microns

$$a_1 = 31.30932\,\theta = 31.30932\left(\frac{5040.17}{T}\right) \quad \text{(C-20)}$$

Approximate expressions for the Gaunt factor $g_I(\nu, n)$ have been derived for quantum levels n = 1 to n = 15 by curve-fitting expressions of the following form to the data of Karzas and Latter (26).

$$g_I(\nu, n) = \sum_{i=0}^{4} C_{ni}\, x^i \quad \text{(C-21)}$$

Where

$$x = \log_e(1/\lambda)$$

λ in microns

The coefficients C_{ni} are presented in Table IX . These approximate expressions represent the values given by Karzas and Latter to within $\pm$ 1%.

For the free-free Gaunt Factors $g_{II}(\nu, T)$, two way interpolation is performed in Table X , which was taken from the data of Karzas and Latter (26).

TABLE IX

Bound-Free Gaunt Factor Coefficients

n	C_{n0}	C_{n1}	C_{n2}	C_{n3}	C_{n4}
1	-0.22562	0.52841	-0.014517	-0.013476	0.0007822
2	0.68116	0.22009	-0.023062	-0.0031543	0.0001566
3	0.88173	0.13846	-0.029257	0.0038457	-0.0006862
4	0.95987	0.085765	-0.0084987	-0.0018784	-0.0000285
5	0.99835	0.065833	-0.0096262	0.0004475	-0.0003724
6	1.02307	0.047595	-0.011946	0.0045831	-0.0010702
7	1.03084	0.042335	-0.0034511	0.00002719	-0.0004090
8	1.03887	0.035587	-0.0015757	0.00000562	-0.0004473
9	1.04378	0.032595	-0.0006065	-0.00099665	-0.0003040
10	1.05048	0.027722	-0.0025525	0.00167602	-0.0007242
11	1.05040	0.032472	0.0002064	-0.00122854	-0.0002464
12	1.05495	0.026047	-0.0002350	0.00027118	-0.0005101
13	1.05632	0.025378	0.0001967	0.00003431	-0.0004727
14	1.05753	0.025188	0.0005817	-0.00024406	-0.0004295
15	1.05985	0.021491	0.0007569	0.00039540	-0.0005509

TABLE X

Free-Free Gaunt Factors

	$\theta = \frac{5040.17}{T}$					
$\ln(1/\lambda)$	0.00958	0.05	0.10	0.15	0.20	0.25
-1.0	8.475	2.418	2.032	1.84	1.71	1.62
-0.8	3.25	2.24	1.88	1.70	1.585	1.506
-0.6	3.025	2.07	1.75	1.585	1.49	1.42
-0.4	2.80	1.904	1.62	1.484	1.402	1.344
-0.2	2.59	1.766	1.514	1.40	1.335	1.29
0.0	2.382	1.645	1.43	1.333	1.28	1.24
0.2	2.19	1.537	1.356	1.272	1.23	1.203
0.4	2.02	1.44	1.295	1.235	1.202	1.18
0.6	1.86	1.367	1.27	1.202	1.177	1.16
0.8	1.74	1.302	1.213	1.177	1.159	1.148
1.0	1.58	1.247	1.183	1.159	1.146	1.138
1.2	1.46	1.204	1.156	1.14	1.132	1.126
1.4	1.35	1.156	1.125	1.116	1.11	1.106
1.6	1.25	1.107	1.087	1.081	1.078	1.075
1.8	1.15	1.048	1.037	1.033	1.03	1.028

	$\theta = \frac{5040.17}{T}$					
$\ln(1/\lambda)$	0.30	0.35	0.40	0.45	0.50	0.60
-1.0	1.55	1.502	1.47	1.435	1.41	1.37
-0.8	1.452	1.418	1.385	1.36	1.34	1.305
-0.6	1.372	1.345	1.315	1.30	1.28	1.252
-0.4	1.307	1.276	1.255	1.234	1.219	1.193
-0.2	1.257	1.23	1.212	1.195	1.182	1.163
0.0	1.214	1.198	1.181	1.167	1.158	1.142
0.2	1.184	1.17	1.16	1.15	1.144	1.134
0.4	1.165	1.154	1.146	1.139	1.133	1.125
0.6	1.149	1.142	1.135	1.13	1.126	1.120
0.8	1.14	1.134	1.13	1.126	1.123	1.118
1.0	1.132	1.127	1.124	1.122	1.120	1.116
1.2	1.121	1.118	1.116	1.114	1.112	1.110
1.4	1.104	1.102	1.100	1.099	1.098	1.096
1.6	1.073	1.071	1.070	1.069	1.068	1.067
1.8	1.027	1.027	1.026	1.025	1.025	1.024

2. Ionized Helium -- He II

Since He II is a hydrogen-like atom, we follow exactly the procedure of the previous sections with the following exceptions:

$$Z = 2$$

$$a_1(\text{He II}) = \frac{h\nu_1(\text{He II})}{kT}$$

$$= 4\, a_1(\text{H I})$$

$$g_I(\nu, n) = 1.0$$

$$g_{II}(\nu, T) = 1.0$$

Since the Gaunt factors are unknown, we simply set them to unity. The actual ionization frequencies of He II are determined from the Rydberg for helium, which is slightly different from the Rydberg for hydrogen. For convenience's sake, we have assumed the Rydberg to be the same in order that the ionization edges coincide and thus insure numerically accurate ν -integrals. Since the charge on the helium nucleus is 2, we sum over twice as many levels as in the case of hydrogen. Numerically, we have for the atomic absorption coefficient of He II, per He II atom in the ground state:

$$a_\nu(T) = 1.6718 \times 10^{-13}\, \lambda^3\, e^{-a_1} \left[\sum_{n^2 \geq \frac{\nu_1}{\nu}}^{30} \frac{e^{a_1/n^2}}{n^3} + \frac{e^{a_1/961}}{2a_1} \right]$$

(C-22)

To convert this to a mass absorption coefficient, we multiply by $N_{II,1}$, the number of He II atoms in the ground state, and divide by the density ρ .

3. Neutral Helium -- He I

Quantum mechanical calculations exist for transitions from bound states n = 1 and n = 2 to free states. Table XI summarizes the data on these transitions and gives the source of the calculations.

TABLE XI

i	Transition	g_i	$1/\lambda_i$ (μ^{-1})	χ_i (ev)	Source
1	$1^1S \rightarrow K^1P$	1	19.8305	0.00	(1)
2	$2^3S \rightarrow K^3P$	3	3.8546	19.82	(1)
3	$2^1S \rightarrow K^1P$	1	3.2033	20.61	(1)
4	$2^3P \rightarrow K^3D$	9	2.9224	20.96	(2)
5	$2^3P \rightarrow K^3S$	9	2.9224	20.96	(3)
6	$2^1P \rightarrow K^1D$	3	2.7176	21.22	(2)
7	$2^1P \rightarrow K^1S$	3	2.7176	21.22	(3)

Sources:
(1) Huang (27)
(2) Goldberg (28)
(3) Ueno (29) Quotes Goldberg as original source.

The following approximate expressions were derived from least-square curve fits to the data as given by the sources listed in Table XI .

$1\,{}^1S \rightarrow \kappa\,{}^1P$

$$a_1(\nu) = \exp(-71.039 + 36.459\,x - 14.694\,x^2 + 2.5057\,x^3 - 0.16249\,x^4) \quad \text{(C-23)}$$

$2\,{}^3S \rightarrow \kappa\,{}^3P$

$$a_2(\nu) = \exp(-43.736 + 5.7414\,x - 3.1768\,x^2 + 0.58587\,x^3 - 0.04232\,x^4) \quad \text{(C-24)}$$

$2\,{}^1S \rightarrow \kappa\,{}^1P$

$$a_3(\nu) = \exp(-38.198 + 0.27730\,x - 1.1451\,x^2 + 0.247371\,x^3 - 0.021336\,x^4) \quad \text{(C-25)}$$

$2\,{}^3P \rightarrow \kappa\,{}^3D$

$$a_4(\nu) = \exp(-36.375 - 1.4957\,x - 0.62184\,x^2 + 7.8167\,x^3 - 0.0004734\,x^4) \quad \text{(C-26)}$$

$2\,{}^3P \rightarrow \kappa\,{}^3S$

$$a_5(\nu) = \exp(-38.487 - 3.3\,x) \quad \text{(C-27)}$$

$2\,{}^1P \rightarrow \kappa\,{}^1D$

$$a_6(\nu) = \exp(-35.747 - 3.2129\,x + 0.007567\,x^2 - 0.033804\,x^3 + 0.0032075\,x^4) \quad \text{(C-28)}$$

$2\,{}^1P \rightarrow \kappa\,{}^1S$

$$a_7(\nu) = \exp(-38.296 - 3.6\,x) \quad \text{(C-29)}$$

where

$$x = \log_e (1/\lambda)$$

λ in microns

The contribution from these transitions to the bound-free absorption coefficient of He I, per He I atom in the ground state, is

$$a_\nu(T; n \leq 2) = \sum_{\substack{i=1 \\ \lambda_i > \lambda}}^{7} g_i \, a_i(\nu) \, e^{-\frac{\chi_i}{kT}} \qquad \text{(C-30)}$$

Hydrogenic forms are used for levels with quantum number $n \geq 3$. For levels $n = 3$ and $n = 4$, the exact term values and statistical weights are used; data is given in Table XII.

Shielding by the inner electron is approximated by setting

$$Z = Z_{eff} = 1.1$$

and the Gaunt factors are assumed to be unity. We thus have the following as the contribution to the bound-free absorption coefficient of He I, per He I atom in the ground state:

$$a_\nu(T; n = 3,4) = 1.53 \times 10^{-14} \lambda^3 \left[\frac{1}{243} \sum_{\substack{i=8 \\ \lambda_i > \lambda}}^{12} g_i \, e^{-\frac{\chi_i}{kT}} + \frac{1}{1024} \sum_{\substack{i=13 \\ \lambda_i > \lambda}}^{18} g_i \, e^{-\frac{\chi_i}{kT}} \right] \qquad \text{(C-31)}$$

TABLE XII

n	i	Level	g_i	$1/\lambda_i$ (μ^{-1})	χ_i (ev)
3	8	3^3S	3	1.5074	22.716
	9	3^1S	1	1.3446	22.968
	10	3^3P	9	1.2746	23.005
	11	3^3D and 3^1D	20	1.2208	23.072
	12	3^1P	3	1.2101	23.085
4	13	4^3S	3	0.8013	23.592
	14	4^1S	1	0.7371	23.671
	15	4^3P	9	0.7094	23.706
	16	4^3D and 4^1D	20	0.6866	23.734
	17	4^3F and 4^1F	28	0.6858	23.735
	18	4^1P	3	0.6818	23.740

Complete hydrogenic forms are assumed for quantum levels $n \geq 5$, adopting:

$$g_n = 4n^2$$
$$Z = Z_{eff} = 1.1$$
$$a_n(\text{He I}) = a_n(\text{H I})$$

(C-32)

$$a_\nu(T; n \geq 5) = 1.53 \times 10^{-14} \lambda^3 \left[4 \sum_{\substack{n=5 \\ n^2 \geq \frac{\nu_1}{\nu}}}^{15} \frac{e^{a_n}}{n^3} \right.$$

$$\left. + \frac{2}{a_1} \left(e^{a_{16}} - 1 \right) \right] \qquad \text{(C-33)}$$

The same procedure is followed for computing the free-free atomic absorption coefficient of He I as was outlined for H I in equation (C-11) through (C-17), except that we do not make the substitution for a_1 given in equation (C-15). We obtain

$$a_\nu(T; \kappa) = \frac{64\pi^2 e^6 kT}{3\sqrt{3}\, h^4 c} \frac{1}{\nu^3} e^{-I/kT} \qquad \text{(C-34)}$$

or

$$a_\nu(T, \kappa) = 6.6709 \times 10^{-16} \frac{\lambda^3}{\theta} 10^{-24.585\theta} \qquad \text{(C-35)}$$

The total continuous atomic absorption coefficient of neutral helium, per He I atom in the ground state, is obtained by adding equations (C-30), (C-31), (C-33) and (C-35):

$$a_\nu(T) = a_\nu(T; n \leq 2) + a_\nu(T; n = 3,4)$$

$$+ a_\nu(T; n \geq 5) + a_\nu(T; K) \qquad \text{(C-36)}$$

To convert this to a mass absorption coefficient, multiply by $N_{I,1}$, the number of He I atoms in the ground state, and divide by the density ρ .

APPENDIX D

An Approximate Expression For the Hopf $q_0(\tau)$ Function

The Hopf $q_0(\tau)$ function, which expresses the variation with optical depth of the source function in a semi-infinite plane-parallel gray atmosphere, has been discussed at length by Kourganoff (4). King (5) has given a simple expression for this function of the form

$$q_0(\tau) = A + B\,E_2(\tau) + C\,E_3(\tau) \qquad \text{(D-1)}$$

where E_n is the n^{th}-order exponential integral. Using the Schwarzschild-Milne integral equation for the source function, flux and K-integrals at the top of a semi-infinite gray atmosphere, we have

$$B(0) = \frac{1}{2}\int_0^\infty B(\tau)\,E_1(\tau)\,d\tau \qquad \text{(D-2)}$$

$$F = 2\int_0^\infty B(\tau)\,E_2(\tau)\,d\tau \qquad \text{(D-3)}$$

$$K(0) = \frac{F}{4}\,q_0(\infty) = \frac{1}{2}\int_0^\infty B(\tau)\,E_3(\tau)\,d\tau \qquad \text{(D-4)}$$

Substituting

$$B(\tau) = \frac{3F}{4}\left[\tau + q_0(\tau)\right] \qquad \text{(D-5)}$$

into equations (D-2), (D-3) and (D-4) we have three integral constraints upon the Hopf function.

$$\int_0^\infty q(\tau)\, E_1(\tau)\, d\tau = \frac{2}{\sqrt{3}} - \frac{1}{2} \tag{D-6}$$

$$\int_0^\infty q(\tau)\, E_2(\tau)\, d\tau = \frac{1}{3} \tag{D-7}$$

$$\int_0^\infty q(\tau)\, E_3(\tau)\, d\tau = \frac{2}{3} q(\infty) - \frac{1}{4} \tag{D-8}$$

When equation (D-1) is substituted into (D-6), (D-7) and (D-8) and the coefficients A, B and C determined, King finds that the approximate expression (D-1) reproduces the exact $q(\tau)$ with an error of +0.24 per cent at $\tau = 0$ and less than $\pm$ 0.1 per cent error for $\tau \geq 0.01$.

A more accurate expression may be derived with slight additional effort by adding two constraints to the constraints in equations (D-6), (D-7) and (D-8). The two constraints are

$$q(0) = \frac{1}{\sqrt{3}} = 0.57735027 \tag{D-9}$$

and

$$q(\infty) = \frac{6}{\pi^2} + \frac{1}{\pi} \int_0^{\pi/2} \left(\frac{3}{\theta^2} - \frac{1}{1 - \theta \cot \theta} \right) d\theta$$
$$= 0.71044609 \tag{D-10}$$

These additional constraints merely have the effect of making the approximate expression exact at $\tau = 0$ and $\tau = \infty$, which is of considerable importance in certain applications.

We continue the series approximation for $q_f(\tau)$ in equation (D-1) by

$$q_f(\tau) = A + B E_2(\tau) + C E_3(\tau) + D E_4(\tau) + E E_5(\tau) \tag{D-11}$$

substitute this expression into our five constraints and obtain the linear set of equations

$$\left.\begin{aligned}
A + B F_{12} + C F_{13} + D F_{14} + E F_{15} &= \frac{2}{\sqrt{3}} - \frac{1}{2} \\
\tfrac{1}{2} A + B F_{22} + C F_{23} + D F_{24} + E F_{25} &= \frac{1}{3} \\
\tfrac{1}{3} A + B F_{23} + C F_{33} + D F_{34} + E F_{35} &= \tfrac{2}{3} q_f(\infty) - \tfrac{1}{4} \\
A &= q_f(\infty) \\
A + B + \tfrac{1}{2} C + \tfrac{1}{3} D + \tfrac{1}{4} E &= q_f(0)
\end{aligned}\right\} \tag{D-12}$$

where the functions F_{nm} are defined by

$$F_{nm} = \int_0^\infty E_n(\tau)\, E_m(\tau)\, d\tau \tag{D-13}$$

and are tabulated by Kourganoff (4).

The value of $q_f(\infty)$ was obtained by expanding the integrand of equation (D-10) in an infinite series:

$$f(\theta) = \frac{3}{\theta^2} - \frac{1}{1 - \theta \cot \theta}$$

$$= \frac{\sum_{n=1}^{\infty} F_n \, \theta^{2(n-1)}}{\sum_{n=1}^{\infty} G_n \, \theta^{2(n-1)}} \tag{D-14}$$

$$= \sum_{n=1}^{\infty} R_n \, \theta^{2(n-1)} \tag{D-15}$$

where

$$F_n = (-1)^{n+1} \cdot \left[(2n+3)(2n+1) \cdot (2n-1)! \right]^{-1}$$

$$G_n = (-1)^{n+1} \cdot \left[(2n+1) \cdot (2n-1)! \right]^{-1} \tag{D-16}$$

$$R_n = \left[F_n - \sum_{j=1}^{n-1} G_{j+1} \, R_{n-j} \right] \cdot G_1^{-1}$$

Thus

$$q(\infty) = \frac{6}{\pi^2} + \frac{1}{\pi} \sum_{n=1}^{\infty} \frac{R_n}{2n-1} \left(\frac{\pi}{2} \right)^{2n-1} \tag{D-17}$$

Computations using an IBM 7094 computer in double precision yielded

$$q(\infty) = 0.71044\ 60895\ 98763 \tag{D-18}$$

The coefficients determined from equations (D-12) have the values

$$A = +0.71044609$$
$$B = -0.28303851$$
$$C = +0.57975839 \qquad \text{(D-19)}$$
$$D = -0.75751038$$
$$E = +0.45026781$$

Calculations of this $q_\delta(\tau)$ approximate expression compare well with the exact $q_\delta(\tau)$ values given by King (5), the error being less than 0.0032 per cent for all optical depths. Shown in Table XIII is a comparison between the values computed with this approximate function and the exact values given by King (5).

TABLE XIII

Comparison of Approximate $q_3(\tau)$ Function with Exact Values

τ	Exact	Approximate	Per Cent Error
0.00	0.577350	0.577350	0.0000
0.01	0.588236	0.588219	-0.0029
0.02	0.595391	0.595383	-0.0013
0.03	0.601242	0.601242	0.0000
0.05	0.610758	0.610770	0.0020
0.10	0.627919	0.627939	0.0032
0.20	0.649550	0.649556	0.0009
0.30	0.663365	0.663355	-0.0015
0.40	0.673090	0.673072	-0.0027
0.60	0.685801	0.685782	-0.0028
0.80	0.693535	0.693524	-0.0016
1.00	0.698540	0.698541	0.0001
2.00	0.707916	0.707938	0.0031
3.00	0.709806	0.709821	0.0021
∞	0.710446	0.710446	0.0000

APPENDIX E

NUMERICAL QUADRATURE FORMULAE

1. The Schwarzschild-Milne Integrals

The solution to the equation of radiative transfer was shown in Chapter V to involve integrals of the form

$$I = \int_{\tau_\nu}^{\infty} S_\nu(x_\nu)\, E_n(x_\nu - \tau_\nu)\, dx_\nu$$

$$-(-1)^n \int_0^{\tau_\nu} S_\nu(x_\nu)\, E_n(\tau_\nu - x_\nu)\, dx_\nu \qquad \text{(E-1)}$$

We will henceforth suppress the subscript ν on all independent variables, with the understanding that we always integrate on a τ_ν or x_ν scale. We write equation (E-1) in general terms

$$I = I_1 - (-1)^n I_2 \qquad \text{(E-2)}$$

where

$$I_1 = \int_{\tau}^{\infty} S(x)\, E_n(x-\tau)\, dx \qquad \text{(E-3)}$$

and

$$I_2 = \int_0^{\tau} S(x)\, E_n(\tau - x)\, dx \qquad \text{(E-4)}$$

We make the following transformations in the integrals I_1 and I_2

I_1: $u = x - \tau$

$du = dx$

I_2: $u = \tau - x$

$du = -dx$

Thus the integrals become

$$I_1 = \int_0^\infty S(\tau + u)\, E_n(u)\, du \tag{E-5}$$

$$I_2 = \int_0^\tau S(\tau - u)\, E_n(u)\, du \tag{E-6}$$

In evaluating the first of these integrals, it is seen that a practical upper limit may be taken to be

$u = 20$

since

$$E_n(20) \sim 10^{-10}$$

We divide the range $0 \le u \le 20$ into m-1 intervals, denoting the k^{th} interval by $[u_{k-1}, u_k]$ where

$u_1 = 0$

$u_m = 20$

Our integrals thus become

$$I_1 = \sum_{k=2}^{m} \int_{u_{k-1}}^{u_k} S(\tau+u)\, E_n(u)\, du \qquad \text{(E-7)}$$

and

$$I_2 = \sum_{k=2}^{j} \int_{u_{k-1}}^{u_k} S(\tau-u)\, E_n(u)\, du + \int_{u_j}^{\tau} S(\tau-u)\, E_n(u)\, du \qquad \text{(E-8)}$$

where in the second integral we perform the indicated summation over the basic intervals up to the largest u_j that is smaller than τ. We then must compute the contribution of this partial interval to the integral as a whole.

We note that the basic integral to be evaluated is of the general form

$$\int_A^B f(x,\tau)\, w(x)\, dx$$

where w(x) is a weighting function. We can evaluate such integrals by means of a Gaussian quadrature, in which the weighting function does not appear explicitly, provided the moments of the weighting function exist.

Moments are defined by

$$\alpha_\ell (A,B) = \int_A^B x^\ell \, w(x)\, dx \qquad \ell = 0, 1, 2, \ldots \tag{E-9}$$

Since the limits of the integral in the last term of equation (E-8) are variable, we cannot evaluate this integral in terms of a fixed set of points and weights. Instead we transform the integral to the interval (-1, +1) and employ Gauss-Legendre quadrature. A list of the roots and associated weights of the Legendre polynomials is given by Lowan, Davids and Levenson (30). We write

$$\int_{u_j}^{\tau} S(\tau-u)\, E_n(u)\, du$$

$$= \frac{\tau-u_j}{2} \int_{-1}^{+1} S\left[\tfrac{1}{2}(\tau-u_j)(1-x)\right] E_n\left(\frac{\tau+u_j}{2} + \frac{\tau-u_j}{2}x\right) dx$$

$$= \frac{\tau-u_j}{2}\left[\sum_{i=1}^{\ell} S\left[\tfrac{1}{2}(\tau-u_j)(1-x_i)\right] \times W_i\, E_n\left(\frac{\tau+u_j}{2} + \frac{\tau-u_j}{2}x_i\right)\right] \tag{E-10}$$

Divisions x_i and weights w_i for this quadrature are given in Table XIV . It has been found that, because the argument of S is rather close to the origin and hence S might be more ill-behaved than elsewhere, a four-point formula, exact for polynomials of seventh degree, was advisable.

TABLE XIV

i	Quadrature for the Incomplete Interval x_i	w_i
1	-0.86113631	0.34785485
2	-0.33998104	0.65214515
3	+0.33998104	0.65214515
4	+0.86113631	0.34785485

The procedure for deriving the divisions and weights which are used to evaluate the remaining integrals in equations (E-7) and (E-8) are best illustrated by an example. We choose to evaluate the integral over the interval $[u_{k-1}, u_k]$ by a two-point formula. This will be exact for all polynomials of third degree or less. We also choose to illustrate our procedure by the first exponential integral. We are then attempting to evaluate the elementary integral in the following manner.

$$\int_{u_{k-1}}^{u_k} f(x) E_1(x) dx = W_{1k} f(x_{1k}) + W_{2k} f(x_{2k}) \qquad \text{(E-11)}$$

We denote the general moment of the first exponential integral over the interval $[u_{k-1}, u_k]$ by

$$\alpha_{kl} = \int_{u_{k-1}}^{u_k} x^l E_1(x) dx \qquad \text{(E-12)}$$

Assuming for the moment that these moments exist and can be computed, we have the following four conditions to be satisfied in order that our quadrature formula be exact for all polynomials of third degree or less.

$$\left.\begin{aligned} W_{1k} &+ W_{2k} = \alpha_{k0} \\ W_{1k}\, x_{1k} &+ W_{2k}\, x_{2k} = \alpha_{k1} \\ W_{1k}\,(x_{1k})^2 &+ W_{2k}\,(x_{2k})^2 = \alpha_{k2} \\ W_{1k}\,(x_{1k})^3 &+ W_{2k}\,(x_{2k})^3 = \alpha_{k3} \end{aligned}\right\} \qquad \text{(E-13)}$$

This is a set of equations linear in the w_{ik}'s, but non-linear in the x_{ik}'s. We separate the linear and non-linear variables and solve for them in turn. Kopal (31) has shown that the divisions x_{ik} are the roots of the equation

$$x^2 + c_1 x + c_2 = 0 \qquad \text{(E-14)}$$

where the c_i's are defined by a simultaneous linear system

$$\left.\begin{aligned} \alpha_{k2} &+ c_2\,\alpha_{k1} + c_1\,\alpha_{k0} = 0 \\ \alpha_{k3} &+ c_2\,\alpha_{k1} + c_1\,\alpha_{k1} = 0 \end{aligned}\right\} \qquad \text{(E-15)}$$

Once the roots have been computed, we obtain the corresponding Gaussian weights w_{ik} from any 2 of the 4 equations in (E-13). This method can be extended to a larger number of divisions and weights in an obvious manner.

We turn now to the calculation of the general moments of the n^{th} exponential integral,

$$\alpha_{nkl} = \int_{u_{k-1}}^{u_k} x^l\, E_n(x)\, dx \qquad \text{(E-16)}$$

$$l = 0, 1, 2, \cdots$$

We integrate by parts n times and obtain

$$\alpha_{nkl} = \left[\frac{x^{l+1}}{l+1} E_n(x) + \frac{x^{l+2}}{(l+1)(l+2)} E_{n-1}(x) + \cdots + \frac{x^{l+n}}{(l+1)(l+2)\cdots(l+n)} E_1(x) \right] \Bigg|_{u_{k-1}}^{u_k} + \frac{1}{(l+1)(l+2)\cdots(l+n)} \int_{u_{k-1}}^{u_k} x^{l+n-1} e^{-x} dx \qquad \text{(E-17)}$$

which can be written

$$\alpha_{nkl} = \left[\sum_{i=1}^{n} \frac{l!}{(l+i)!} x^{l+i} E_{n+i-1}(x) \right] \Bigg|_{u_{k-1}}^{u_k} + \frac{l!}{(l+n)!} \int_{u_{k-1}}^{u_k} x^{l+n-1} e^{-x} dx \qquad \text{(E-18)}$$

We expand e^{-x} in the last integral, and the resulting expression for α_{nkl} is

$$\alpha_{nkl} = \left[\sum_{i=1}^{n} \frac{l!}{(l+i)!} x^{l+i} E_{n+i-1}(x) + \frac{l!}{(l+n)!} \sum_{i=0}^{\infty} \frac{(-1)^i}{(l+n+i)\cdot i!} x^{l+n+i} \right] \Bigg|_{u_{k-1}}^{u_k} \qquad \text{(E-19)}$$

Following the procedures just described, Gaussian divisions and weights were computed for the first and second exponential integrals. The selection of the intervals $[u_{k-1}, u_k]$ is to a certain degree arbitrary, but we are guided in our selection by wishing to employ as few points as possible to represent the integrals in (E-1),

yet retain a prescribed accuracy. The optimum procedure was to select the distribution of the u_k such that the resulting moments α_{nkl} turned out to be approximately the same order of magnitude. The u_k scale adapted and the resulting Gaussian divisions and weights for 2, 3 and 4 points per interval are shown in Tables XV XVI and XVII respectively for the first exponential integral, while Tables XVIII, XIX and XX present the corresponding data for the second exponential integral.

The accuracy of these quadrature formulae was judged by computing the mean intensity and flux integrals for a gray atmosphere in radiative equilibrium

$$J(\tau) = \frac{1}{2}\int_{\tau}^{\infty} S(t)\, E_1(t-\tau)\, dt + \frac{1}{2}\int_{0}^{\tau} S(t)\, E_1(\tau-t)\, dt \qquad \text{(E-20)}$$

$$F = 2\int_{\tau}^{\infty} S(t)\, E_2(t-\tau)\, dt - 2\int_{0}^{\tau} S(t)\, E_2(\tau-t)\, dt \qquad \text{(E-21)}$$

The source function S(t) for a gray atmosphere is given by

$$S(t) = \frac{3}{4} F \left[t + q_0(t) \right] \qquad \text{(E-22)}$$

where q(t) is the Hopf function, discussed in Appendix D, where a highly accurate expression was derived.

As Unsöld (32) pointed out, the effect of the $\Lambda_\tau^{(1)}$ operator, defined in equation (V-64) of Chapter V, is to render an approximate source function more exact. We therefore have the following integral equations to be satisfied

$$\tau + q(\tau) = \frac{1}{2}\int_\tau^\infty \left[t + q(t)\right] E_1(t-\tau)\,dt + \frac{1}{2}\int_0^\tau \left[t + q(t)\right] E_1(\tau-t)\,dt \qquad \text{(E-23)}$$

$$\frac{4}{3} = 2\int_\tau^\infty \left[t + q(t)\right] E_2(t-\tau)\,dt - 2\int_0^\tau \left[t + q(t)\right] E_2(\tau-t)\,dt \qquad \text{(E-24)}$$

The accuracy of the expression derived in Appendix D for the Hopf q(t) function is considered to be such that if the above integral equations, when evaluated numerically using the approximate expression for q(t) and the quadrature formulae in Tables XV through XX , should be satisfied to within the known error in our q(t). We should thus be able to test the accuracy of our quadratures to within 1 part in 10^4.

The accuracy ascribed to any quadrature formula is of course dependent upon the test function; it is believed that our choice of the source function for a gray atmosphere in radiative equilibrium is a realistic choice.

The results of numerical calculations of equations (E-23) and (E-24) are given in Tables XXI and XXII for the $\Lambda_\tau^{(1)}$ and $\Lambda_\tau^{(2)}$ quadratures, for 2, 3 and 4 points per interval. Also given in column two for comparison is the relative error $\frac{\Delta S^*}{S^*}$ in per cent for the approximate $S(\tau)$ expression. Note that the quadrature errors in Table XXI follow the error of the approximate $S(\tau)$ expression, both in magnitude and sign, except in the vicinity of $\tau = 0.01$. Note also that the errors given in Table XXI for all three quadrature formulae are practically identical at all optical depths.

The integral equation for the source function in a non-gray stellar atmosphere, equation (V-81) of Chapter V is solved by iteration, and the effect of an accumulated systematic error in the quadrature formula must be investigated. A practical means of doing this is to compute model atmospheres starting from identical initial conditions, changing only the quadrature formulae. This was tried on several different model atmospheres and revealed that the monochromatic source functions, mean intensities and fluxes agreed to within one part in 10^4 for all quadrature formulae. It is concluded that the errors inherent in the quadrature formulae given in Tables XV through XX are less than the errors given in Tables XXI and XXII.

TABLE XV

Divisions and Weights for the First Exponential Integral

No. points per interval =2

u_{k-1}	u_k	x	w
0.000	0.018	3.2293625 (-3)	4.4230031 (-2)
		1.3873008 (-2)	3.5854506 (-2)
0.018	0.045	2.3422959 (-2)	4.1758942 (-2)
		3.9045883 (-2)	3.7735955 (-2)
0.045	0.080	5.2111943 (-2)	4.1348963 (-2)
		7.2337290 (-2)	3.8110536 (-2)
0.080	0.125	8.9170756 (-2)	4.2255826 (-2)
		1.1516441 (-1)	3.9136544 (-2)
0.125	0.180	1.3622547 (-1)	4.1516308 (-2)
		1.6798828 (-1)	3.8545482 (-2)
0.180	0.248	1.9386802 (-1)	4.1360736 (-2)
		2.3313289 (-1)	3.8321230 (-2)
0.248	0.334	2.6548995 (-1)	4.1725380 (-2)
		3.1514234 (-1)	3.8416279 (-2)
0.334	0.444	3.5627381 (-1)	4.1674317 (-2)
		4.1977333 (-1)	3.8002246 (-2)
0.444	0.592	4.7372988 (-1)	4.2274960 (-2)
		5.5914546 (-1)	3.7883306 (-2)
0.592	0.803	6.3381530 (-1)	4.2738696 (-2)
		7.5553210 (-1)	3.7187322 (-2)
0.803	1.146	8.6905778 (-1)	4.3946839 (-2)
		1.0666433 (0)	3.5939053 (-2)
1.146	1.800	1.2642311 (0)	4.1571698 (-2)
		1.6389589 (0)	2.9649589 (-2)
1.800	5.000	2.1652675 (0)	3.7051527 (-2)
		3.7610834 (0)	1.0767260 (-2)

u_{k-1}	u_k	x	w
5.000	20.000	5.5194879 (0)	8.5591913 (-4)
		8.0818947 (0)	1.4054982 (-4)

The number within parentheses indicates the power of 10 by which the Table entry must be multiplied.

TABLE XVI

Divisions and Weights for the First Exponential Integral

No. points per interval = 3

u_{k-1}	u_k	x	w
0.000	0.018	1.7050739 (-3)	2.6863438 (-2)
		8.5788997 (-3)	3.4241477 (-2)
		1.5842587 (-2)	1.8979622 (-2)
0.018	0.045	2.0917022 (-2)	2.3972841 (-2)
		3.1218285 (-2)	3.5136203 (-2)
		4.1853498 (-2)	2.0385853 (-2)
0.045	0.080	4.8820057 (-2)	2.3561209 (-2)
		6.2205936 (-2)	3.5215749 (-2)
		7.5943256 (-2)	2.0682542 (-2)
0.080	0.125	8.4924142 (-2)	2.4031785 (-2)
		1.0214444 (-1)	3.6099371 (-2)
		1.1979053 (-1)	2.1261214 (-2)
0.125	0.180	1.3102631 (-1)	2.3587863 (-2)
		1.5207919 (-1)	3.5523790 (-2)
		1.7363645 (-1)	2.0950136 (-2)
0.180	0.248	1.8744649 (-1)	2.3510218 (-2)
		2.1346511 (-1)	3.5359783 (-2)
		2.4012511 (-1)	2.0811965 (-2)
0.248	0.334	2.5739675 (-1)	2.3758627 (-2)
		2.9026764 (-1)	3.5561759 (-2)
		3.2401687 (-1)	2.0821274 (-2)
0.334	0.444	3.4597747 (-1)	2.3793488 (-2)
		3.8795424 (-1)	3.5349006 (-2)
		4.3118533 (-1)	2.0534069 (-2)
0.444	0.592	4.6001233 (-1)	2.4255433 (-2)
		5.1632677 (-1)	3.5545588 (-2)
		5.7464816 (-1)	2.0357245 (-2)
0.592	0.803	6.1458221 (-1)	2.4723787 (-2)
		6.9447352 (-1)	3.5406397 (-2)
		7.7799452 (-1)	1.9795834 (-2)

u_{k-1}	u_k	x	w
0.803	1.146	8.3887879 (-1)	2.5855303 (-2)
		9.6738374 (-1)	3.5285656 (-2)
		1.1044188 (0)	1.8744933 (-2)
1.146	1.800	1.2110479 (0)	2.5329369 (-2)
		1.4501491 (0)	3.1158198 (-2)
		1.7165780 (0)	1.4733720 (-2)
1.800	5.000	2.0214225 (0)	2.7029580 (-2)
		2.9599028 (0)	1.7603695 (-2)
		4.3884949 (0)	3.1855122 (-3)
5.000	20.000	5.3706538 (0)	7.1771342 (-4)
		7.0695086 (0)	2.6932351 (-4)
		1.0768523 (+1)	9.4320227 (-6)

The number within parentheses indicates the power of 10 by which the Table entry must be multiplied.

TABLE XVII

Divisions and Weights for the First Exponential Integral

No. points per interval = 4

u_{k-1}	u_k	x	w
0.000	0.018	1.0489777 (-3)	1.8037488 (-2)
		5.5908984 (-3)	2.7008755 (-2)
		1.1809116 (-2)	2.3446900 (-2)
		1.6687671 (-2)	1.1591393 (-2)
0.018	0.045	1.9810018 (-2)	1.5307783 (-2)
		2.6707305 (-2)	2.6794238 (-2)
		3.5904015 (-2)	2.4819948 (-2)
		4.3074022 (-2)	1.2572927 (-2)
0.045	0.080	4.7366786 (-2)	1.4972071 (-2)
		5.6342889 (-2)	2.6652480 (-2)
		6.8252164 (-2)	2.5049848 (-2)
		7.7514040 (-2)	1.2785099 (-2)
0.080	0.125	8.3049668 (-2)	1.5252098 (-2)
		9.4601725 (-2)	2.7269100 (-2)
		1.0990889 (-1)	2.5721957 (-2)
		1.2180680 (-1)	1.3149216 (-2)
0.125	0.180	1.2873154 (-1)	1.4960744 (-2)
		1.4285773 (-1)	2.6808314 (-2)
		1.6156319 (-1)	2.5333119 (-2)
		1.7609888 (-1)	1.2959613 (-2)
0.180	0.248	1.8461150 (-1)	1.4914836 (-2)
		2.0206971 (-1)	2.6704495 (-2)
		2.2519428 (-1)	2.5194430 (-2)
		2.4317312 (-1)	1.2868206 (-2)
0.248	0.334	2.5382169 (-1)	1.5087060 (-2)
		2.7587420 (-1)	2.6919842 (-2)
		3.0511812 (-1)	2.5275494 (-2)
		3.2788354 (-1)	1.2859264 (-2)
0.334	0.444	3.4142533 (-1)	1.5132265 (-2)
		3.6957926 (-1)	2.6854458 (-2)
		4.0698193 (-1)	2.5029584 (-2)
		4.3615387 (-1)	1.2660255 (-2)

u_{k-1}	u_k	x	w
0.444	0.592	4.5393834 (-1)	1.5469468 (-2)
		4.9168903 (-1)	2.7179033 (-2)
		5.4200872 (-1)	2.4996878 (-2)
		5.8138838 (-1)	1.2512887 (-2)
0.592	0.803	6.0604384 (-1)	1.5842728 (-2)
		6.5955343 (-1)	2.7368027 (-2)
		7.3128212 (-1)	2.4610709 (-2)
		7.8773823 (-1)	1.2104554 (-2)
0.803	1.146	8.2540617 (-1)	1.6730270 (-2)
		9.1132844 (-1)	2.7897151 (-2)
		1.0278773 (0)	2.3924450 (-2)
		1.1207281 (0)	1.1334022 (-2)
1.146	1.800	1.1869960 (0)	1.6729416 (-2)
		1.3463581 (0)	2.5855415 (-2)
		1.5681607 (0)	1.9960175 (-2)
		1.7497742 (0)	8.6762813 (-3)
1.800	5.000	1.9487884 (0)	2.0017436 (-2)
		2.5741250 (0)	1.9381005 (-2)
		3.6030888 (0)	7.0111172 (-3)
		4.6567863 (0)	1.4092283 (-3)
5.000	20.000	5.2869272 (0)	6.0945754 (-4)
		6.5655010 (0)	3.4980321 (-4)
		9.1121393 (0)	3.6692300 (-5)
		1.3583756 (+1)	5.1589969 (-7)

The number within parentheses indicates the power of 10 by which the Table entry must be multiplied.

TABLE XVIII

Divisions and Weights for the Second Exponential Integral

No. points per interval = 2

u_{k-1}	u_k	x	w
0.000	0.100	2.0015666 (-2)	4.4085002 (-2)
		7.7875580 (-2)	3.9623539 (-2)
0.100	0.250	1.3003107 (-1)	4.8435533 (-2)
		2.1664212 (-1)	4.3171800 (-2)
0.250	0.500	2.9906121 (-1)	5.5634087 (-2)
		4.4327069 (-1)	4.7445675 (-2)
0.500	0.900	5.7632904 (-1)	5.3222702 (-2)
		8.0663716 (-1)	4.2678684 (-2)
0.900	1.500	1.0106560 (0)	3.9544535 (-2)
		1.3550066 (0)	2.9418954 (-2)
1.500	2.400	1.6579186 (0)	2.2992746 (-2)
		2.1711358 (0)	1.5341360 (-2)
2.400	3.800	2.6264829 (0)	9.5637226 (-3)
		3.4128939 (0)	5.3585606 (-3)
3.800	8.000	4.2382190 (0)	2.7514763 (-3)
		6.1979275 (0)	7.0044441 (-4)
8.000	20.000	8.5399923 (0)	2.6685720 (-5)
		1.1172691 (+1)	4.4949231 (-6)

The number within parentheses indicates the power of 10 by which the Table entry must be multiplied.

TABLE XIX

Divisions and Weights for the Second Exponential Integral

No. points per interval = 3

u_{k-1}	u_k	x	w
0.000	0.100	1.0763460 (-2)	2.5350680 (-2)
		4.8893366 (-2)	3.7000253 (-2)
		8.8313669 (-2)	2.1357609 (-2)
0.100	0.250	1.1618066 (-1)	2.7849995 (-2)
		1.7322168 (-1)	4.0583704 (-2)
		2.3239111 (-1)	2.3173633 (-2)
0.250	0.500	2.7654248 (-1)	3.2374966 (-2)
		3.7089751 (-1)	4.5601857 (-2)
		4.7016828 (-1)	2.5102939 (-2)
0.500	0.900	5.4153235 (-1)	3.1479201 (-2)
		6.9088973 (-1)	4.2307457 (-2)
		8.5116163 (-1)	2.2114728 (-2)
0.900	1.500	9.6063919 (-1)	2.3835407 (-2)
		1.1816598 (0)	3.0288479 (-2)
		1.4246266 (0)	1.4839603 (-2)
1.500	2.400	1.5874506 (0)	1.4224364 (-2)
		1.9122289 (0)	1.6689008 (-2)
		2.2820653 (0)	7.4207332 (-3)
2.400	3.800	2.5276120 (0)	6.1501069 (-3)
		3.0151453 (0)	6.3695363 (-3)
		3.6031161 (0)	2.4026401 (-3)
3.800	8.000	4.0713533 (0)	2.0507175 (-3)
		5.2294758 (0)	1.2270770 (-3)
		7.1011594 (0)	1.7412620 (-4)
8.000	20.000	8.3812974 (0)	2.2193380 (-5)
		1.0112495 (+1)	8.6565973 (-6)
		1.3811874 (+1)	3.3066644 (-7)

The number within paraentheses indicates the power of 10 by which the Table entry must be multiplied.

TABLE XX

Divisions and Weights for the Second Exponential Integral

No. points per interval = 4

u_{k-1}	u_k	x	w
0.000	0.100	6.6783673 (-3)	1.6211446 (-2)
		3.2205834 (-2)	2.8260364 (-2)
		6.6263566 (-2)	2.6082825 (-2)
		9.2850071 (-2)	1.3153907 (-2)
0.100	0.250	1.1004711 (-1)	1.7787383 (-2)
		1.4826651 (-1)	3.1095908 (-2)
		1.9928544 (-1)	2.8487252 (-2)
		2.3923430 (-1)	1.4236788 (-2)
0.250	0.500	2.6652974 (-1)	2.0818984 (-2)
		3.2967778 (-1)	3.5510944 (-2)
		4.1467596 (-1)	3.1450654 (-2)
		4.8181645 (-1)	1.5299180 (-2)
0.500	0.900	5.2597122 (-1)	2.0432986 (-2)
		6.2578014 (-1)	3.3685733 (-2)
		7.6167911 (-1)	2.8458950 (-2)
		8.7035685 (-1)	1.3323716 (-2)
0.900	1.500	9.3810836 (-1)	1.5641682 (-2)
		1.0855779 (0)	2.4764408 (-2)
		1.2891614 (0)	1.9748170 (-2)
		1.4544895 (0)	8.8092280 (-3)
1.500	2.400	1.5553564 (0)	9.4782276 (-3)
		1.7716605 (0)	1.4167581 (-2)
		2.0762471 (0)	1.0383212 (-2)
		2.3293380 (0)	4.3050848 (-3)
2.400	3.800	2.4817275 (0)	4.1942542 (-3)
		2.8058274 (0)	5.7312450 (-3)
		3.2767689 (0)	3.6594776 (-3)
		3.6835313 (0)	1.3373065 (-3)
3.800	8.000	3.9846615 (0)	1.5409671 (-3)
		4.7631316 (0)	1.4061089 (-3)
		6.0745447 (0)	4.3605402 (-4)
		7.5027444 (0)	6.8790779 (-5)

u_{k-1}	u_k	x	w
8.000	20.000	8.2889068 (0)	1.8525605 (-5)
		9.5644378 (0)	1.1284676 (-5)
		1.2053906 (+1)	1.3439943 (-6)
		1.6203619 (+1)	2.6367847 (-8)

The number within parentheses indicates the power of 10 by which the Table entry must be multiplied.

TABLE XXI

Per Cent Errors in the $\Lambda^{(1)}$ Quadrature

τ	$\frac{\Delta S^\circ}{S^\circ}$	No. of points per interval		
		2	3	4
0.00	0.0000	0.0006	0.0001	0.0000
0.01	0.0028	-0.0128	-0.0130	-0.0130
0.02	0.0013	0.0016	0.0013	0.0013
0.03	0.0000	0.0002	0.0000	0.0000
0.04	-0.0009	-0.0008	-0.0010	-0.0010
0.06	-0.0019	-0.0020	-0.0022	-0.0022
0.08	-0.0023	-0.0021	-0.0025	-0.0026
0.10	-0.0027	-0.0024	-0.0026	-0.0026
0.20	-0.0007	-0.0005	-0.0007	-0.0007
0.30	0.0010	0.0009	0.0008	0.0008
0.40	0.0017	0.0014	0.0013	0.0013
0.60	0.0015	0.0016	0.0011	0.0010
0.80	0.0007	0.0006	0.0005	0.0005
1.00	-0.0001	0.0001	0.0001	0.0001
2.00	-0.0008	0.0000	-0.0002	-0.0002
3.00	-0.0004	0.0000	0.0000	0.0000
4.00		0.0000	0.0000	0.0000
6.00		0.0000	0.0000	0.0000
8.00		0.0000	0.0000	0.0000
10.00		0.0000	0.0000	0.0000

TABLE XXII

Per Cent Errors in the $\Lambda^{(2)}$ Quadrature

τ	$\frac{\Delta S^\circ}{S^\circ}$	No. of points per interval		
		2	3	4
0.00	0.0000	0.0033	0.0007	0.0002
0.01	0.0028	0.0016	0.0002	0.0000
0.02	0.0013	0.0011	0.0001	0.0001
0.03	0.0000	0.0008	0.0001	0.0001
0.04	-0.0009	0.0007	0.0001	0.0001
0.06	-0.0019	0.0005	0.0002	0.0002
0.08	-0.0023	0.0005	0.0002	0.0002
0.10	-0.0027	-0.0025	-0.0008	-0.0004
0.20	-0.0007	-0.0007	-0.0008	-0.0008
0.30	0.0010	-0.0010	-0.0006	-0.0006
0.40	0.0017	-0.0005	-0.0005	-0.0005
0.60	0.0015	0.0000	0.0005	0.0005
0.80	0.0007	0.0007	0.0008	0.0008
1.00	-0.0001	-0.0002	0.0014	0.0014
2.00	-0.0008	-0.0002	0.0000	0.0000
3.00	-0.0004	-0.0008	-0.0006	-0.0007
4.00		-0.0014	-0.0006	-0.0006
6.00		-0.0002	-0.0002	-0.0002
8.00		-0.0003	-0.0002	-0.0002
10.00		-0.0001	-0.0002	-0.0002

2. Frequency Integrals

In the course of the computation of a model stellar atmosphere, integrals of the form

$$\int_0^\infty f(\nu)\, d\nu \tag{E-25}$$

arise, where the integrand $f(\nu)$ is not necessarily a continuous function, due to the ionization edges of the mass absorption coefficient. It is thus necessary to integrate separately the frequency regions between adjacent ionization limits. In order to keep to a minimum the number of frequencies necessary to compute integrals of the form (E-25) to within a prescribed accuracy, we choose a Gaussian formula with two points fixed at the limits of the integration region between adjacent ionization edges.

We fix our attention upon the frequency region between two adjacent ionization edges ν_1 and ν_2. The contribution of this region to the total integral is

$$I = \int_{\nu_1}^{\nu_2} f(\nu)\, d\nu \tag{E-26}$$

We transform this integral by the substitution

$$\nu = \left(\frac{\nu_2 + \nu_1}{2}\right) + \left(\frac{\nu_2 - \nu_1}{2}\right) x \tag{E-27}$$

and obtain

$$I = \left(\frac{\nu_2-\nu_1}{2}\right)\int_{-1}^{+1} f\left[\frac{\nu_2+\nu_1}{2} + \frac{\nu_2-\nu_1}{2}\,x\right] dx \qquad \text{(E-28)}$$

This is evaluated by a n-point quadrature of the form

$$I = \frac{\nu_2-\nu_1}{2}\left[W_1 f(\nu_1) + W_n f(\nu_2) + \sum_{i=2}^{n-1} W_i f\left[\frac{\nu_2+\nu_1}{2} + \frac{\nu_2-\nu_1}{2}\,x_i\right]\right] \qquad \text{(E-29)}$$

Values of the divisions x_i and weights w_i for this type of quadrature are given by Kopal (31) for n = 3, 4, ... 10.

The limits given for the complete integral in (E-25) are not practical from a numerical standpoint. Instead, we choose as our upper limit the highest ionization frequency to be encountered in our model atmosphere. If the contribution to the total integral becomes negligible at a lower frequency, as is the general case in cool stars, we choose a lower ionization frequency. Suitable upper limits for various effective temperatures are given in Table XXIII . Also given in Table XXIII are practical lower limits for the frequency integrals.

We adapt as our criterion of accuracy one part in 10^4 to be compatible with the accuracy of the quadrature in the preceeding section and present in Table XXIV a set of standard frequencies, expressed in terms of inverse wavelength, and corresponding weights.

The integrals which must be computed with maximum accuracy are the integrals for the total flux at depth τ , equation (V-102) of Chapter V. For these integrals we obtain asymptotic expressions to approximate the contributions from the frequencies above the upper limit and below the lower limit. We assume that the monochromatic flux for frequencies above the upper limit at depth τ resembles the Planck function in the limit of $\nu \to \infty$

$$F_\nu(\tau) = C\,\nu^3 \exp\left(-\frac{h\nu}{k\,T(\tau)}\right)$$

$$\nu > \nu_{max} \qquad \text{(E-30)}$$

where the constant C is determined by fitting to the monochromatic flux at a frequency just above the upper limit ν_{max} . For small frequencies, we assume

$$F_\nu(\tau) = C'\,\nu^2$$

$$\nu < \nu_{min} \qquad \text{(E-31)}$$

and determine C' by fitting to the monochromatic flux at a frequency just below the lower limit ν_{min} .

TABLE XXIII

Frequency Upper Limits for Model Atmospheres

T_e (°K)	Ionization edge of	λ (A)	$1/\lambda$ (μ^{-1})
20000	He II	227	43.871032
15000	He I	504	19.8305
10000	H I	911	10.967758

Frequency Lower Limits for Model Atmospheres

T_e (°K)	Ionization edge of	λ (A)	$1/\lambda$ (μ^{-1})
20000	H I (n=5)	22794	0.43871032
10000	H I (n=6)	32823	0.30465993
5000	H I (n=7)	44676	0.22383179

TABLE XXIV
Standard Frequencies and Weights

Ionization Edge	$1/\lambda$ (μ^{-1})	W
He II		
	43.871010	4.0067551
	31.850765	16.027020
	19.830520	4.0067551
He I		
	19.830480	1.4771237
	15.399129	5.9084949
	10.967778	1.4771237
H I		
	10.967738	0.26129293
	10.183879	1.0451717
	9.400000	0.30583793
	9.2522568	0.22272500
	9.0132031	0.22272500
	8.8654620	0.044545000
HeH^+		
	8.8654580	0.30617603
	7.8080923	1.6669584
	5.8036997	2.1772519
	3.7993071	1.6669584
	2.7419414	0.30617603
H I		
	2.7419374	0.076164982
	2.4789064	0.41467602
	1.9802896	0.54161765
	1.4816727	0.4147602
	1.2186417	0.076164982
H I		
	1.2186377	0.044429573
	1.0712793	0.22214787
	0.83284523	0.22214787
	0.68548505	0.044429573
H I		
	0.68548465	0.041129091
	0.56209758	0.16451636
	0.43871050	0.041129091
H I		
	0.43871010	0.022341695
	0.37168512	0.08936678
	0.30466013	0.022341695
H I		
	0.30465973	0.013471290
	0.26424586	0.053885160
	0.22383199	0.013471290
H I		

REFERENCES

1. Corbató, F.J., J. Chem. Phys., Vol. 24, p. 452, 1956.

2. Ruedenberg, K., Roothaan, C.C.J. and Jaunzemis, W., J. Chem. Phys., Vol. 24, p. 201, 1956.

3. Ruedenberg, K., J. Chem. Phys., Vol. 19, p. 1459, 1951.

4. Kourganoff, V., "Basic Methods in Transfer Problems", Clarendon Press, Oxford, 1952.

5. King, J.I.F., Ap. J., Vol. 132, p. 509, 1960.

6. Bates, D.R., Monthly Notices of the Royal Astronomical Society, Vol. 111, p. 303, 1951.

7. Bates, D. R., Monthly Notices of the Royal Astronomical Society, Vol. 112, p. 40, 1952.

8. Mulliken, R.S., J. Chem. Phys., Vol. 7, p. 20, 1939.

9. Bates, D.R., and Carson, T.R., Proc. Roy. Soc. A, Vol. 234, p. 207, 1956.

10. Arthurs, A.M., Bond, R.A.B. and Hyslop, J., Proc. Phys. Soc. A, Vol. 70, p. 617, 1957.

11. Arthurs, A.M. and Hyslop, J., Proc. Phys. Soc. A, Vol. 70, p. 849, 1957.

12. Eddington, A.S., "Internal Constitution of the Stars", Cambridge University Press, London, 1926.

13. Evett, A.A., J. Chem. Phys., Vol. 24, p. 150, 1956.

14. Anex, B.G., J. Chem. Phys., Vol. 38, p. 1651, 1963.

15. Hart, J.F. and Herzberg, G., Phys. Rev., Vol. 106, p. 79, 1957.

16. Chandrasekhar, S., Ap. J., Vol. 102, p. 223, 1945.

17. Münch, G., "The Theory of Model Stellar Atmospheres", Chapter 1 of Stellar Atmospheres, editor Greenstein, University of Chicago Press, Chicago, 1960.

18. Cohen, E.R., Crowe, K.M. and Dumond, J.W.M., "The Fundamental Constants of Physics", Interscience Publishers, New York, 1957.

19. Bates, D.R., J. Chem. Phys., Vol. 19, p. 1122, 1951.

20. Gingerich, O., Ap. J., Vol. 134, p. 653, 1961.

21. Chandrasekhar, S. and Breen, F.H., Ap. J., Vol. 104, p. 430, 1946.

22. Krook, M., Ap. J., Vol. 137, p. 863, 1963.

23. Avrett, E.H. and Krook, M., Ap. J., Vol. 137, p. 874, 1963.

24. Schwarzschild, K., Gottinger Nachr., No. 41, 1906.

25. Krishna Swamy, K.S., Ap. J., Vol. 134, p. 1017, 1961.

26. Karzas, W.J. and Latter, R., Ap. J. Supplement No. 55, Vol. VI, 1961.

27. Huang, Su-Shu, Ap. J., Vol. 108, p. 354, 1948.

28. Goldberg, L., Ap. J., Vol. 90, p. 414, 1939.

29. Ueno, S., Cont. Inst. Ap. Univ. Kyoto, No. 42, 1953.

30. Lowan, A.N., Davids, N. and Levenson, A., "Table of the zeros of the Legendre polynomials of Order 1 - 16 and the weight coefficients for Gauss' mechanical quadrature formula", Tables of Functions and of Zeros of Functions, National Bureau of Standards, Washington, D.C., 1954.

31. Kopal, Z., "Numerical Analysis", Wiley and Sons, New York, Chapter VII, 1955.

32. Unsöld, A., Zs. f. Ap., Vol. 24, p. 363, 1948.

33. Kramers, H.A. and ter Haar, D., B. A. N., Vol. 10, p. 137, 1946.

34. Pauling, L. and Wilson, E.B., "Introduction to Quantum Mechanics", McGraw-Hill, New York, p. 188, 1935.

35. Roothaan, C.C.J., J. Chem. Phys., Vol. 19, p.1445, 1951.

36. Herzberg, G., "Spectra of Diatomic Molecules", D. van Nostrand Co., Princeton, New Jersey, 1950.

37. Bates, D. R. and Dalgarno, A., "Atomic and Molecular Processes", editor Bates, Academic Press, New York, Chapter 7, 1962.

38. Stecher, T. P. and Milligan, J. E., Ap. J., Vol. 136, p. 1, 1962.

39. Pecker, J. C., C. R., Vol. 254, p. 821, 1962.

40. Hoyle, F. and Wickramasinghe, N. C., Monthly Notices of the Royal Astronomical Society, Vol. 126, p. 401, 1963.

41. Aller, L. H., "Interpretation of Normal Stellar Spectra", Chapter 5 of Stellar Atmospheres, editor Greenstein, University of Chicago Press, 1960.